The Role of Phosphatidylinositol Metabolism and Actin in Polarized Biosynthetic Traffic

by

Christopher James Guerriero

B.S. Biology and Chemistry, West Liberty State College, 2003

Submitted to the Graduate Faculty of

The School of Medicine in partial fulfillment

of the requirements for the degree of

Doctor of Philosophy

University of Pittsburgh

2008

UNIVERSITY OF PITTSBURGH

School of Medicine

This dissertation was presented

by

Christopher James Guerriero

It was defended on

September 24, 2008

and approved by

Dr. Gerard L. Apodaca, Committee Chair, Department of Medicine

Dr. Meir Aridor, Department of Cell Biology and Physiology

Dr. Jes K. Klarund, Department of Biochemistry and Molecular Genetics

Dr. Paul R. Kinchington, Department of Molecular Biology and Microbiology

Dr. Ora A. Weisz, Dissertation Advisor, Department of Medicine

The Role of Phosphatidylinositol Metabolism and Actin in Polarized Biosynthetic Traffic

Christopher James Guerriero, PhD

University of Pittsburgh, 2008

Polarized epithelial cell function relies on the proper sorting and distribution of newly synthesized proteins to either the cells apical or basolateral domains. If trafficking is altered by disruptions either the fidelity or efficiency of this sorting then disease can result. There is an increasing appreciation for the role of phosphatidylinositol metabolism in membrane traffic, including the sorting and delivery of newly synthesized proteins. I have studied how biosynthetic delivery pathways are regulated by the expression of phosphatidylinositol-metabolizing enzymes. The phosphatidylinositol 4,5-bisphosphate (PIP_2)-synthesizing enzyme, murine phosphatidylinositol 4-phosphate 5-kinase I alpha (PI5KIα) localizes to the apical pole of Madin-Darby canine kidney (MDCK) cells and increases cellular PIP_2 concentrations over control cell levels. Interestingly, expression of exogenous PI5KIα stimulated the rate of surface delivery of a subset apical proteins that associate with lipid rafts, including influenza hemagglutinin (HA). Conversely, overexpression of the PIP_2-5'-phosphatase OCRL (oculocerebrorenal syndrome of Lowe), which is defective or absent in patients with Lowe syndrome, decreased cellular PIP_2 levels and inhibited the rate of HA delivery.

The observation that increases in PIP_2 stimulate apical delivery of HA suggests the possibility that depletion of OCRL may have a similar effect to overexpression of PI5K. I used siRNA to knock down OCRL in MDCK cells and human proximal tubule (HK2) cells and

examined the consequence on HA surface delivery. Knockdown of OCRL slightly increased cellular PIP_2 levels but did not stimulate HA delivery.

PI5K-mediated increases in PIP_2 results in activation of neuronal Wiskott-Aldrich syndrome protein (N-WASP) leading to downstream actin cytoskeleton rearrangements including the formation of actin comets. To examine the potential role of N-WASP in HA delivery I expressed a dominant negative inhibitor of N-WASP function, the WA domain from a WASP family member, WAVE1. Expression of the WA domain significantly and selectively inhibited the rate of HA surface delivery. siRNA-mediated knockdown of N-WASP also inhibited HA delivery, confirming a role for N-WASP in biosynthetic traffic. Consistent with this, PI5KIα and HA (but not p75) were visualized on actin comets in formaldehyde-fixed MDCK cells. In summary, my data support a role for PI5K-stimulated actin comet formation in apical delivery of a subset of newly synthesized proteins.

TABLE OF CONTENTS

LIST OF TABLES

LIST OF FIGURES

PREFACE

My completion of this work would not have been possible without the generous support of several individuals. I would like to take this opportunity to thank my advisor, Dr. Ora Weisz. Ora's thoughtful guidance over the past 5 years has given me a very positive graduate school experience. Thank you for granting me the freedom to explore my interests and for all of your mentoring which has made me a better scientist. Your dedication has solidified my path in science and given me the tools necessary to blaze that path. I would also like to thank the members of my thesis committee, Drs. Gerard Apodaca, Meir Aridor, Jes Klarlund, and Paul Kinchington for their always helpful advice and support.

I would like to thank all of the members of the Weisz lab both past and present who have supported me enormously when I started and throughout my research. I would especially like to thank Dr. Kelly Weixel who was always available for insightful and informative discussions about my project or science in general as well as for teaching me the art of microscopy. I would like to thank my fellow graduate student Mark Miedel, who began this journey with me, for always being a good friend, collaborator, and distraction when needed. Beth Potter was also a great friend and colleague who never turned me away when I needed help with an experiment or presentation, and her husband Mike who inadvertently became the Wiesz Lab presentation design consultant. I also acknowledge all of the other lab members who have been there when I needed technical advice or someone with which to share my good or bad data; Jennifer Bruns,

Mark Ellis, Kerry Cresawn, Yumei Lai, as well as newer lab members, Polly Matilla, Shanshan Cui, and Di Mo who have been a pleasure to work with over the years. The Renal-Electrolyte Division has provided me with an excellent training environment and my success would have been diminished without the gracious effort of all its members for provide reagents, technical assistance, and a friendly atmosphere in which to work.

I owe my family tremendous thanks for being supportive of me throughout my graduate career. My mother, whose career as a medical technician sparked my interest in laboratories and experiments. My father, a well rounded college music professor, taught me to appreciate music, play the trumpet, and has equipped me with invaluable life skills. Mom and Dad, you have provided me with so much love, support, and opportunities over the years that I cannot begin to find the words to thank you for everything. You were an inspiration to me and kindled my love of both music and science. I love you very much and you have made me the confident, inquisitive, and hard working individual I am today. Anita and Bridget, a brother could not ask for two better sisters. Anita, your hard work in college and medical school set the bar high and helped to foster my own interest in science. Bridget, you have made me proud because you are an excellent music teacher and you worked very hard during the summers to obtain your masters degree. I am glad that all three of us can share of love of music and science in our lives. Last but not least, I would like to thank my wife. Emily, you have been an unending source of love, patience, understanding, and support. I could not ask for a better partner in science or in life. You are always there when I need you whether its help with a grant I am writing, preparing for a presentation, or to listening to me vent about a frustrating day. Thank you for everything and I hope I can be there as much for you as you begin your masters degree as a physician assistant.

ABBREVIATIONS

AP	Adaptor protein
ATP	Adenosine triphosphate
ADP	Adenosine diphosphate
AV	Adenovirus
Arf	ADP-ribosylation factor
Arp	Actin-related protein
CCP	Clathrin coated pit
CCV	Clathrin coated vesicle
CI-MPR	Cation-independent mannose 6-phosphate receptor
COPII	Coat protein complex II
CLASP	Clathrin-associated sorting protein
DAG	Diacylglycerol
DOX	Doxycycline
EEA1	Early endosome antigen 1
Endo H	Endoglycosidase H
EGF	Epidermal growth factor
ER	Endoplasmic reticulum

ERAD	ER-associated degradation
ERGIC	ER-to-Golgi intermediate compartment
FAPP	Four-phosphatase-adaptor proteins
FYVE	Fab1, YOTB, Vac1, EEA1
GAP	GTPase-activating protein
GEF	Guanine nucleotide exchange factor
GFP	Green fluorescent protein
GGA	γ-adaptin ear-containing, Arf binding
GPCR	G protein coupled receptor
GPI	Glycophosphatidylinositol
GTP	Guanosine triphosphate
HA	Hemagglutinin
HPLC	High pressure liquid chromatography
Inpp5b	Neuraminidase
IP_3	Inositol 1,4,5-trisphosphate
LDL	Low density lipoprotein
lmwp	Low molecular weight proteinuria
MDCK	Madin-Darby canine kidney
m.o.i.	Multiplicity of infection
NPF	Nucleation promoting factor
NSF	N-ethylmaleimide-sensitive factor

N-WASP	neuronal Wiskott-Aldrich syndrome protein
OCRL	Oculocerebrorenal syndrome of Lowe
oligo	Oligonucleotide
OSBP	Oxysterol binding protein
PA	Phosphatidic acid
PC	Phosphatidylcholine
PDK	Phosphoinositide-dependent kinase
PH	Plekstrin homology
pptase	Phosphatase
PI	Phosphatidylinositol
PIP	Phosphatidylinositol phosphate
PI5K	Phosphatidylinositol 4-phosphate 5-kinase
pIgR	polymeric Immunoglobulin Receptor
PLC	Phospholipase C
PLD	Phospholipase D
PMA	Phorbol myristate acetate
PKC	Protein kinase C
PKD	Protein kinase D
PTEN	Phosphatase and Tensin homolog
PTC	Proximal tubule cells
PX	Phox homology

RNAi	RNA interference
RTK	Receptor tyrosine kinase
SHIP2	Src homology 2-containing inositol-5-pptase
siRNA	Small interfering RNA
SNARE	soluble NSF attachment receptors
SNX	Sorting nexin
syndapin I	syntaptic dynamin-associated protein I
TGN	*trans*-Golgi network
Tfn	Transferrin
TLC	Thin layer chromatography
VSV-G	Vesicular stomatitis virus G protein
WAS	Wiskott-Aldrich syndrome
WASP	Wiskott-Aldrich syndrome protein
WAVE	WASP family verprolin homologues
wisk	wiskostatin

1.0 INTRODUCTION

1.1 OVERVIEW

The function of polarized epithelial cells depends largely on their ability to maintain a barrier between internal and external environments, as well as their ability to perform specialized tasks, including ion transport across the barrier or binding to surface-specific ligands. Barrier function is maintained by a series of junctional proteins surrounding cells giving them a cobblestone appearance and preventing paracellular flow of solutes (Figure 1.1). Tight junctions also prevent the intramembranous flow of proteins and lipids dividing the membrane into two distinct domains: apical (luminal; green in Figure 1.1) and basolateral (ablumenal; orange in Figure 1.1). Because polarized epithelial cells have two separate membrane domains, they must accurately deliver and maintain proteins at their appropriate sites of function. My work concentrates on the role of lipids in the delivery of newly synthesized proteins to the plasma membrane, termed biosynthetic traffic.

The plasma membrane is composed of a diverse array of lipids that provide it with structural and functional attributes. An important class of lipids is the phosphatidylinositol phosphates (PIPs), which exist in many different varieties due to multiple phosphorylation arrangements. These lipids have important roles in cellular signaling and regulation of membrane traffic. One mechanism by which they affect membrane traffic is through interacting with

proteins that modulate actin cytoskeletal dynamics. Actin is broadly important as a structural component of cells, but it also has a crucial role in the movement of vesicles. My primary goal was to determine if there is a role for PIP metabolism in polarized biosynthetic traffic and if so, to determine if actin is directly involved. The following introduction provides the framework with which to put my studies into perspective with the current literature on PIPs and polarized biosynthetic traffic.

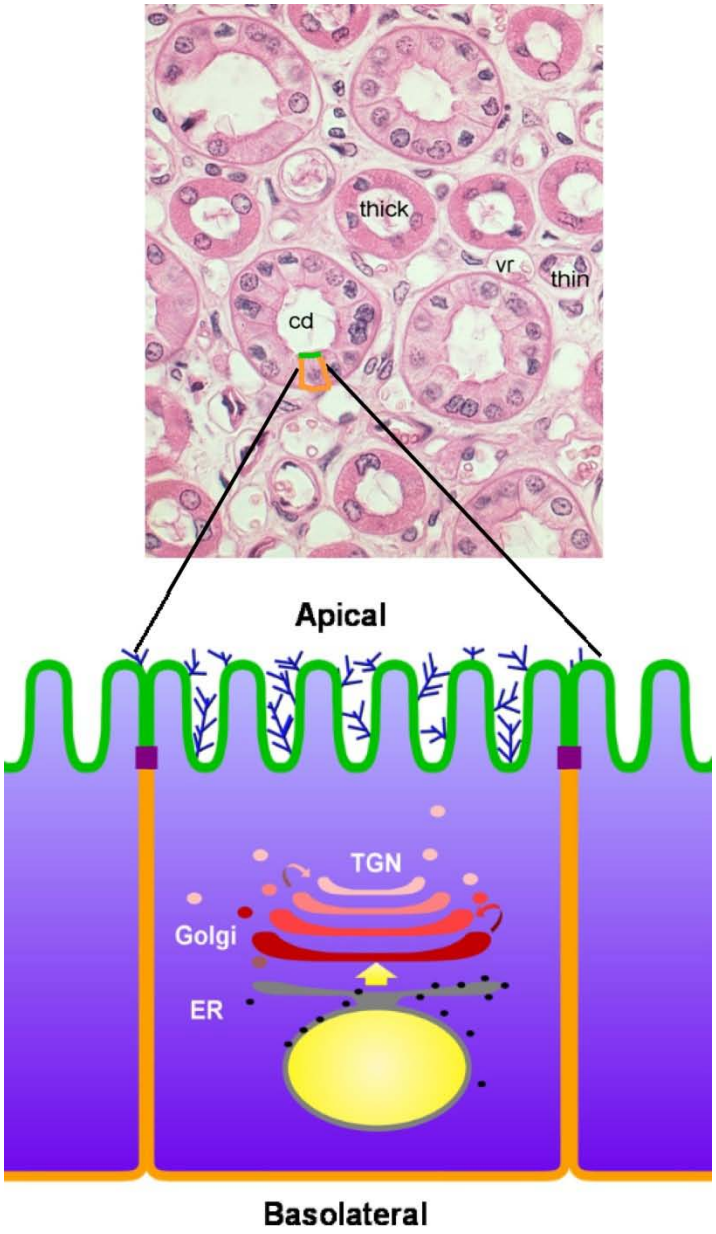

Figure 1.1 Renal tubule cells and a schematic of a polarized epithelial cell. The top panel is a cross section of stained kidney tubules from the Indiana University online histology tutorial. Collecting duct (cd) segments, the thin (descending) and thick (ascending) limbs of the loop of Henle, and a renal vein (vr) are labeled. The bottom panel is a schematic drawing of polarized epithelial cells with the apical (green) and basolateral (orange) surfaces highlighted. Highly glycosylated proteins (blue) decorate the apical surface of these cells forming a protective barrier (glycolcalyx). Also depicted are the nucleus (yellow) ER (grey) studded with ribosomes (black spots), Golgi (red) and *trans*-Golgi network (pink). Arrows depict the direction of movement for biosynthetic traffic from ER to Golgi to cell surface. Note how the cells are arranged in the kidney tubule and how this orientation relates to the polarized cell schematic.

1.2 BIOSYNTHETIC TRAFFIC: THE ENDOPLASMIC RETICULUM AND BEYOND

The biosynthetic sorting of proteins begins immediately upon protein synthesis. Cytosolic proteins are synthesized in the cytoplasm, while nascent proteins containing a hydrophobic signal sequence are recognized by a signal recognition particle (SRP) and shuttled to the endoplasmic reticulum (ER). Coincident with their translation, transmembrane proteins are inserted into the lipid bilayer, while secreted proteins are deposited in the ER lumen. ER-resident chaperones sense the folding state of the newly synthesized protein to determine whether it is fit for delivery. Misfolded proteins are candidates for ER associated degradation (ERAD) via the proteasome (1). During/after co-translational insertion into the ER, proteins can be altered by post-translational modifications and assembled into multisubunit oligomeric protein complexes.

Non-ER resident proteins exit the ER via a mechanism dependent upon the coat protein complex II (COP II) (2). COP II contains the components necessary for formation and release of a vesicle from an ER exit site. COPII consists of Sec 23/24, Sec 13/31, and the small GTPase Sar1. Sec 23/24 form the cargo recognition component of the coat and are recruited to the ER membrane by GTP-bound Sar1. The Sec13/31 complex is subsequently recruited to the ER and forms a cage that promotes vesicle budding. Uncoating of the vesicle occurs when COP II components stimulate the GTPase activity of Sar1, which prepares the vesicle for future fusion events (3). After exiting the ER, proteins transit through the ER-to-Golgi intermediate compartment (ERGIC) before reaching the flattened cisternae of the Golgi complex. The ERGIC is a major site of both anterograde (forward) and retrograde (reverse) traffic between the ER and Golgi and is thought to contribute to both protein folding and quality control (4).

Proteins are further processed in the Golgi complex before packaging and delivery to the plasma membrane. In this compartment proteins can be cleaved by proteases and undergo processing of core N-glycans added to them in the ER. O-glycans are also added and extended in this organelle. After reaching the *trans*-Golgi network (TGN) proteins may be delivered to the plasma membrane by either a direct or indirect pathway. The TGN was long thought to be the primary site at which targeting information within proteins was recognized and translated into delivery instructions. However, recent evidence suggests that some proteins take an "indirect pathway" and traverse endosomal compartments *en route* to the cell surface (5-7). The observation that biosynthetic cargo also intersects with these compartments raises the possibility that sorting of some proteins may occur in endosomes.

Polarized epithelial cells are unique because they require additional sorting to their two distinct membrane domains. Wherever the site of biosynthetic sorting, several signals have been identified that are important for polarized delivery. For basolateral proteins, sorting information is most often found within the cytoplasmic tail of the protein, ideal for recognition by cytoplasmic sorting machinery. Apical sorting signals are more pleomorphic, and include lumenal N- and O-linked carbohydrates, transmembrane domains, lipid anchors, and cytoplasmic peptide motifs. A common sorting mechanism for these diverse signals is difficult to envision; therefore the possibility exists for multiple transport mechanisms. Some data suggest that diverse classes of apical proteins take different pathways to the cell surface (7-9). However, the trafficking machinery involved for each apical pathway has yet to be determined.

1.2.1 Basolateral Sorting in Polarized Epithelial Cells

Basolateral proteins contain short linear peptide motifs that are recognized by the heterotetrameric adaptor protein (AP) complexes. Four AP complexes have been identified: AP-2 for endocytosis, and AP-1, AP-3, and AP-4, which are localized to the TGN and endosomal compartments where they can interact with different signals (10). Basolateral sorting by AP complexes can be conferred by the tyrosine-base tetrapeptide motif YXXΦ or by a dileucine motif, [D/E]XXXL[L/I] among others. These signals not only function as basolateral targeting signals, but can also function as sorting signals for endocytosis and lysosomal delivery (11). Of particular interest, there is an epithelial specific isoform of the AP-1 μ subunit (μ1-B). AP1B complexes containing this subunit are required for efficient sorting of the basolateral proteins transferrin (Tfn) receptor and low-density lipoprotein (LDL) receptor in polarized LLC-PK1 cells (12;13). The ability of AP complexes to interact with both cargo and clathrin allows proteins to be concentrated in clathrin coated vesicles (CCVs), facilitating their delivery to the basolateral surface. Additionally, clathrin itself has been shown to be indispensible for the polarized delivery of basolateral proteins, as demonstrated by their apical missorting upon RNA interference (RNAi) of clathrin (14).

1.2.2 Apical Sorting in Polarized Epithelial Cells

Polarized epithelial cells must be able to recognize and sort the diverse apical sorting signals presented by proteins. Some apical proteins, such as rhodopsin and the renal scavenger receptor megalin contain cytoplasmic peptide motifs that are important for their apical delivery (15;16). Addition of O-linked and N-linked glycosylation is necessary for the apical sorting of proteins

like the neurotrophin receptor, p75 and the sialomucin endolyn, respectively (17;18). Finally, sorting of some apical proteins depends on their association with the lipid bilayer. This is the case for some proteins modified by glycophosphatidylinositol (GPI) anchors (e.g. placental alkaline phosphatase) as well as for some transmembrane proteins that contain apical sorting information within their transmembrane domain, such as influenza hemagglutinin (HA) and neuraminidase (NA) (19;20). It is plausible that receptor-mediated sorting is used for peptide- and glycan-dependent signals; however, this mechanism is less likely for proteins whose apical targeting is lipid-dependent. A potential mechanism for sorting of proteins with lipid-dependent signals is selective inclusion of these proteins into sphingolipid-enriched detergent-resistant microdomains termed lipid rafts.

In 1988 Kai Simons proposed a model stating that the asymmetric lipid distribution of polarized epithelial cells is established by lateral segregation of lipids into microdomains destined for either the apical or basolateral surface (21). Support for this model came in 1992 when Deborah Brown demonstrated that GPI-anchored proteins can be isolated in glycolipid-enriched low density membranes, later termed lipid rafts (22). Lipid rafts have since been reported to play important roles in signal transduction, cytoskeletal organization, pathogen entry, and membrane traffic (23). However, the existence of these domains has been challenged largely due to the inability to visualize them in living cells, to inconsistency in their predicted size, and to the controversial methods used to test for raft function, such as acute cholesterol depletion (24). Lipid raft-association of a given protein is best determined by gradient centrifugation and largely relies on the characteristic insolubility of rafts in non-ionic detergents and their low buoyant density. While the size and dynamics of rafts continue to be elusive, it is clear that a

protein's ability to partition with raft membranes does provide relevant information about the trafficking of that protein (25).

Both GPI-anchored proteins and HA have been demonstrated to associate with lipid-rafts, as assessed by their characteristic insolubility in cold Triton X-100 (26;27). Lipid-rafts have been implicated in sorting of proteins to the apical plasma membrane of polarized epithelial cells (28;29). Lipid-rafts are highly concentrated in sphingolipids with saturated fatty acid side chains and cholesterol allowing them to pack tightly and serve as both signaling and sorting platforms (29;30). The lipid phosphatidylinositol 4,5-bisphosphate (PIP_2) has been proposed to be enriched in rafts, however the presence of PIP_2 in rafts has been challenged (31). Hydrolysis of PIP_2 can contribute to membrane traffic and signaling cascades by producing second messengers such as inositol trisphosphate (IP_3) and diacylglycerol (DAG) (32-34). Given the fact that some apical proteins partition into lipid rafts, it is tempting to speculate that PIP_2 may be important for the traffic of some apical proteins, but a relationship between these phenomenon has not been discovered.

1.3 PHOSPHATIDYLINOSITOLS AND THEIR METABOLISM

PIPs are inner leaflet lipids anchored in the membrane by a diacylglycerol tail, which is linked via a phosphodiester to an inositol sugar headgroup (Figure 1.2) (35). Phosphatidylinositol (PI) is made in the ER and is transported throughout the cell via vesicular transport or by PI transfer proteins (36). The inositol headgroup contains five free hydroxyl groups, and the 3', 4' and 5' positions are differentially phosphorylated to produce a diverse array of PIP species (37). The versatility of PIPs contributes to myriad cellular functions, including cell signaling, regulation of

ion channels, and membrane trafficking. Cells specifically localize PI kinases and PI phosphatases to maintain a compartmentalized distribution of PIPs. Below I discuss the cellular localization of the major PIP species, as well as the enzymes that are responsible for their synthesis and degradation.

1.3.1 Phosphatidylinositol Localization

In order to accurately study the function of PIPs, it is important to know their steady state subcellular localization. This has been difficult as PIPs exist at low abundance and are turned over rapidly. *In vitro*, cellular PIPs can be extracted and analyzed by thin layer chromatography (TLC), high pressure liquid chromatography (HPLC), and mass spectroscopy, but within cells identification is more complicated (38). Much of what is known about the cellular localization of these lipids comes from work employing high specificity probes such as conserved PIP binding domains (to be discussed in Chapter 1.4.2.1). These domains have allowed researchers to determine the steady state intracellular distribution of individual PIP species (Figure 1.3) (39).

PIPs are compartmentalized within cells and their general steady state distributions and basic functions are detailed in the sections to follow (Figure 1.3). Phosphatidylinositol 3-phosphate (PI3P) is localized primarily to endosomes and lysosomes. PI3P is thought to provide organellar identity to early endosomes, but it also participates functionally in tethering, fusion, signaling, and motility (36). In contrast, phosphatidylinositol 4-phosphate (PI4P) is found primarily in the Golgi complex. Golgi-localized PI4P has been shown to participate either directly or indirectly in membrane trafficking through the actions of various effector molecules. PI4P recruits AP-1, lipid-transfer proteins, such as four-phosphatase-adaptor proteins 2 (FAPP2), and other proteins greatly influencing membrane traffic from the Golgi (40).

Most of the cellular PIP_2 is localized at the plasma membrane, where it functions in cellular signaling and endocytosis (36;41). However, evidence suggests that there is also a minor pool PIP_2 in the Golgi complex. First, it has been demonstrated that PIP_2 can be formed on isolated Golgi membranes *in vitro* (42). Second, immunoelectron microscopy studies using the PIP_2 binding domain of phospholipase C (PLC) have detected a small pool of PIP_2 in the Golgi (43). Finally the PIP_2-hydrolyzing enzyme OCRL localizes primarily to the TGN (in addition to coated pits, and endosomes) suggests the availability of substrate at that site (44). While these data hint that a pool of PIP_2 is present in the Golgi, the role of PIP_2 in polarized biosynthetic traffic is uncertain. In chapter 2, I modulate cellular PIP_2 levels in order to determine the consequences on polarized biosynthetic traffic.

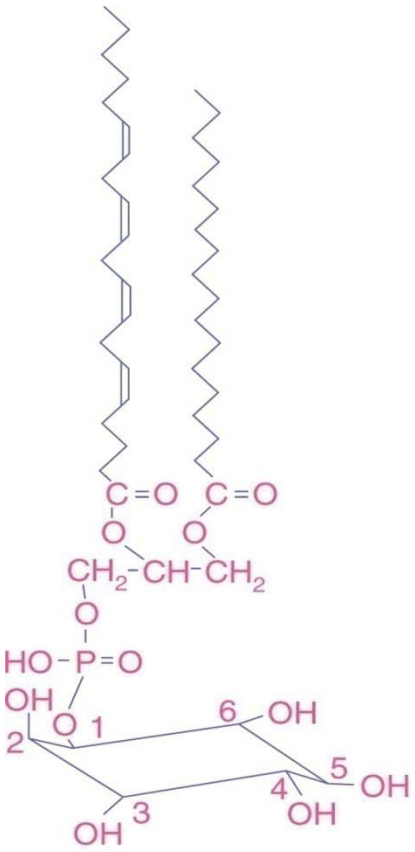

Figure 1.2 Structural diagram of phosphatidylinositol.

The diacylglycerol tail anchors the PIP into the membrane and may contain unsaturated carbons (as depicted). A phosphodiester link connects the tail to the inositol headgroup which can be phosphorylated at the D3, D4, or D5 positions on the inositol ring. Figure taken from Irvine et al. 2002, full reference in text.

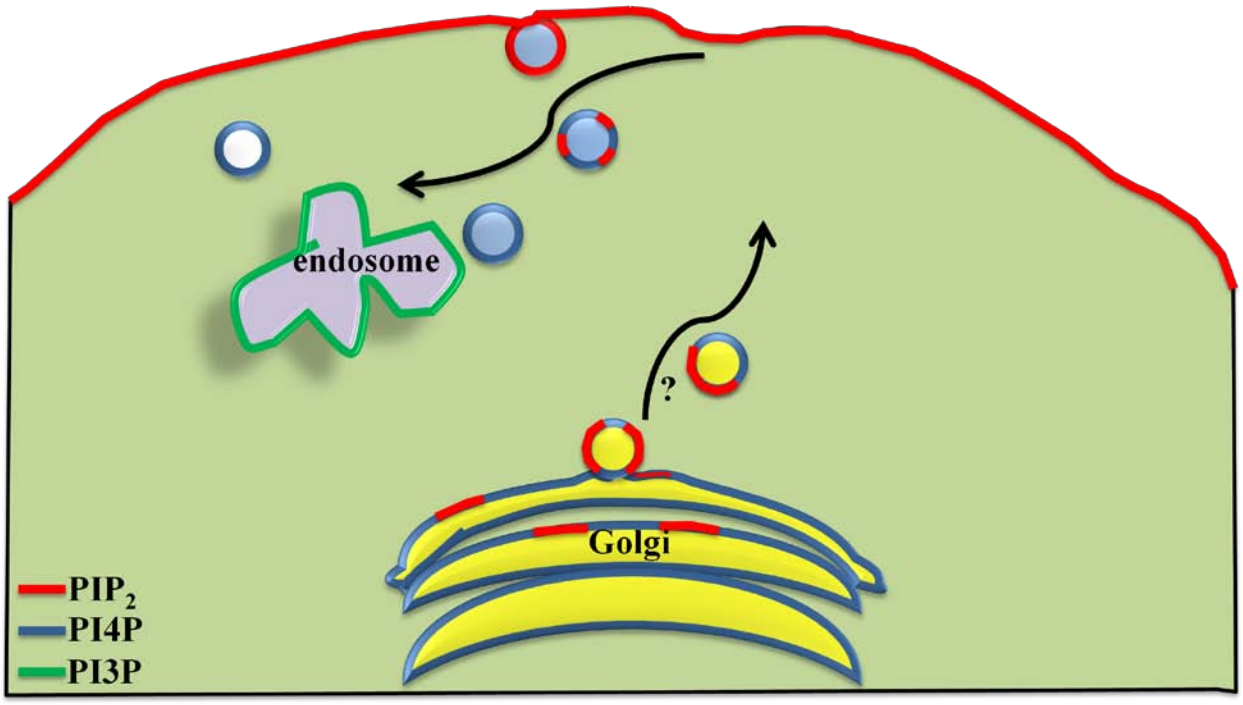

Figure 1.3 Intracellular localization of PIPs.
PIP_2 at the plasma membrane functions in recruitment of endocytic machinery. PI3P is localized mainly to the endosomal system and is important for multivesicular body formation. PI4P is primarily found within the Golgi complex and a small pool of PIP_2 has been localized the Golgi as well. The question mark (?) refers to possible localization of PIP_2 on post-Golgi vesicles and the potential role for actin in their movement (to be discussed later). Figure adapted from De Mateteis et al. 2004, full reference in the text.

1.3.2 Phosphatidylinositol Kinases

Cells maintain their steady state distribution of PIPs by compartmentalizing their synthesis via PI-kinases. PIP-synthesizing enzymes are classified based on the substrate they act upon and the product they generate. These enzymes fall into three general families, phosphatidylinositol 3-kinases (PI3Ks), phosphatidylinositol 4-kinases (PI4Ks), and phosphatidylinositol 5-kinases (PI5Ks). These kinases are present and conserved throughout higher and lower eukaryotes suggeststheir importance to cell physiology (45). Table 1.1 and Figure 1.4 show some of the kinase and phosphatase isoforms, their localization, substrate specificity, and the reactions they catalyze (39).

PI3Ks are a diverse group of enzymes involved in numerous signaling and trafficking processes. PI3Ks were first identified by their interaction with oncoproteins and cellular growth factor receptors (45). More broadly, they are implicated in cell proliferation and survival, membrane ruffling, neurite outgrowth, actin reorganization, and chemotaxis. The PI3K family can be further sub-divided into 3 classes based on structure, substrate specificity, and sensitivity to the fungal metabolite wortmannin (46). In general, these enzymes contain a domain that interacts with a regulatory subunit and a catalytic domain (45). Class I enzymes are the best characterized and are sensitive to wortmannin in the nanomolar range (47). Class I PI3Ks and are composed of a 110kDa catalytic subunit and an 85kDa regulatory subunit to generate PI3P, $PI3,4P_2$, and $PI3,4,5P_3$.

PI4Ks phosphorylate PI to generate PI4P, which can then be used to produce both $PI3,4P_2$ and $PI4,5P_2$. PI4Ks are subdivided into class II and III, each having an alpha and beta isoform. The class II enzymes are approximately 55kDa in size and are insensitive to wortmannin but sensitive to adenosine (48). The class III enzymes are approximately 210 kDa

(α) and 110 kDa (β), and are sensitive to wortmannin in the micromolar range (49). The different PI4K isoforms localize to distinct compartments within the cell, including the ER, Golgi, and endosomes. PI4KIIIβ localizes to the Golgi complex and plays an important role in biosynthetic traffic in polarized epithelial cells. Overexpression of PI4KIIIβ inhibits the rate of TGN-to-apical surface delivery of the lipid raft-associated protein HA. Conversely, overexpression of a kinase dead version of the enzyme stimulates the rate of delivery of HA (50). These data highlight an important role for PIP metabolism within the Golgi. Additionally, since PI4P is a substrate for production of PIP_2 the possibility exists that regulated PIP_2 metabolism in the Golgi may also be important for polarized biosynthetic traffic.

There are three isoforms of the Type I PI5Ks, which phosphorylate PI4P at the D5 position to generate PIP_2 (53). The alpha and beta isoforms were cloned in 1996 in both human and mouse, but they were unfortunately named in reciprocal manner (51;52). I use murine PI5KIα in my studies; therefore I have used the mouse nomenclature throughout. This enzyme is equivalent to human PI5KIβ. The PI5K gamma isoform was cloned in 1998 and found to have two splice variants, a short isoform (PI5KIγ635) and a longer isoform (PI5KIγ661) with a 26 amino acid insertion near the carboxy-terminal end that can target it to focal adhesions (53;54). The central kinase domain of the three isoforms is highly conserved, with greater than 80% sequence identity. *In vitro*, all three isoforms have similar kinetics and are activated by phosphatidic acid (PA), ser/thr dephosphorylation, and small GTPases. However, the isoforms have divergent amino and carboxy terminal regions that are likely to be responsible for isoform specific function and localization (55). PI5Ks are cytosolic proteins, but they can associate with the plasma membrane via two invariant lysine residues within the specificity loop and two highly conserved basic residues in the kinase domain (55). However, stimulation by GTPases and

binding to specific partners has also been shown to enhance their membrane association and localization (36;56-58). In nonpolarized cells all three isoforms are found on the plasma membrane, but the reason for this redundancy is unknown (59). The functions and localization of PI5K isoforms in polarized epithelial cells have been largely unexplored. However, some evidence suggests that PI5K isoforms localize to different surfaces in polarized epithelial cells where they may regulate functionally distinct pools of PIP_2.

Table 1.1 Activity and localization of PI-kinases and -phosphatases.

PI-kinase	Localization	Substrate		PI-phosphatase	Localization	Substrate
PI3K P110	PM, N	$PI4,5P_2$		PTEN (3-pptase)	PM, GC, N	$PI3,4,5P_3$ $PI3,5P_2$
PI4KIIα	GC, E	PI		Type I and II 4-pptase	E, PM	$PI3,4P_2$
PI4KIIβ	PM, GC	PI				
PI4KIIIα	GC, ER	PI		OCRL (5-pptase)	CCV,GC,E	$PI4,5P_2$
PI4KIIIβ	GC, N	PI		Synaptojanin 1	SV, MI	$PI4,5P_2$
PI5Kα,β,γ	PM	PI4P		Inpp5b	ND	$PI4,5P_2$

The known localization and *in vivo* substrate specificity for the discussed PI-kinases and PI-phosphatases (pptase). Plasma membrane (PM), Golgi complex (GC), endosomes (E), endoplasmic reticulum (ER), mitochondria (MI), clathrin coated vesicle (CCV), synaptic vesicle (SV), nucleus (N), and not determined (ND). Table adapted from De Matteis et al. 2004, full reference in text.

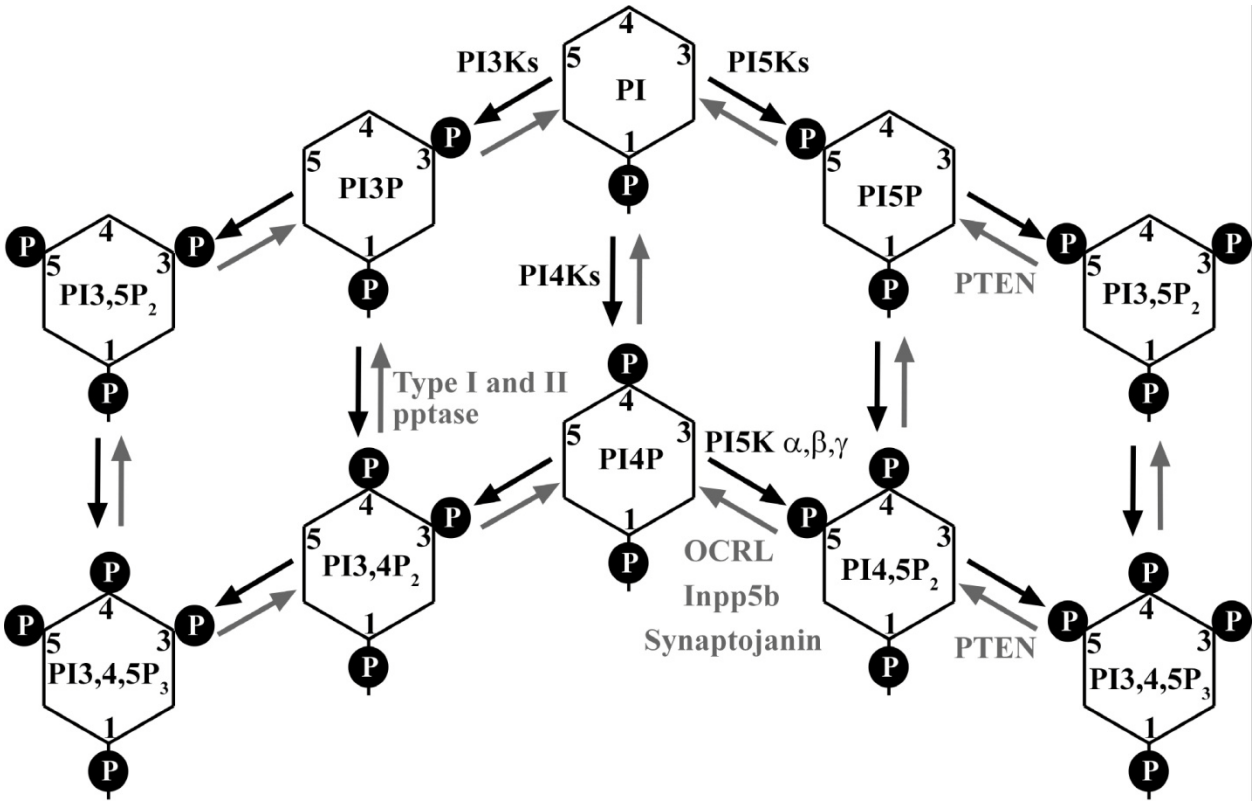

Figure 1.4 Summary of known reactions in PIP metabolism and the some of the relevant enzymes.

This figure is a graphic representation of the known PIP metabolism reactions within cells. Depicted is the inositol ring and the location of the phosphates for each of the different PIP species. The relevant enzymes discussed are labeled above or below the reaction arrows depending on the particular reaction they catalyze. Figure adapted from De Matteis et al. 2004, full reference in text.

1.3.3 Phosphatidylinositol Phosphatases

The regulation of cellular PIP levels is controlled not only by their synthesis, but by thier phosphatase-mediated degradation as well. Naming of the PIP-phosphatases (pptases) does not follow the logical convention used for the naming of other enzymes and fails to reveal any information about their activity or specificity. PIP-pptases dephosphorylate the inositol ring at the 3', 4' or 5' positions to convert PIPs. In general, these enzymes are divided into three families based upon the position of the inositol ring on which they act.

The family of 3-pptases dephosphorylate PI3P, PI3,4P_2, PI3,5P_2, and PI3,4,5P_3 at the 3-position and are important for regulating growth factor signaling. These enzymes can be found in the nucleus, Golgi, ER, and the plasma membrane (Table 1.1). Phosphatase and tensin homologue (PTEN) is a ubiquitously expressed 3-pptase that is a known tumor suppressor. PTEN dephosphorylates PI3,4,5P_3 (PIP_3) generating PIP_2 which halts PI3K signaling. Loss of PTEN leads to increased PIP_3 at the plasma membrane and sustained activation of a signaling kinase, Akt/PKB. Akt/PKB can influence a number of signaling pathways leading to cell growth and proliferation, so sustained activation ultimately causes protection from apoptosis (60).

Inositol polyphosphate 4-pptases are categorized into types I and II which share 37% sequence identity (61). The type I enzymes have been shown to participate in cell growth regulation by converting PI3,4P_2 to PI3P in the endosomal system (62). Recently, Ungewickell et al. identified and characterized type I and II 4-pptases that act on PIP_2, are ubiquitously expressed, and localize to endosomes and lysosomes (63). Overexpression of either enzyme increased epidermal growth factor-(EGF)-receptor degradation following EGF stimulation. Additionally, Zou et al. recently found a role for the type I PIP_2 4-pptase in stimulating p53-dependent apoptosis in cells following DNA damage (64).

The inositol polyphosphate 5-pptase (Inpp5p) family is well described and includes 10 members (Figure 1.5) (65). These enzymes dephosphorylate PIP_2 at the 5' position of the inositol ring to produce PI4P. They contain a central catalytic domain flanked by various protein-protein interaction domains (66). Below I discuss three of these enzymes and their roles in membrane traffic.

Synaptojanin is the prototypical Inpp5p involved in clathrin-mediated endocytosis. There are two isoforms of this enzyme: synaptojanin 1, which is primarily expressed in neuronal tissue, and synaptojanin 2, which is ubiquitously expressed (67). Synaptojanin 1 functions at nerve terminals and participates in synaptic vesicle endocytosis. At the synapse, PIP_2 helps recruit the clathrin adaptor AP-2, and other accessory proteins resulting in the formation and budding of clathrin coated vesicles. After endocytosis, synaptojanin 1 dephosphorylates PIP_2 causing clathrin to dissociate from vesicles (67).

Inpp5b is a PIP_2 5-pptase with a central 5-phosphatase domain and a carboxy-terminal Rho GTPase-activating protein (GAP)-like domain (44). The functional significance of the RhoGAP domain is unknown as it lacks a critical catalytic residue GAP activity (68). PIP_2 is the preferred substrate for Inpp5b, but it also displays some activity toward PIP_3, inositol (1,4,5) trisphosphate $(IP)_3$ and I(1,3,4,5) tetrakisphosphate $(IP)_4$ (44). Inpp5b localizes to both the ER-to-Golgi intermediate compartment (ERGIC) and endosomes through interaction with various RabGTPases (69). A knockout mouse model of Inpp5b only exhibited male sterility, revealing little about its functions (70). However, consistent with its localization to the early secretory pathway, a group has recently reported a role for Inpp5b in membrane traffic at the ERGIC (70).

OCRL is the protein encoded by the *OCRL1* gene that is mutated or absent in Lowe syndrome, a rare X-linked disorder (to be discussed in Chapter 1.5.1). OCRL is highly

homologous to Inpp5b, with which it shares 45% amino acid sequence identity, a similar domain organization, and substrate specificity. There are two splice variants of OCRL: the longer isoform OCRLa is ubiquitously expressed albeit at lower levels than the shorter form OCRLb. OCRLb is expressed in all tissues except brain, where OCRLa is most abundant (71). OCRL is localized to the TGN, cytoplasmic CCVs, endosomes, and to clathrin coated pits (CCPs) (72-76). Localization to the Golgi and endosomes is dependent upon OCRL binding to Rabs, while its presence at CCPs is due to the a conserved C-terminal clathrin binding motif (44;77). OCRL binds to Rac1 through its RhoGAP domain and translocates to the plasma membrane upon growth factor activation of Rac1 (78;79). OCRL's activity as a PIP_2 5- pptase and its localization led to the suggestion that OCRL participates in clathrin-mediated trafficking at the TGN and endosome interface. Indeed, Choudhury et al. demonstrated that expression of a pptase domain-deficient version of OCRL inhibited the trafficking of Shiga toxin from endosomes to the TGN. Moreover, siRNA-mediated silencing OCRL caused a partial redistribution of the cation-independent mannose 6-phosphate receptor (CI-MPR) from the TGN to endosomes (75). Given its intracellular distribution, it is possible that OCRL may also regulate biosynthetic traffic at either the TGN on endosomes, but this possibility has not been tested (5;80). In chapter 2, I use siRNA to silence OCRL in MDCK cells to determine whether OCRL is important for biosynthetic traffic.

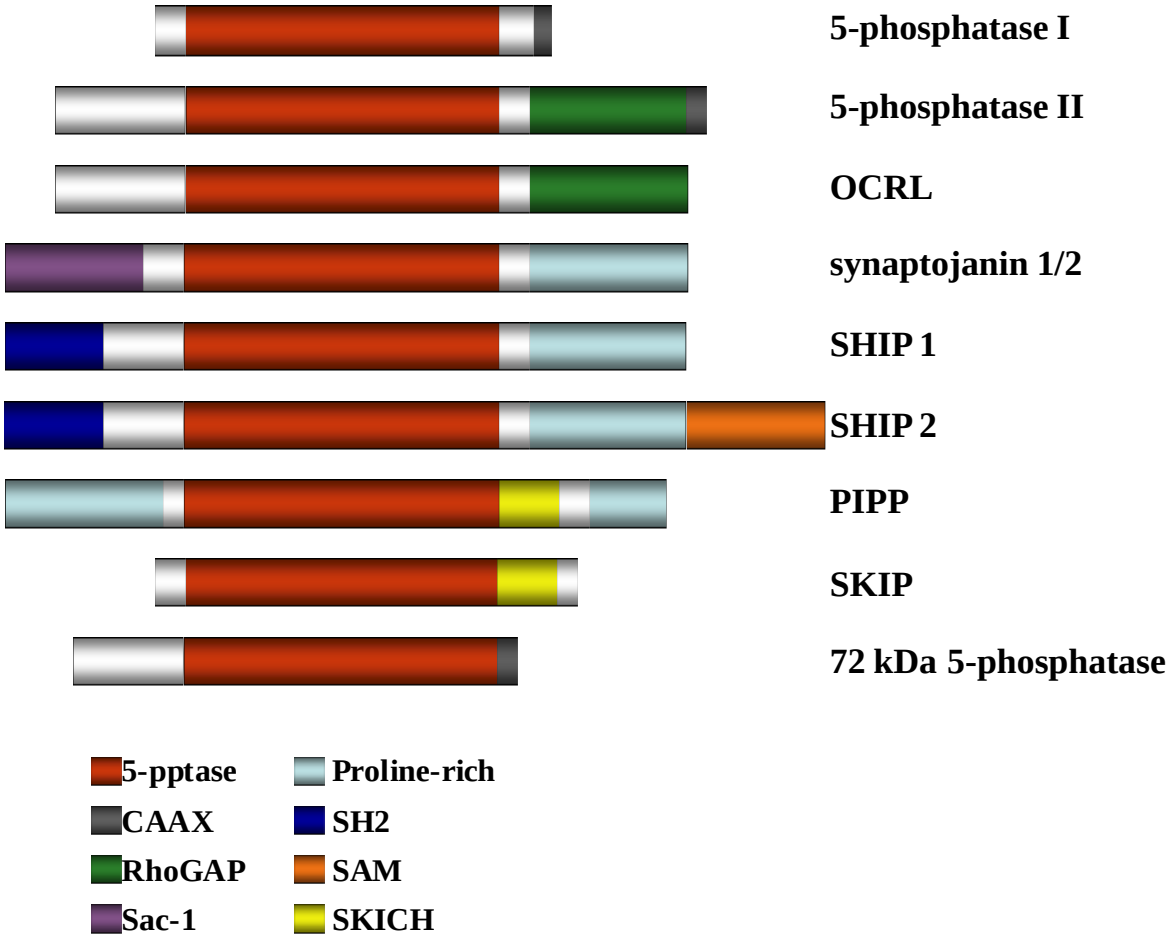

Figure 1.5 Domain organization of the known mammalian 5-phosphatases.

Each of the 10 mammalian 5-pptases are drawn to indicate their overall domain organization. All of the enzymes contain a central catalytic domain. The legend reveals the identity of each domain by color, the white areas represents segments without characterized domains. Inpp5b is listed in this figure as 5-phosphatase II. Proline-rich inositol polyphosphatase 5-phosphatase (PIPP) and SKIP (a skeletal muscle and kidney enriched inositol polyphosphate 5-phosphatase) contain a unique C-terminal SKICH domain that is important for their membrane localization. Synaptojanin 1/2 contain an extra N-terminal catalytic domain (Sac-1) that has very broad specificity toward PI3P, PI4P and $PI(3,5P)_2$. SHIP2 contains a sterile α motif (SAM) which is a protein interaction motif, along with SH2 domains and praline-rich domains. Inpp5b and OCRL both contain C-terminal RhoGAP-like domains, whose true function is unknown as they lack a critical residue for GAP activity. This figure was modified from Astle et al. 2007, full reference in text.

1.4 PHOSPHATIDYLINOSITOLS AND THEIR FUNCTIONS

1.4.1 Phosphatidylinositols and Signaling

Synthesis and degradation of PIPs plays an important role in signal transduction from the plasma membrane and can influence the temporal characteristics of a signal or the type of signaling cascade. Cleavage of PIP by phosphatases can terminate a signal. Alternatively, ligand binding to a G-protein coupled receptor (GPCR) can result in activation of PLC and the formation of the second messengers IP_3 and DAG (81). IP_3 can diffuse throughout the cytosol until it encounters an IP_3 receptor leading to rapid release of calcium from intracellular stores such as the ER (82). Signaling pathways that increase cytosolic calcium are tightly regulated and cells are quick to restore calcium levels to their normal steady state (83). Released calcium binds to and modulates the activities of many cellular proteins making it a potent signaling molecule. Membrane-embedded DAG activates PKC which phosphorylates many cellular targets influencing proliferation, differentiation, and survival through pathways such as MAP kinase and nuclear factor (NF)κB. Moreover, DAG has also been shown to participate in cell signaling via non-PKC-dependent DAG receptors (84).

Alternatively, phosphorylation of PIP_2 to generate PIP_3 can terminate PIP_2 signaling and give rise to growth factor-like signaling via the PI3K/Akt pathway. In general, response to growth factors leads to activation of receptor tyrosine kinases (RTKs) and increased PIP_3 production. The formation of PIP_3 recruits the ser/thr kinase Akt/PKB to the plasma membrane where it is subsequently phosphorylated by mammalian target of Rapamycin (mTOR) and phosphoinositide-dependent kinase 1 (PDK1) (85). Once activated, Akt can affect numerous cellular targets to induce downstream effects on growth and metabolism.

1.4.2 Phosphatidylinositols in Membrane Traffic

PIPs can influence membrane traffic by recruiting proteins to the inner leaflet of cell membranes, affecting membrane curvature and modulating the actin cytoskeleton. These three mechanisms aid in vesicle formation or propulsion driving exocytosis, endocytosis, and biosynthetic transport. The ability of the cell to compartmentalize PIPs translates into highly regulated recruitment of effector proteins to a particular site. This specificity combined with the tightly controlled synthesis and degradation of PIPs allows for spatio-temporal regulation of PIP-mediated processes. In the next three sections, I discuss various domains that enable proteins to bind selectively to PIPs at specific intracellular sites, and the role of these domains in membrane traffic and in the modulation of actin cytoskeletal dynamics.

1.4.2.1 Phosphatidylinositol Binding Domains

The ability of proteins to transiently associate with the cytosolic aspect of membranes is important for many cellular processes including signaling, maintaining cell structure, and membrane trafficking (86). Much of this binding is mediated by interaction to PIPs through diverse mechanisms including sensing of acidic phospholipids, basic motifs, or conserved PIP-specific binding domains. There are 10 distinct PIP binding domains that fall into two different groups based on their overall specificity (86). Generally, lower specificity domains can impart temporal characteristics to recruitment, but lack the spatial control of the more highly specific domains. The higher specificity binding domains have been successfully used as probes to study the steady state localization of individual PIP species within cells (87;88). Below I briefly discuss some of the major PI-binding domains including their general structures and affinities for PIPs.

The Fab1, YOTB, Vac1, EEA1 (FYVE) domain is a 60-70 amino acid zinc finger domain that contains a conserved basic motif that allows it to interact with PI3P (89-91). FYVE domain-containing proteins bind specifically to PI3P, which is primarily found in the endosomal system (89). A prototypical FYVE domain-containing protein is early endosome antigen 1 (EEA1), which is important for endosome fusion. Dimerization of FYVE domain-containing proteins through a coiled-coil domains has been shown to increase the efficiency of PI3P-binding (92;93).

The phox (PX) domain was first identified as a part of the NADPH oxidase complex and was later determined to bind to PI3P (94;95). PX domains are approximately 130 amino acids in length and in addition to binding PI3P they also bind to $PI3,4P_2$ or PIP_2 (96;97). PX domains are found in all sorting nexins (SNX), a diverse group of proteins important for several membrane trafficking steps (98). These domains also require some degree of dimerization or interaction with an oligomeric complex to increase their efficiency for PI3P binding (99;100).

Pleckstrin homology (PH) domains are approximately 100 amino acid motifs originally described in the protein pleckstrin, and were shown to bind phosphoinositides (101). The PH domain of phospholipase $C\delta_1$ (PLCδ) was demonstrated to bind specifically to PIP_2 and has been used as a probe to study PIP_2 (102;103). The crystal structure of the PLCδ-PH reveals seven β-strands and one α-helix and a deep pocket containing charged residues that are important for PIP_2 binding (104).

A key mechanism by which PIPs act as markers of organelle identity or to recruit proteins is via coincidence detection. The principle behind coincidence detection is that low affinity interactions of a protein with PIPs can be enhanced by binding to a second signal, and that this dual interaction increases the strength and specificity of the interaction. The second

signal can be another lipid, a protein, or a curved membrane domain (105). For example, the recruitment of FAPPs to the Golgi complex requires binding to both PI4P and the small GTPase Arf1 (106). Also, SNXs use coincidence detection to recognize PI3P via a PX domain and highly curved endosomal tubules through their Bin/Amphiphysin/Rvs domain (107). Coincidence detection, through combination of signals, increases the number of ways PIPs can be engaged by cytoplasmic proteins to ensure spatial control over cellular processes.

1.4.2.2 Phosphatidylinositols in Exocytosis and Endocytosis

The formation of vesicles during endocytosis and the fusion of two membranes during exocytosis rely on a significant contribution by the phospholipids in both membranes. Phosphatidylinositols, particularly PIP_2, have been demonstrated to be important in both pathways to regulate recruitment of adaptor proteins and to serve as a biochemical marker of membrane identity.

The events leading up to exocytosis are tethering, docking, priming, and fusion (108). The overall goal is to bring the two membranes within close proximity of each other so that the vesicle may either fuse or partially fuse to release its contents. The core machinery responsible for the fusion event is the soluble N-ethylmaleimide-sensitive factor attachment protein receptor (SNARE) proteins. Once a vesicle is tethered, v-SNARES and t-SNARES interact to bring the vesicle into close proximity with the membrane (109). Increases in Ca^{2+} are sensed by synaptotagmin which is thought to induce final fusion of the complex by helping to overcome the energy barrier of fusion (110). Synaptotagmin has a single transmembrane domain and it interacts with PIP_2 in a Ca^{2+}-dependent fashion to stimulate vesicle fusion in conjunction with increases in Ca^{2+} (36;111;112). PIP_2 may also play a role in marking the plasma membrane as a site for fusion and in cooperating with t- and v-SNARE pairing (36;109). Consistent with this,

PIP_2 forms clusters on the plasma membrane near areas of high syntaxin-(t-SNARE) density that contain docked vesicles. Increases in PIP_2 show a positive correlation with the number of syntaxin clusters and the magnitude of the Ca^{2+}-dependent exocytic response (113-116). In polarized epithelial cells, fusion of vesicles with the basolateral surface may be mediated by interactions with the exocyst, a known tethering complex, which has been shown to interact with PIP_2 (117).

PIP_2 also acts as a recruitment factor for endocytic proteins, and is important for all forms of endocytosis (36). All of the AP complexes and other clathrin adaptors, such as AP180 and epsin, bind to PIP_2 at the plasma membrane (67;118;119). Assembly of CCVs requires the coordinated action of protein-lipid and protein-protein interactions. Briefly, PIP_2 at the plasma membrane can recruit the AP-2 complex, which interacts with cargo containing tyrosine- or dileucine-based endocytic signals. Subsequently, clathrin triskelia assemble onto the AP-2-cargo complex to form a clathrin lattice (120). This assembly is partially responsible for the invagination of the membrane. The vesicle is ultimately severed from the membrane by the PIP_2-interacting GTPase, dynamin (121;122). In addition to these classical players in clathrin-mediated endocytosis, an additional family of adaptors termed clathrin-associated sorting proteins (CLASPs) bind to PIP_2, APs, and to other cargo endocytic signals, thus increasing the range of cargo recruited to coated pits (123). The actin cytoskeleton is also important for efficient CCV endocytosis (124). A potent stimulator of actin polymerization, neuronal Wiskott-Aldrich syndrome protein (N-WASP) is recruited by PIP_2 and is thought to help provide the force to propel detached CCVs into the cytosol (125). Once endocytosis occurs, pptases such as synaptojanin quickly dephosphorylate PIP_2 to PI4P allowing the coat components to dissociate so they may be recycled for another round of endocytosis (126). Increases in PIP_2 at the plasma

membrane have been suggested as a mechanism to modulate the rate/efficiency of clathrin mediated endocytosis presumably by increasing recruitment of proteins that mediate/regulate endocytosis. This phenomenon has been observed in nonpolarized cells in which overexpression of PI5Ks stimulates the rate of Tfn receptor endocytosis and in IgA endocytosis polarized epithelial cells (59;127).

1.4.2.3 Phosphatidylinositols in Biosynthetic Membrane Traffic

PIPs are important for the recruitment of cytoplasmic machinery for cargo selection, vesicle formation, and the movement of proteins though the biosynthetic pathway (128;129). Consistent with this, exit from the ER is dependent on COP II, which consists of Sec 23/24, Sec 13/31, and the small GTPase Sar1. In studies using liposomes, the recruitment of Sec 23/24 was shown to depend on acidic phospholipids, such as phosphatidic acid (PA) and PIP_2. Phospholipase D (PLD) activity has also been shown to be important for ER exit (130). PLD cleaves an abundant membrane constituent, phosphatidylcholine (PC) into PA, a known cofactor/activator of many PIP kinases (131). Recently, Blumental-Perry et al. showed that PI4P is locally concentrated at ER exit sites. Sar1 was shown to transiently stimulate PI4P and PIP_2 formation on ER membranes. By expressing PIP-binding domains to sequester PIPs, they demonstrated that both PI4P and PIP_2 were necessary for efficient ER export (132). Together these studies highlight the importance of PIPs in the binding of coat proteins to the ER and the formation of ER vesicles.

The Golgi complex contains the majority of cellular PI4P. As described earlier, PI4P in the Golgi is generated by the action of PI4Ks. Weixel et al. demonstrated that two different PI4Ks, PI4KIIα and PI4KIIIβ localize to different subdomains of the Golgi and can regulate distinct pools of PI4P (49). One mechanism by which PIPs may affect the Golgi is through alterations in membrane curvature. The flattened cisternae of the Golgi have highly curved

surfaces at the ends of each stack, which may rely on PI4P to maintain their structure and/or stimulate vesicle budding from these sites. In support of this, studies using the expression of catalytically-inactive forms of PI4Ks or siRNA knockdown have revealed that PI4P is important for Golgi structure and biosynthetic traffic from the TGN (50;133;134). In addition, Golgi reformation is markedly delayed in cells expressing a dominant-negative PI4K, indicating a possible requirement for PI4P in Golgi biogenesis.

In addition to direct effects on membrane curvature PI4P may influence the Golgi through the recruitment of effectors. Indeed, several effector proteins bind to PI4P in the Golgi including epsinR, AP-1, four-phosphatase-adaptor proteins (FAPPs), and oxysterol binding protein (OSBP) (106;133;135;136). Synthesis of PI4P at the Golgi may be important for continued recruitment of effectors in a positive feedback loop that modulates Golgi function. In support of this, FAPP binds to PI4P and ADP-ribosylation factor 1 (Arf1) at Golgi exit sites. Knockdown or displacement of FAPPs with a competing PH domain disrupts Golgi to plasma membrane transport (106). The small GTPase Arf1 is important for vesicle budding because it recruits numerous effectors and PI4KIIIβ to Golgi membranes (137;138). Arf1 is also responsible for recruiting coat complexes to the Golgi, including the aforementioned AP-1, COP I for retrograde transport, and the Golgi-associated, γ-adaptin ear-containing, Arf binding (GGA) proteins for Golgi-to-endosome transport (139). These data represent a pathway of Arf activation leading to increased PI4P synthesis that allows the recruitment of factors such as FAPPs to influence membrane traffic.

A positive feedback loop involving Arf1 has also been proposed to influence PIP_2 in the Golgi. Arf1 can stimulate the activity of PLD, resulting in increased cleavage of PC to PA, which is a cofactor/activator of PI5K. PI5K could increase Golgi PIP_2 by utilizing PI4P as a

substrate. PIP_2 has also been shown to stimulate Arf activity which would in theory lead to a positive feedback loop for increasing PIP_2 at the Golgi (58). While there is no direct evidence for the existence of this pathway, the circumstantial evidence is strong. Arf1 can also recruit PI5K to Golgi membranes to generate PIP_2 (42). Although no PI5K isoform has been localized to the Golgi, the presence of OCRL in the TGN makes a strong case for regulated PIP_2 metabolism in the Golgi. Several studies have alluded to the possible roles of PIP_2 in biosynthetic traffic at the Golgi, but these have not been directly tested. It is possible that PIP_2 could help regulate Golgi traffic by recruiting coat complexes, specific sorting receptors, or proteins that can modulate actin cytoskeletal dynamics. In chapter 3, I explore the role of PIP_2 and actin in biosynthetic traffic by modulating PIP_2 levels or the activity of the PIP_2-dependent stimulator of actin polymerization N-WASP.

1.4.2.4 PIP-mediated Modulation of Actin

Actin plays an important role in many cellular processes including maintenance of cell shape, cell motility, and vesicular traffic. Actin is a small globular protein (~42 kDa) that is highly conserved throughout higher and lower eukaryotes. In its monomeric form actin is referred to as globular or G-actin. Actin monomers have a binding site for ATP and they will dimerize upon ATP binding to create a "nucleation site" for the polymerization of additional actin monomers, which assemble into an actin filament (F-actin) with increasing efficiency. Growth of the actin filament occurs at what is termed the barbed end (plus end), while depolymerization occurs as the slower growing pointed end (minus end). A number of actin accessory proteins exist to modify actin filaments by crosslinking, capping, or severing actin filaments. Actin polymerization can be regulated by GTPases, nucleation promoting factors (NPFs), or by PIPs (140-142).

PIPs can modulate actin polymerization through recruitment of proteins that directly bind to actin. For example, the recruitment and activation of N-WASP by PIP_2 influences vesicle movement via actin-mediated propulsion. N-WASP is a ubiquitously expressed neuronally-enriched member of the Wiskott-Aldrich syndrome protein (WASP)/WASP family verprolin homologues (WAVE) family of proteins. Wiskott-Aldrich syndrome (WAS) is a rare X-linked disorder caused by mutations in the gene for WASP and symptoms include bloody diarrhea, eczema, and greater susceptibility to infections (143;144). WASP is only expressed in hematopoietic cells and WAS fits into a group of cytoskeletal diseases including hereditary spherocytosis, hereditary elliptocytosis, and Duchenne muscular dystrophy because WASP is part of a cytoskeletal complex (145). A known peculiarity of these diseases is the presence of surface proteins with abnormal glycosylation or deficiencies in surface glycoproteins, implicating the requirement for a normal cytoskeleton in order to properly traffic proteins to the cell surface (145). Since N-WASP is ubiquitously expressed it may have roles in protein trafficking in all cell types. Below I discuss the functions of N-WASP-Arp2/3 complex and how it is regulated by PIP_2 and accessory proteins.

1.4.2.5 N-WASP Function in Membrane Traffic

N-WASP participates in cellular functions from cell motility to vesicular traffic. The N-WASP-knockout mouse embryo survives past gastrulation, but severe developmental delays are evident followed by death on or before embryonic day 12 (146). This highlights the importance of N-WASP in development, maintenance of cell shape, and organ integrity.

N-WASP is well known for its role in the actin-based motility of pathogens such as *Shigella flexneri*, but it is also important for the movement of organelles and vesicles. Some bacteria and virus have evolved mechanisms to highjack the cellular machinery controlling actin

polymerization in order to enhance their spread (147;148). *S. flexneri* possesses a protein, VirG, that recruits host cell N-WASP to the tip of the bacterium allowing it to exhibit actin-based motility (149). By contrast, *Listeria monocytogenes* uses a protein, ActA, that mimics the function of N-WASP giving it the capability to rocket around the host cell and into adjacent cells (150). In either case, rocketing is mediated by the localized and highly efficient formation of branched actin filaments at the surface of the pathogen. It is apparent that N-WASP is important for the movement of intracellular bacteria, but at the time of these studies its role in vesicular traffic was not clear.

N-WASP participates in endocytic traffic by interacting with endocytic complexes and helping to promote vesicle scission. N-WASP was first identified by Miki et al. in 1996 as an actin-depolymerizing protein that transiently associates with activated epidermal growth factor (EGF) receptor (151). The first link between N-WASP and endocytic traffic came from the discovery of an interaction between N-WASP and syntaptic dynamin-associated protein I (syndapin I). Syndapin I interacts with dynamin I, synaptojanin, and N-WASP providing evidence that N-WASP may influence endocytosis (152). Direct evidence demonstrating that N-WASP is involved in endocytosis was observed in 2002. Kessels et al. disrupted N-WASP function or localization and found a profound negative effect on receptor-mediated endocytosis (153). It was later shown that N-WASP is recruited to CCVs during the late stages of vesicle formation and disrupting recruitment causes an accumulation of CCVs at the plasma membrane (154;155). Together, these data indicate that N-WASP is recruited to the site of clathrin-mediated endocytosis and is important for mediating vesicle scission or movement away from the membrane.

N-WASP has also been proposed to function in vesicle propulsion at the Golgi. In 1999, a group studying vaccinia virus actin-based motility found that “little actin tails” (LATs) were associated with clathrin, but not with an endocytic protein (transferrin receptor) (156). They interpreted their data to mean that these structures originated from the Golgi complex. Interestingly, the outer membrane of vaccinia virus derives from TGN membrane during the enveloping process (157). Vaccinia has since been shown to recruit N-WASP, which is responsible for its actin-based motility (146). In 2000, Rozelle et al. showed that actin comets whose formation was stimulated by PI5K overexpression were enriched in proteins that associate with lipid-rafts. They examined the number of comets associated with HA or VSV-G at time points between 2 and 6 hours post-infection and found comets to be more enriched in HA than VSV-G (158). While these data support a role for N-WASP comets in biosynthetic traffic, it cannot be determined from their studies whether actin comets affect the kinetics or some other aspects of the transport of these proteins. Therefore, prior to my research, the actual contribution of N-WASP in vesicular traffic from the Golgi remains unclear. In chapter 2, I explore the role of N-WASP in TGN-to-plasma membrane delivery of raft- and non-raft-associated proteins by perturbing N-WASP function.

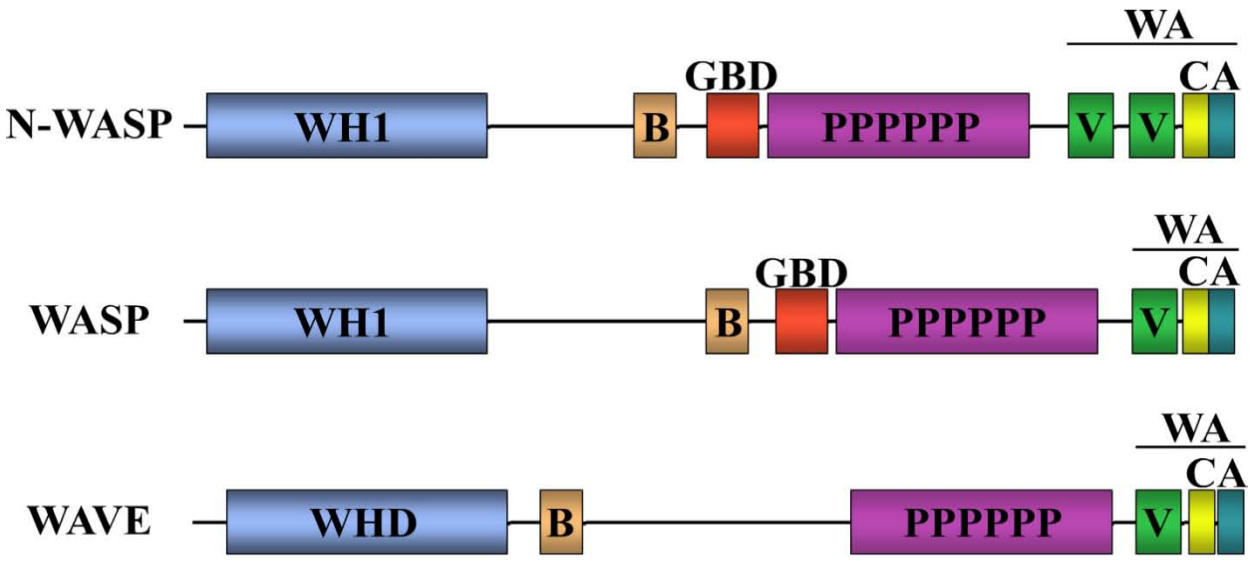

Figure 1.6 Domain organization of N-WASP, WASP and WAVE. The various domains of N-WASP, WASP and WAVE are indicated starting with the highly conserved N-terminal WASP homology domain (WHD) which is highly conserved and is important for interaction with WASP-interacting proteins (WIPs). The B motif is a highly basic region that mediates interaction with PIP_2. WASP and N-WASP contain a GTPase binding domain (GBD) causing them to interact with GTPases like Cdc42. The poly-proline (P) domain of each is important for protein-protein interactions. The verprolin homology (V) domain, which binds to actin monomers, the cofilin homology (C), and the central acidic (A) domain, which binds to Arp2/3, collectively make up the highly conserved functional WA domain. This figure was adapted from Stradal et al. 2004, full reference in text.

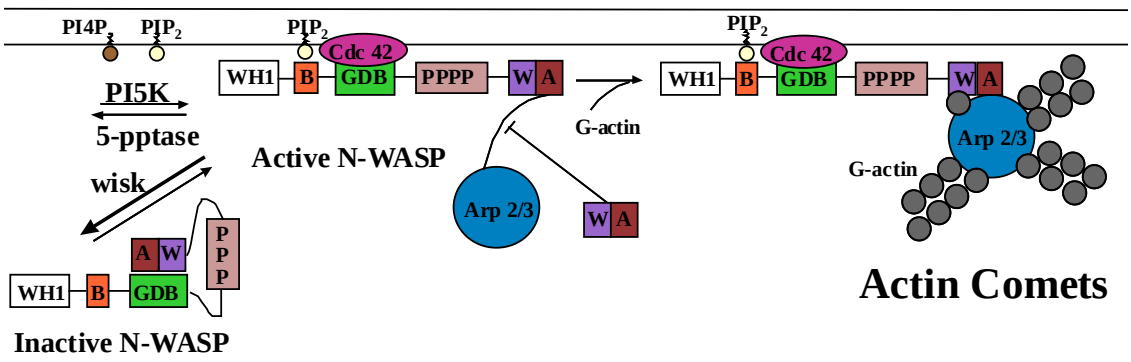

Figure 1.7 Model for N-WASP activation and actin comet formation. N-WASP assumes an autoinhibitory conformation and remains inactive in the cytoplasm. Following PIP_2 synthesis, N-WASP is recruited to the membrane through an interaction between the B motif and PIP_2. Cdc42 can bind to the GBD domain to help activate N-WASP, which can then recruit Arp2/3 leading to branched actin filament formation or actin comet formation. Wiskostatin (wisk) can stabilize the autoinhibitory conformation locking N-WASP in an inactive state or the WA domain can be used to inhibit the association of Arp2/3 with N-WASP. Figure adapted from Bompard et al. 2004, full reference in text.

1.4.2.6 N-WASP-Arp2/3 and its Regulation

N-WASP is regulated in a number of ways to ensure exquisite spatial and temporal control of N-WASP-dependent functions. The V,C, and A domains are collectively termed the VCA region (WA domain), where the V (W) domain interacts with actin monomers and the CA (A) domain interact with the Arp2/3 complex (159-162) (Figure 1.6). The Arp2/3 complex binds to an existing actin filament and uses itself as a nucleation site for the polymerization of a new actin filament at a 70º angle to the existing actin filament (163;164). N-WASP is normally folded in an autoinhibitory conformation in which the WA domain binds to the GBD domain. This interaction prevents the recruitment of the Arp2/3 complex to N-WASP, thereby inhibiting actin polymerization (165). Autoinhibition is relieved through dual activation of N-WASP by Cdc42 and PIP_2 (160;161;165-167). The lysine-rich B motif of N-WASP binds to PIP_2, while GTP-bound Cdc42 binds to the GBD, inducing a change in conformation leading to N-WASP activation at the target membrane (168;169). It has also been shown that increases in local PIP_2 concentration can recruit, unfold, and activate N-WASP even in the absence of Cdc42 (158;170). N-WASP binds numerous SH3 domain-containing proteins through its proline-rich region allowing it to be recruited to specific sites (171-173). Phosphorylation of N-WASP's GDB domain by Src-family tyrosine kinases plays an important role in N-WASP's sustained activation presumably by relieving autoinhibition (174-176). To support this, mutations in key N-WASP tyrosine residues that mimic phosphorylation result in constitutive activation of N-WASP (168).

Several approaches have been used to inhibit N-WASP function. The WA domain of N-WASP or other WAVE family proteins has been used as a dominant negative construct for N-WASP (158;161). When used for *in vitro* actin polymerization experiments, the WA domain acts

as a constitutively active construct because it not autoinhibited like full-length N-WASP (177). However, *in vivo* the WA domain binds to and sequesters Arp2/3 from N-WASP thereby inhibiting actin polymerization downstream of N-WASP (Figure 1.7) (169). Use of the WA domain lacks complete specificity as this domain is highly conserved among the WASP/WAVE family; therefore, this construct could also inhibit Arp2/3-mediated actin polymerization downstream of other NPFs such as WAVEs. A more selective way to inhibit N-WASP was described in 2003 by Peterson et al., who conducted a screen for compounds that inhibit PIP_2-stimulated actin polymerization *in vitro*. The study identified wiskostatin as a small molecule inhibitor that binds to and stabilizes the autoinhibitory conformation of N-WASP (wisk; Figure 1.7). Using assays that measure the rate and extent of actin polymerization the group showed that wiskostatin potently inhibits N-WASP activity *in vitro* (178). In addition to this approach, some groups have also used either siRNA or a knockout mouse to study the role of N-WASP in various cellular processes. In chapter 3, I explore the role of N-WASP in polarized biosynthetic traffic using expression of the WA domain, wiskostatin, and siRNA-mediated knockdown to disrupt N-WASP function.

1.5 PHOSPHATIDYLINOSITOL METABOLISM AND DISEASE

Given the multiple roles of PIPs in cell homeostasis it is not surprising to find diseases resulting from aberrant PIP metabolism. Loss of proper PIP metabolism and signaling has been linked to diseases such as cancer, Type 2 diabetes, Down syndrome, and Lowe syndrome (179). The fundamental differences between these diseases reinforce the diversity of cellular functions that

rely on efficient PIP metabolism. In the following sections, I briefly discuss the faulty pathway that leads to each disease.

PI3K/PTEN-regulated PIP_3 metabolism is involved in cell proliferation, apoptosis, metabolism, signaling, and cell growth (180). The gene for PTEN was first identified as a tumor suppressor located in an area of chromosome 10 associated with breast and prostate cancer (181;182). The ability of PTEN to suppress tumors was later found to be the result of its ability to dephosphorylate PIP_3 (183;184). Mutations in PTEN cause the inherited diseases Cowden disease and Bannayan-Zonana syndrome, which are characterized by multiple hamartomas (benign growths) but also an increased risk of malignant tumors (179). Mutations that increase PI3K activity have also been linked to certain cancers, such as colorectal cancer and glioblastomas (85).

Type 2 diabetes results from a decreased or loss of response to insulin leading to hyperglycemia. A number of proteins normally act as modifiers of this pathway by suppressing downstream signaling from the insulin receptor, including the PIP_3 5-pptase Src homology 2-containing inositol-5-phosphatase (SHIP2) (179). Insulin signaling is mediated through the PI3K/Akt pathway, and SHIP2 activity suppresses insulin signals by decreasing the available PIP_3. In a study that compared 4 control subjects and 8 patients with type 2 diabetes, it was found that one disease patient was lacking a 16 bp region of the SHIP2 3' untranslated region. Deletion of this region increases SHIP2 expression thereby dampening insulin signaling resulting in type 2 diabetes (185;186).

Symptoms of complex multi-gene disorders, such as Down syndrome, have been attributed to problems with PIP_2 metabolism. Down syndrome is caused by chromosome 21 trisomy, and therefore patients have an extra copy of chromosome 21 genes, including

synaptojanin 1 (*synj1*). Researchers discovered that the Down syndrome model mouse has a defect in PIP_2 homeostasis. As discussed earlier, regulation of PIP_2 metabolism is important for synaptic vesicle cycling, therefore dysregulation of PIP_2 may be responsible for altered cognitive function in Down patients. Furthermore, altered PIP_2 metabolism is recapitulated in transgenic mice designed to contain an extra copy of *Synj1* causing the mice to have a deficit in completing cognitive tasks (187).

1.5.1 Lowe Syndrome

Lowe syndrome results from mutations in the gene *OCRL1*. Lowe syndrome is a rare X-linked disorder characterized by mental retardation, congenital cataracts, poor muscle tone, and renal Fanconi syndrome (low molecular weight proteinuria (lmwp), hypercalciuria, and nephrocalcinosis) (44;188). The cause of the pathologies of Lowe syndrome are not known, but it is hypothesized that they may be due to defects in membrane traffic. OCRL is a 105kDa PIP_2 5-pptase that was originally localized to lysosomes, but has since been found primarily in the TGN, endosomes, and CCPs (73;75;76). The localization of OCRL is not coincident with the major pool of PIP_2 in the plasma membrane. Therefore, OCRL may function to regulate a small pool of PIP_2 that is generated and important at intracellular sites.

OCRL shares a similar phenotype with another X-linked disorder, Dent disease, which arises from mutations in the chloride-proton antiporter, ClC-5, and ultimately results in renal Fanconi syndrome (lmwp, glycosuria, aminoaciduria, and phosphaturia) (189;190). While Dent disease is predominantly caused by ClC-5 mutations, some Dent patients were found to have mutations in OCRL. These patients exhibited lmwp, but not the other main clinical phenotypes of Lowe syndrome (189;191). A detailed study comparing the kidney phenotype of Dent patients

and Lowe patients revealed that Lowe syndrome seems to result in a selective proximal tubule dysfunction, and lack the glycosuria found in Dent disease (192). Of note, are mutations OCRL that cause Dent disease are often found on or before exon 7 of the OCRL gene. However, this finding provides little insight into the mild Lowe phenotype of these patients as the mutations frequently result in complete loss of protein expression (189;193). The similarities in the reneal symptoms between the Dent disease and Lowe syndrome suggest that they share a common mechanism underlying their pathophysiology. Fanconi syndrome in Dent disease is thought to be caused by a loss of function of the multi-ligand scavenger receptor megalin, which reabsorbs proteins and other ligands in the kidney proximal tubule (194). It has been hypothesized that the Fanconi syndrome phenotype in Lowe syndrome is similarly caused by aberrant megalin trafficking, but this has not been examined directly.

Megalin is a member of the LDL-receptor family that is trafficked through the secretory pathway in association with its chaperone receptor associated protein (RAP), which prevents premature ligand binding to the receptor. At the cell surface megalin associates and traffics with a co-receptor cubilin. Together, megalin and cubilin internalize over 20 different ligands from the kidney filtrate. Once the ligand has been internalized and dissociates from the receptor, megalin then recycles to the cell surface (195). Interestingly, Lowe syndrome patients have been shown to shed less megalin in their urine, also a feature of Dent disease. Megalin normally undergoes regulated intramembranous proteolysis at a low basal rate, therefore less megalin in the urine suggests that less of the receptor is present at the apical surface at steady state (196;197). Since OCRL has been localized to both endosomes and the TGN, it is reasonable to hypothesize that OCRL activity may influence membrane traffic of megalin along either the biosynthetic or the endocytic/recycling routes (75). Indeed, OCRL has been shown to play a role

in endosome-to-TGN traffic of CI-MPR, but whether OCRL is involved in membrane traffic along the biosynthetic pathway remains to be tested.

1.6 GOALS OF THIS DISSERATION

For my dissertation I investigated the role of PIP metabolism in biosynthetic traffic. In polarized epithelial cells, biosynthetic transport of proteins is directed by sorting at either the TGN or endosomes that ensures proteins are sent to the correct membrane domain. Some information is available about the mechanisms that regulate basolateral sorting, however those that govern the sorting of distinct classes of apical proteins have not been thoroughly investigated. Lipids, including phosphatidylinositols, play important roles in vesicular traffic. PI4P is highly enriched in the Golgi complex and influences membrane traffic through that organelle. PI4P may also serve as a substrate for synthesis of PIP_2 in the Golgi. The role of PIP_2 metabolism in polarized biosynthetic traffic is not well known but could involve PIP_2 effector proteins, such as N-WASP to engage the actin cytoskeleton. In addition, while actin is known to be important for membrane traffic, the involvement of N-WASP in biosynthetic traffic has been largely unexplored.

To explore the role of phosphatidylinositol metabolism in polarized biosynthetic traffic, I have studied the effect of overexpression or knockdown of PIP_2-metabolizing enzymes on biosynthetic traffic of apical and basolateral proteins. The first goal of this study was to determine if there is a role for PIP_2-metabolism in biosynthetic traffic and to characterize proteins that are sensitive to PIP_2 levels based on their sorting signal. The second goal of my work was to determine if actin polymerization via N-WASP/Arp2/3 is important in biosynthetic

traffic. These studies fill an important gap within the literature and have the potential to contribute to therapeutic treatments for Lowe syndrome.

2.0 THE ROLE OF PHOSPHATIDYLINOSITOL METABOLISM IN POLARIZED BIOSYNTHETIC TRAFFIC

2.1 INTRODUCTION

The maintenance of polarized cell function requires continuous active sorting and delivery of newly synthesized proteins and lipids to differentiated apical and basolateral plasma membrane domains. Tight junctions between the cells prevent the diffusion of surface proteins between these domains, but polarity is established and maintained largely by the selective delivery and recycling of proteins to their appropriate site of function. In polarized renal cells, it is thought that newly synthesized proteins are sorted initially at the *trans*-Golgi network (TGN) into distinct carriers destined for the apical or basolateral domain (29;198). Transport of some proteins to their ultimate destination may be indirect and include passage through endosomal compartments or the opposite surface domain (198).

The sorting of individual proteins to the apical and basolateral cell surface domains is signal-mediated. Basolateral sorting signals generally reside in the cytoplasmically-disposed regions of proteins whereas glycan-, lipid-, and peptide-dependent signals have been identified that reside in the lumenal, membrane-associated, or cytoplasmic regions of distinct apically-targeted proteins (198). Little is known about how the sorting machinery recognizes these diverse signals. A current model suggests that preferential incorporation of a subset of apical

proteins, including those with glycosphingolipid anchors or sorting signals within their transmembrane domains, into glycolipid-enriched microdomains (lipid rafts) is important for their polarized delivery (29). Interestingly, apical delivery of raft vs. non-raft proteins may involve distinct transport carriers that are independently regulated (9;199).

There is increasing evidence for a role of phosphatidylinositols in the regulation of biosynthetic membrane traffic (59). The Golgi contains a sizable pool of PI4P and harbors two PI4P-synthesizing enzymes (PI4KIIIβ and PI4KIIα) (49;50;134;200). Previously it has been demonstrated that overexpression of PI4KIIIβ inhibits the rate of apical membrane delivery of the raft-associated protein influenza HA, whereas expression of a kinase-deficient mutant stimulates delivery (50). However, it is conceivable that these effects are due to a downstream metabolite of PI4P, such as PIP_2. Indeed, although there is only a small amount of this lipid that can be visualized in the Golgi complex (43), PIP_2 is readily generated on isolated Golgi membranes incubated with phosphatidylinositol 4-phosphate 5-kinases [PI5Ks; (42)] and several possible functions for PIP_2 in biosynthetic membrane traffic have been postulated (59;201;202). Additionally, the presence of OCRL, a TGN-localized PIP_2 5-pptase that is defective or absent in patients with oculocerebrorenal syndrome of Lowe, lends further support to a role for PIP_2 metabolism in that compartment (72;73).

Lowe syndrome is characterized by mental retardation, congenital cataracts, and renal Fanconi syndrome (44;188). While the degree of each phenotype may vary, Lowe Syndrome patients universally have renal Fanconi syndrome, which is characterized by defective absorption of low molecular weight proteins in the proximal tubule. Protein uptake from the apical surface of these cells is dependent on megalin, a recycling receptor that mediates the uptake and ultimate degradation of protein ligands (195). Observations made in cells from Lowe syndrome patients

reveals that PIP_2 levels are slightly increased due to lack of OCRL, consistent with its function as a PIP_2 5-pptase (203). While a role for OCRL in endosome to TGN traffic has been reported, the role of OCRL-regulated PIP_2 metabolism in biosynthetic traffic has not been explored (75). Here I have examined the effect of increasing PIP_2 synthesis on polarized biosynthetic traffic in Madin-Darby canine kidney (MDCK) cells.

2.2 RESULTS

2.2.1 Localization of PI5K and OCRL in MDCK Cells

The localization of murine PI5KIα (PI5K) and human OCRL was determined via adenoviral (AV)-mediated overexpression in MDCK cells, as they are a well established model to study trafficking in polarized epithelial cells. Due to the lack of available antibodies that recognize endogenous canine PI5K, indirect immunofluorescence was performed to visualize the HA epitope tag of overexpressed PI5K. In nonpolarized MDCK cells, PI5K localizes to the plasma membrane and also to filamentous structures in the cytoplasm (Figure 2.1 top row). This localization is reminiscent of the observed localization of PI5Ks in other adherent cell lines (204). However, in polarized MDCK cells, PI5K is highly concentrated in the apical pole of the cells and is absent from the basolateral surface (Figure 2.1 middle and bottom panels). By contrast, in nonpolarized cells OCRL has a very defined localization to cytoplasmic punctae and the juxtanuclear region consistent with its reported localization in endosomes and the TGN (Figure 2.1 top row). Prior to this work, the localization of OCRL in polarized epithelial cells had not been examined. My data indicate that OCRL is localized to punctae in the periphery of the cell and above the nucleus (Figure 2.1 middle and bottom panels). Since the OCRL antibody I used only recognized exogenously expressed OCRL, these data must be interpreted cautiously. However, the bright OCRL staining above the nucleus and below the tight junctions (not shown) is consistent with Golgi localization, while the lateral punctae may be endosomal compartments.

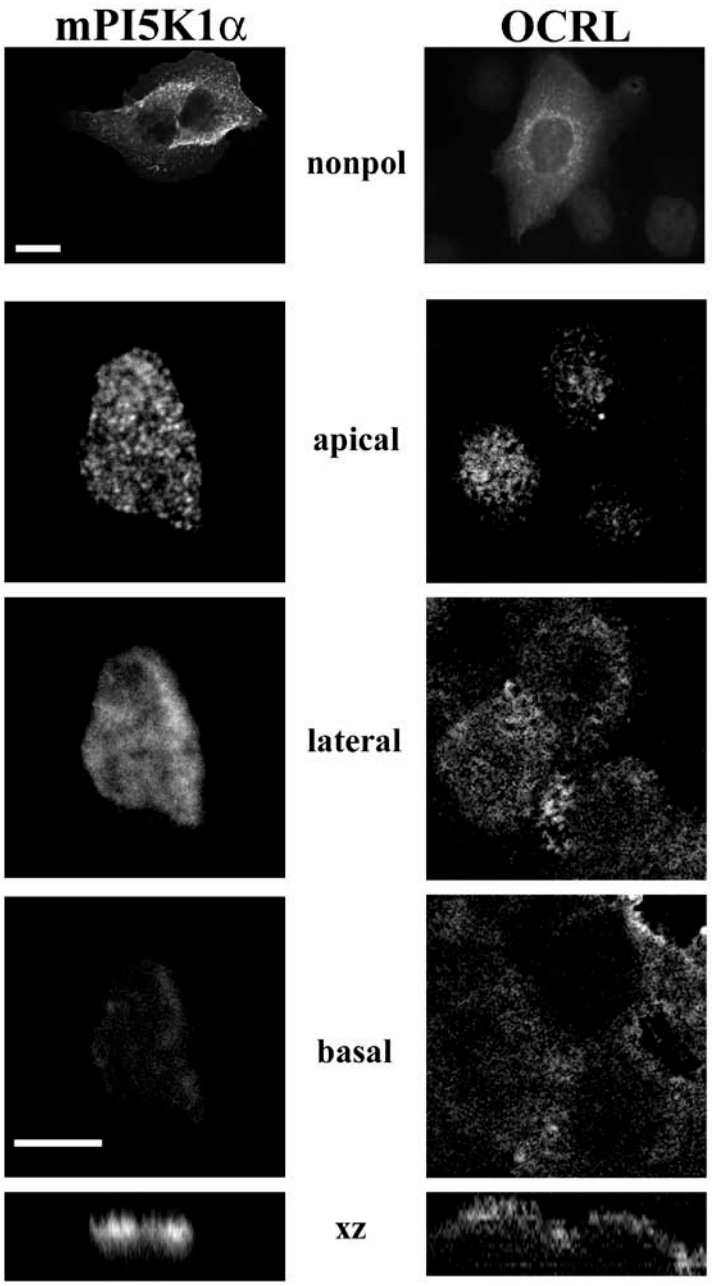

Figure 2.1 Localization of OCRL and PI5K in nonpolarized and polarized MDCK cells. MDCK cells were electroporated with a cDNA construct encoding mPI5KIα, or infected with AV-OCRL and plated sparsely on coverslips (top row) or plated onto Transwell filters for 3 days prior to fixation and processing for immunofluorescence(remaining panels). HA-tagged PI5K and OCRL were detected using a monoclonal antibodies and an AlexaFluor 488 secondary antibody. Confocal sections were captured using a spinning disc confocal deconvolved using Metamporph software show representative PI5K or OCRL staining from the apical pole, lateral and basal regions of the cell. The bottom row shows deconvolved xz sections from the filter-grown cells. Scale bars represent ~10μm.

2.2.2 PI5K Selectively Stimulates Biosynthetic Delivery on an Apical Raft-associated Protein

I examined the effect of AV-mediated overexpression of PI5K on biosynthetic traffic in polarized MDCK cells. Overexpression of PI5K increased cellular levels of PIP_2 by 2-fold (Figure 2.2) but did not alter intra-Golgi kinetics based on the quantitation of the rate of HA acquisition of endoglycosidase H (endo H) resistance (Figure 2.3A). To examine the effects of PI5K on post-Golgi transport, I staged newly-synthesized HA in the TGN at 19ºC, and using a cell surface trypsinization assay measured the rate of its delivery to the cell surface upon warming to 37ºC. Roughly 50% of the total HA expressed in control cells reached the apical membrane in 1 h (Figure 2.3B). In contrast, HA delivery was markedly stimulated in cells overexpressing PI5K (~67% at 1 h).

I next examined the effect of PI5K on the TGN-to-surface transport kinetics of p75, an apical marker that is not known to associate with lipid rafts in MDCK cells (Figure 2.3 C), as well as on the basolateral marker vesicular stomatitis virus G protein (VSV-G) (Figure 2.3D). PI5K had no effect on the biosynthetic delivery of either of these proteins. Thus, the stimulatory effect of PI5K on surface delivery appears to be selective for raft-associated proteins.

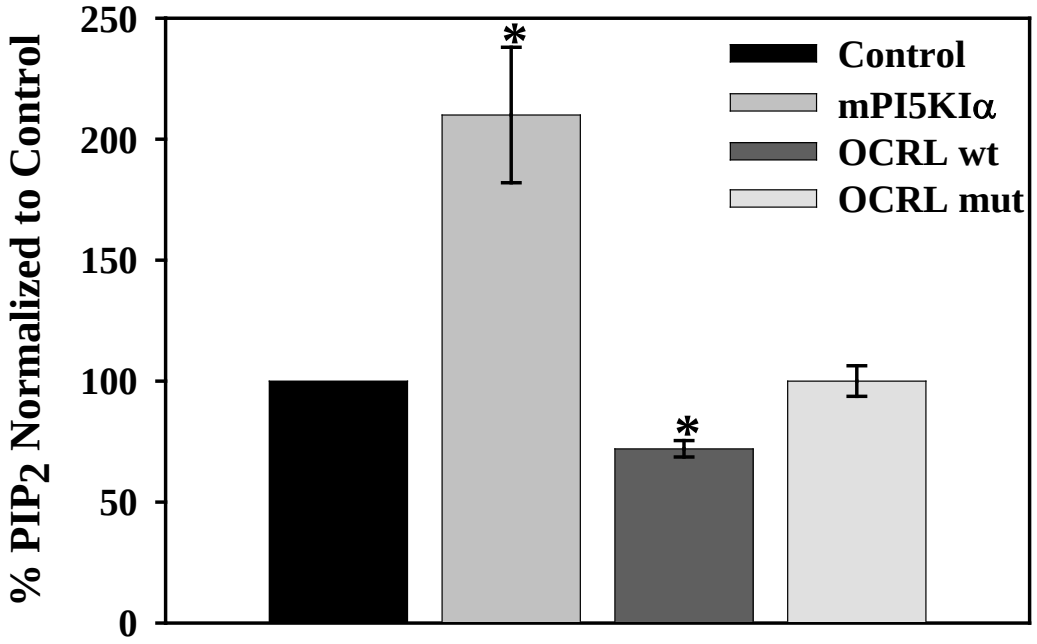

Figure 2.2 Relative PIP_2 levels for AV-infected MDCK cells. Filter-grown MDCK cells were infected with control AV, AV-PI5K, AV-OCRL or AV-OCRL mutant (mut; R483G). To assay for phospholipids levels, cells were incubated briefly in phosphate-free media, labeled for 4 hr with ^{32}P-orthophosphate and extracted using chloroform:methanol:HCl. Extracted lipids were separated using thin layer chromatography (TLC). Densitometry was used to quantify the intensity of each band and relative amounts were determined. Data for PIP_2 were normalized to the control PIP_2 percentage. Error bars represent mean +/- std error for at least n=4 independent experiments. * represents $p \leq 0.004$.

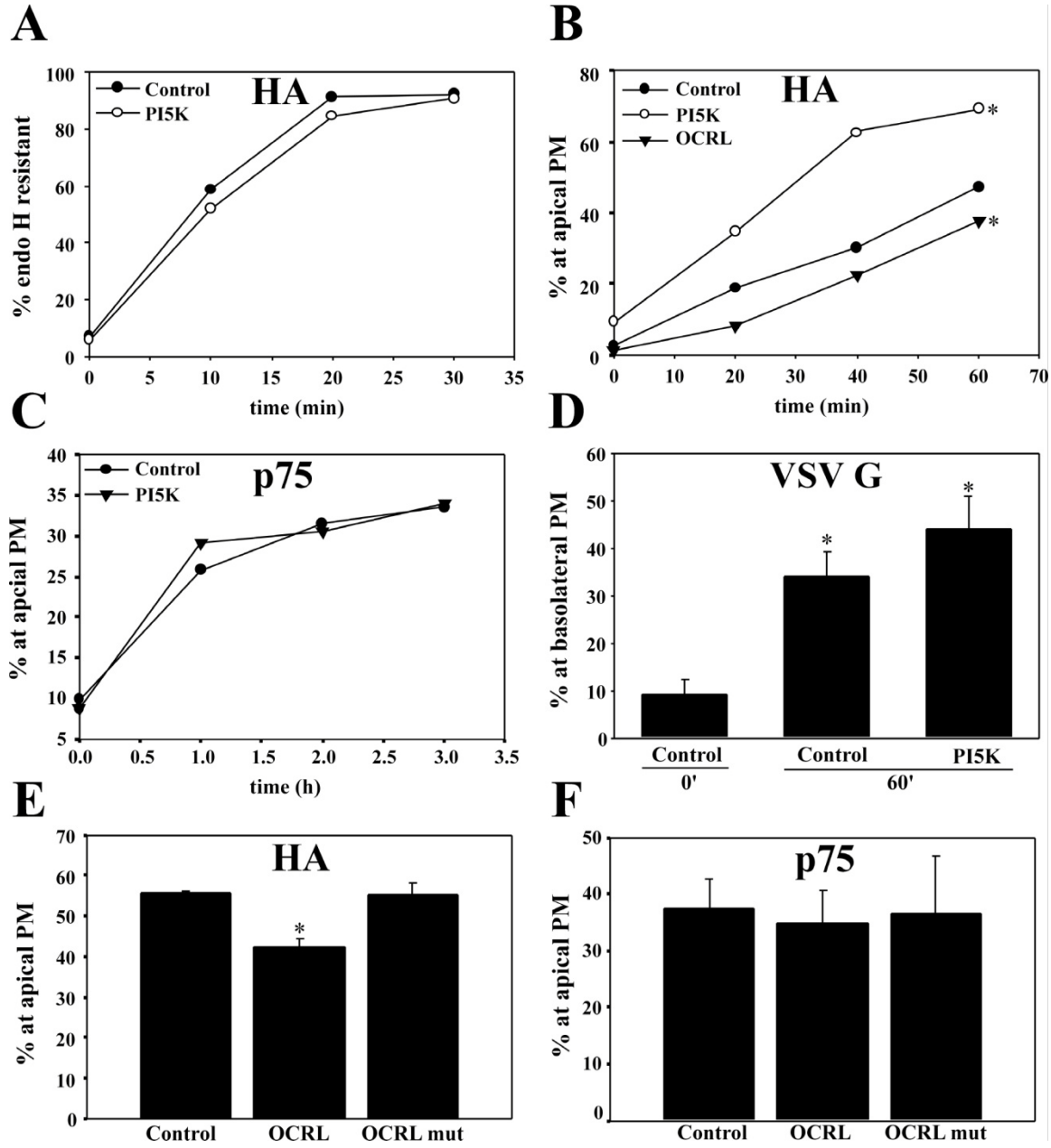

Figure 2.3 TGN to apical membrane delivery of a raft-associated protein is selectively modulated by PI5K and OCRL

A, Filter-grown MDCK cells co-infected with AV-HA and either control AV or AV-PI5K were starved, radiolabeled for 5 min, and chased at 37ºC for the indicated time periods. HA was immunoprecipitated from cell lysates, the samples were treated with endo H, and the fraction of HA that was resistant to endo H at each time point was quantitated. Similar results were obtained in three experiments. *B,* MDCK cells co-infected with AV-HA and either control AV, AV-PI5K or AV-OCRL were radiolabeled for 15 min and chased for 2 h at 19ºC. Apical delivery of HA was quantitated by cell surface trypsinization at various times after warming to 37ºC. Similar results were obtained in 13 experiments comparing HA transport in control and PI5K-expressing cells. *C,* MDCK cells co-infected with AV-p75 and either control AV or AV-PI5K were radiolabeled for 2 h at 18ºC with [^{35}S]-sulfate prior to warming to 37ºC for the indicated times. Apical delivery of p75 was quantitated by domain selective biotinylation. Similar results were obtained in three independent experiments. *D,* MDCK cells co-infected with AV-VSV-G and either control AV or AV-PI5K were radiolabeled and then chased for 2 h at 19ºC prior to warming to 37ºC for 0 or 60 min. Basolateral delivery was quantitated by domain selective biotinylation. The mean +/- S.E.M. of the indicated number of experiments performed in triplicate or quadruplicate is plotted; n=3 for 0'; $n \geq 4$ for 60'. * $p \leq 0.02$ vs. control at 0'. MDCK cells co-infected with AV-HA (*E*) or AV-p75 (*F*) and either control AV or AVs expressing wild-type or kinase-deficient OCRL were starved in sulfate-free media for 30 min and radiolabeled for 2.5 h at 18ºC with [^{35}S]-sulfate prior to warming to 37ºC. Apical delivery of HA (at 1 h) was quantified using cell surface trypsinization; delivery of p75 (at 2 h) was quantitated by domain selective biotinylation. The percent delivery (mean +/- S.E.M.) of HA (n=3) and p75 (n=5-6) is shown. * denotes statistical significance from control measured using Student's t test (p=0.004)

2.2.3 Overexpression of OCRL Selectively Inhibits Biosynthetic Delivery of Influenza HA

To examine whether stimulation of PIP_2 synthesis in the TGN was responsible for the effect of PI5K, I compared the effect of overexpressing the TGN-localized PIP_2 5-pptase OCRL or expressing a phosphatase-deficient mutant of OCRL on the delivery of HA and p75. Overexpression of OCRL decreased PIP_2 levels by approximately 30% while expression of the phosphatase-deficient mutant had no significant effect on PIP_2 levels (Figure 2.2). Because overexpression of both wild type and mutant OCRL slowed intra-Golgi transport as assessed by monitoring endo H kinetics, I used [^{35}S]-sulfate to selectively radiolabel proteins in the TGN. As shown in Figure 1.3B, expression of wild type OCRL inhibited TGN to apical delivery of HA, whereas mutant OCRL had no effect (Figure 2.3E). Consistent with the selective effect of PI5K on HA delivery, neither wild type nor mutant OCRL affected the kinetics of p75 delivery (Figure 2.3F).

2.2.4 Knockdown of OCRL in MDCK Cells

Lowe syndrome patients can have mutations anywhere throughout the coding sequence of *OCRL1* and often, the result of such mutations is complete loss of OCRL protein expression. Therefore, to mimic the conditions in Lowe syndrome patients, I sought to use a knockdown approach to silence expression of endogenous OCRL in MDCK cells. The sequence for a canine-specific OCRL siRNA oligonucleotide (oligo) and a protocol for introducing the oligo into MDCK cells were obtained from Dr. Alex Ungewickell (Washington University). The oligo GGTTCCCTGCCATTTTTCA contains a single mismatch in the 3' end of the sense strand that has been shown to increase the efficiency of siRNA oligos, presumably by enhancing unwinding

and increasing degradation of the target mRNA (205-207). An Amaxa Nucleofector © was used to introduce 2.5 or 5µg of control (firefly luciferase) or OCRL siRNA oligo into MDCK cells cultured to 50% confluence. After electroporation, cells were either allowed to recover for 1 day on a culture dish or plated directly to Transwell filters. After 2-3 days, cells were harvested and Western blotted with an antibody against endogenous OCRL to assay the extent of knockdown. MDCK cells electroporated with 2.5µg siRNA/0.5 x 10^6 cells plated directly onto Transwell filters exhibited approximately 98% knockdown on day 3, while the other conditions exhibited equal or less efficient knockdown (Figure 2.4). In addition to knockdown in polarized MDCK cells, significant knockdown was also achieved in a nonpolarized human proximal tubule (HK2) cell line (not shown).

2.2.5 OCRL Knockdown Increases PIP2 Levels and Stimulates Actin Comets

To determine whether OCRL knockdown recapitulated Lowe syndrome I assayed the published cellular phenotypes of Lowe syndrome cells. One report indicated that proximal tubule cells from Lowe syndrome patients exhibited increased PIP_2 levels (208). Briefly, cellular phospholipids were labeled upon incubation with ^{32}P-orthophosphate prior to extraction with chloroform-methanol and separation by thin layer chromatography (TLC). MDCK cells lacking OCRL had slightly increased PIP_2 levels compared with cells treated with control siRNA (Figure 2.5). While the increase was not statistically significant or as dramatic as that seen with PI5K overexpression, it is consistent with the known localization of OCRL in compartments that have low relative PIP_2 levels.

Abnormalities in the cytoskeleton have also been described in cells from Lowe syndrome patients. Features of this phenotype include decreased stress fibers, increased sensitivity to the

actin depolymerizing agent, cytochalasin D, and increased actin comet formation (209;210). I examined the actin comet phenotype as increases in PIP_2 via PI5K also increase actin comets (158). For these experiments, I generated MDCK cells that were stably transfected with cDNA encoding GFP-actin. These cells were electroporated with either control or OCRL siRNA and then plated onto Transwell filters for 2 days before being grown in culture dishes designed for live cell microscopy. Short movies (3-4 min) were taken of random fields and reviewed for the presence of actin comets. Analysis revealed that OCRL-knockdown cells had an increased frequency of actin comets (~20% of cells) compared to control cells (~4%) (Table 2.1).

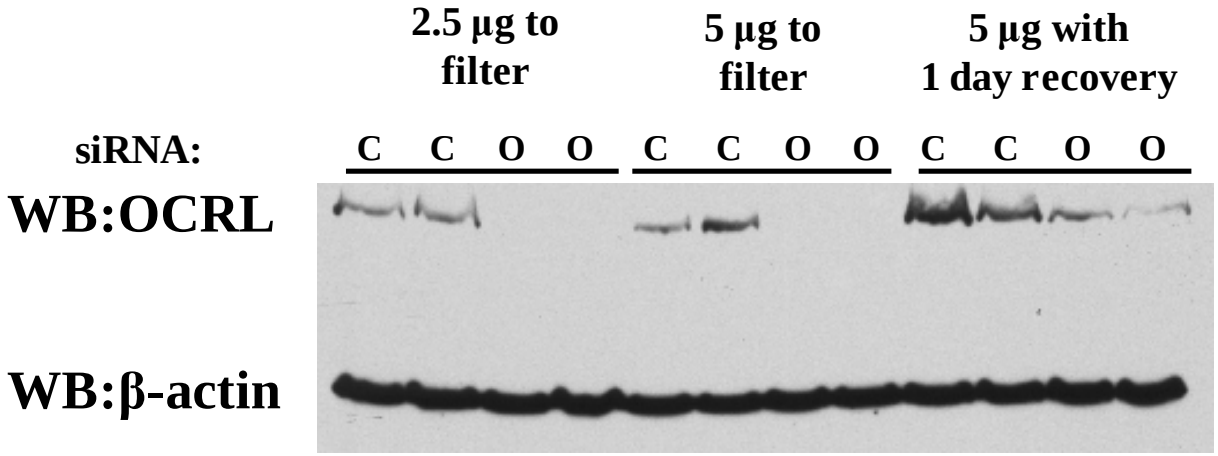

Figure 2.4 Knockdown of OCRL in polarized MDCK cells

Low passage MDCK cells grown to 50% confluence were trypsinized and resuspended into Amaxa solution mix at a density of 1 x 10^6 cells/100ul solution. 100 ul of the cells were mixed with 2.5 or 5 ug of control or OCRL siRNA and placed into a cuvette. Samples were nucleofected using program T-020 and were then either put directly onto filters (left) or allowed to recover for 1 day on a 10 cm dish before being plated to filters for 3 days. Samples were harvested and analyzed by western blot for OCRL and actin as a loading control. Quantitation of data using a VersaDoc (BioRad) and Quantity One software were performed. The left side of the image is labeled to denote the OCRL and β-actin bands. Above the image, the type of siRNA treatment is denoted and below individual lanes are labeled C for control siRNA and O for OCRL siRNA.

.

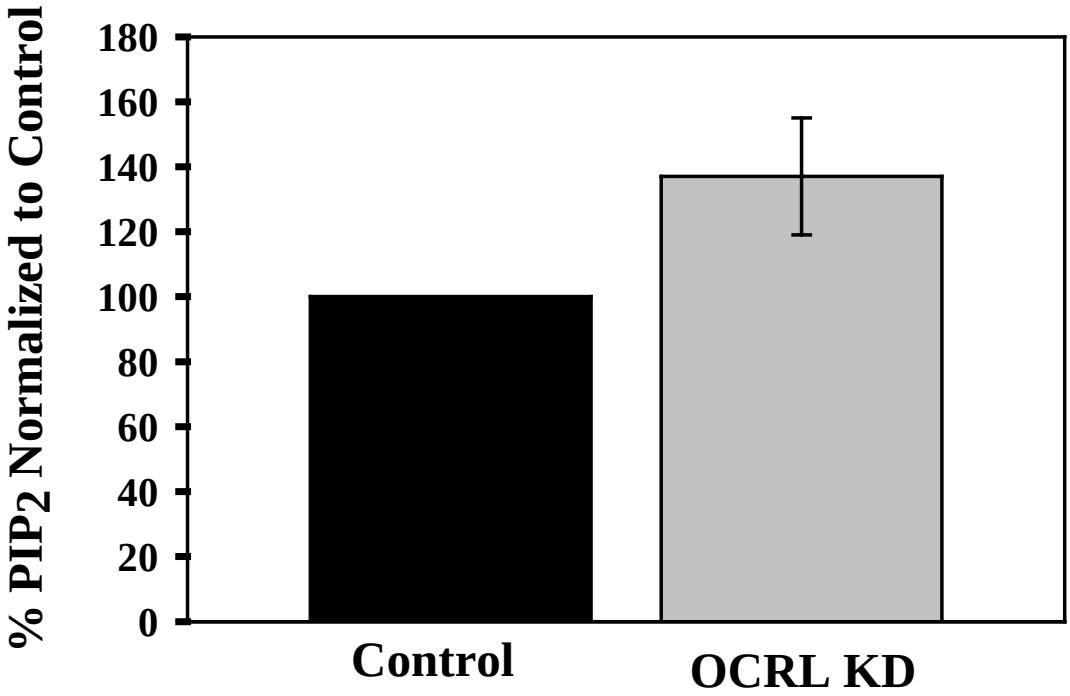

Figure 2.5 PIP_2 levels in OCRL knockdown cells. MDCK cells were treated with either control or OCRL siRNA and plated directly onto filters for 3 days. Phospholipids were labeled with ^{32}P-orthophosphate and analyzed by TLC to determine relative phospholipids levels. PIP_2 values for OCRL knockdown were normalized to control in each of n=3 independent experiments and mean +/- std error is plotted.

Table 2.1 Quantitation of actin comet frequency in MDCK cells.

Condition	% cells with comets	n
OCRL siRNA	22	69
control siRNA	3.6	55
control-AV	7.4	27
AV-PI5K	27	212
AV-WA	0	10
WA+PI5K	0	44
PI5K + OCRL	0	47
PI5K + cyto D	0	10
PMA	31	33
PI5K + 1-butanol	6.7	15
PI5K + OCRL	0	47

MDCK cells stably expressing GFP actin were imaged under the indicated conditions. Three minute movies were taken of random frames with either a 60X or 100 X oil immersion objective. Movies were reviewed multiple times to determine the percentage of cells with actin comets. n represents the number of cells counted for each condition. For siRNA samples, MDCK cells were electroporated with control or OCRL siRNA and plated onto filters for two days before being transferred to Bioptech 0.17 mm ΔT dishes for imaging. For adenovirus infected samples, MDCK cells seeded onto Bioptech dishes were infected with either control AV or AVs encoding WA, PI5K, or OCRL (m.o.i. 100-250). The samples were kept in 0.25 ng/ml DOX overnight to suppress protein expression from the AVs. The next day, DOX was thoroughly washed and random fields were imaged for 3 min intervals starting 5 h later. The effects of PMA and cytochalasin D (cyto D) were determined after a brief treatment with 5 μg/ml of each drug or 1% v/v 1-butanol.

2.2.6 OCRL Knockdown has No Effect on the Biosynthetic Delivery of Influenza HA in MDCK or HK2 Cells

Because increases in cellular PIP_2 levels upon overexpression of PI5K stimulated TGN-to-apical membrane delivery of HA, knockdown of OCRL might also be expected to stimulate the rate of HA delivery. To test this, electroporation of siRNA oligos was used to deplete OCRL from MDCK cells. I examined the effect of OCRL knockdown on the delivery of HA from the TGN to the apical plasma membrane. In several experiments I detected no significant changes in the rate of HA delivery (Figure 2.6 Top). OCRL-null mice show no Lowe syndrome phenotype presumably due to compensation by another related PIP_2 5-pptase, Inpp5b (211). It is unknown whether canine cells lacking OCRL would exhibit the clinical/cellular phenotypes of Lowe syndrome or be rescued by compensation. Therefore, to confirm my results in a species known to have renal phenotype, I tested the effect of OCRL knockdown on HA delivery in the human kidney proximal tubule cell line HK2. Similar to my results in MDCL cells, knockdown of OCRL caused no significant change in the rate of HA delivery in these cells (Figure 2.6 Bottom).

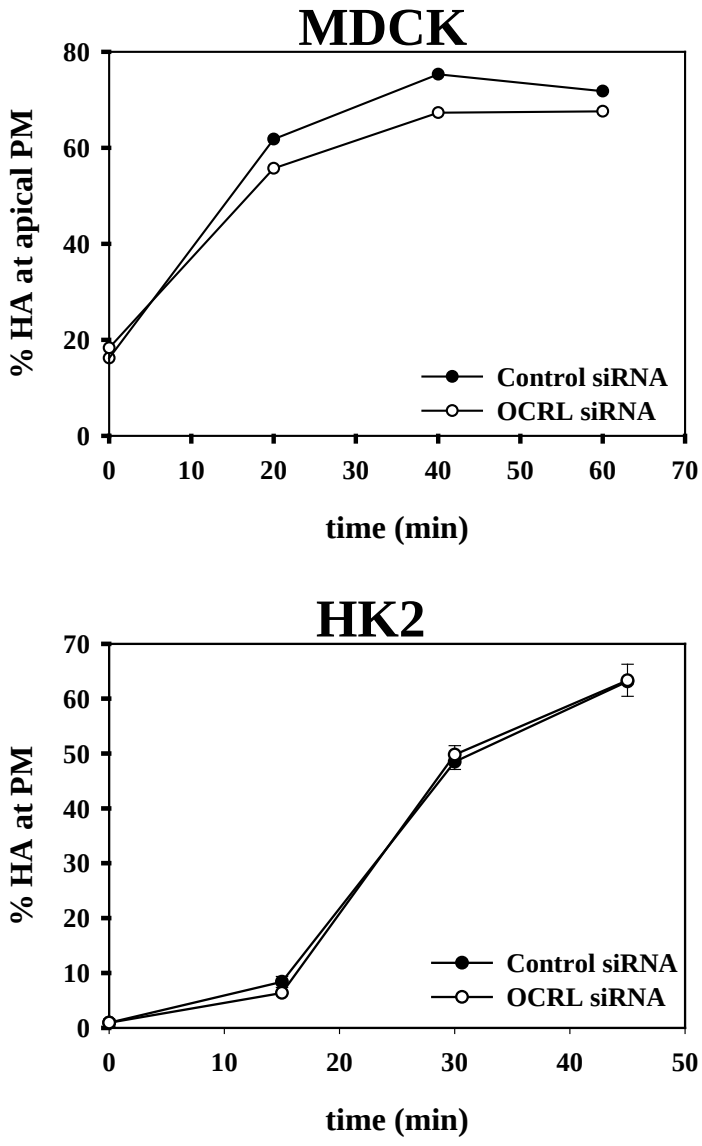

Figure 2.6 TGN to PM delivery of HA is not affected by OCRL knockdown in polarized MDCK cells or HK2 cells.

MDCK or HK2 cells were treated with either control or OCRL siRNA prior to infection with AV-HA. The next day, cells were radiolabeled for 15 min and chased for 2 h at 19ºC. Apical or plasma membrane delivery of HA was quantitated by cell surface trypsinization at various times after warming to 37ºC. One representative experiment is shown for both MDCK (top;n=6) and HK2 (bottom; n=4) error bars in HK2 graph represent the range.

2.3 DISCUSSION

Here I investigated the role of PIP_2 metabolism in polarized biosynthetic traffic. Expression of PI5K in polarized MDCK cells markedly stimulated TGN-to-apical delivery of the lipid raft-associated protein influenza HA, whereas overexpression of OCRL inhibited delivery. Delivery of the non-raft associated apical protein p75 and of the basolateral protein VSV-G were unaffected by PI5K, and expression of OCRL also had no effect on the rate of apical p75 delivery. Knockdown of OCRL slightly stimulated PIP_2 levels and robustly stimulated the formation of actin comets in MDCK cells. However, OCRL knockdown had little to no effect on HA delivery, contrary to my initial predictions that delivery would be stimulated. Together these data suggest a role for PIP_2 in the efficient biosynthetic delivery of a lipid-raft associated protein. However the pathological defects observed in Lowe syndrome appear not to be related to defects in biosynthetic traffic.

It is necessary to consider my results in the context of previous studies on the major Golgi phosphatidylinositol, PI4P. Overexpression of PI4K increases PI4P levels and inhibits HA delivery in MDCK cells (50). The relationship between PI4P and PIP_2 in polarized biosynthetic traffic may be more complex than a simple precursor-product relationship, as PI4P has many functions. A likely scenario is that PI4P and PIP_2 function independently to modulate distinct steps in membrane transport.

The roles of OCRL-mediated PIP_2 metabolism in the pathology of Lowe syndrome remain unclear. The renal Fanconi syndrome common in Lowe patients is likely due to a defect in megalin traffic, however, the site of and mechanism of dysfunction remain to be determined. OCRL could regulate megalin traffic along the biosynthetic or the endocytic/recycling routes. While my data lend less support for a contribution to the biosynthetic route, strong evidence still

exists for OCRL-mediated regulation of megalin endocytosis/recycling, including the observation that Lowe syndrome patients shed less megalin into their urine (196). While I did not identify the compartment to which OCRL localizes in polarized cells, it is possible that the supranuclear punctae represent the apical recycling endosome. The apical recycling endosome is a compartment unique to polarized epithelial cells which is marked by the small GTPase, Rab11. Indeed, this compartment is traversed by megalin in a mechanism dependent on the clathrin sorting adaptor, autosomal recessive hypercholesterolemia (ARH) (212). OCRL has been shown to interact with clathrin through a conserved clathrin-binding motif, and may function in clathrin-mediated vesicular traffic of megalin through the endosomal recycling system.

The site of action of PI5K in TGN-to-apical membrane delivery of HA remains to be determined. Whereas no PI5K isoform has been localized to the Golgi complex, the majority of the PI5K in polarized MDCK cells was associated with actin filaments near the apical surface, close to the supranuclear Golgi complex (Figure 3.1A). There are strong indications that apically-destined proteins traverse endosomal intermediates *en route* to the cell surface suggesting the possibility that the PI5K- and OCRL-mediated effects on HA transport might occur at post-TGN sites (5;213;214). Overall, my data suggest that PIP_2 influences HA traffic through modulation of the actin cytoskeleton, but further research is necessary determine the mechanism of PIP_2's role in biosynthetic traffic.

*Some text in this chapter, Figure 2.3 and portions of Table 2.1 are published in Guerriero et al. *JBC* 2006 and were used with the permission of the Journal of Biological Chemistry.

3.0 THE ROLE OF N-WASP IN BIOSYNTHETIC TRAFFIC

3.1 INTRODUCTION

Polarized epithelial cells line the surfaces of our bodies and maintain internal homeostasis through the regulation of a selective barrier for pathogens and solutes. Both the actin and microtubule cytoskeleton have been implicated in proper biosynthetic membrane traffic. The dynamic polymerization of actin into straight or branched filaments regulates diverse cellular processes including ion transport, membrane trafficking, and cell migration (215-217). An important modulator of actin polymerization is the actin-related protein (Arp)2/3 complex, which nucleates the polymerization of actin on existing filaments to create a branched network. Members of the Wiskott-Aldrich syndrome protein (WASP) and SCAR/WAVE families of proteins activate Arp2/3-mediated actin polymerization, leading to distinct downstream effects. For example, Rac-mediated association of WAVE proteins with Arp2/3 regulates the formation of lamellopodia, whereas Cdc42- and PIP_2-stimulated binding of the ubiquitously expressed WASP family member N-WASP to Arp2/3 has been implicated in the intracytoplasmic propulsion via actin comets of transport vesicles, organelles, and invading pathogens (141;163;218).

N-WASP contains multiple domains that contribute to its function, including a WASP homology (WH)1 domain, a GTPase binding domain (GBD), a proline-rich region, and a WA

domain that binds to both actin and Arp2/3. The protein normally exists in an autoinhibited state that is maintained by *cis* interactions between the GBD and the conserved COOH-terminal WA domain. Interaction with GTP-bound Cdc42 and PIP_2 relieves the autoinhibition and promotes N-WASP-mediated activation of Arp2/3.

Data in chapter 2 show that apical delivery of a lipid raft-associated protein is dependent on PIP_2. Increases in PIP_2 levels upon expression of PI5Ks also leads to production of rapidly nucleating branches of actin filaments termed actin comets, which are capable of propelling transport vesicles through the cytoplasm (219). N-WASP is activated by PIP_2 and transduces elevated PIP_2 levels into an increased frequency of actin comets (220). N-WASP and Arp2/3 are localized to the Golgi complex (among other sites), and a link between actin comets and biosynthetic traffic has been previously suggested (158). Activation of Arp2/3 by WASP and WAVE proteins can be blocked *in vivo* by expression of the highly homologous WA domains of these proteins, which function as dominant-negative inhibitors (162). In addition, wiskostatin, a chemical inhibitor of N-WASP, was recently identified in a high-throughput screen for inhibitors of PIP_2-mediated actin polymerization (221). *In vitro* studies demonstrated that wiskostatin binds to the GBD of N-WASP, thereby stabilizing the autoinhibited conformation of the protein (178). However, the effects of manipulating N-WASP activity on the fidelity or rate of biosynthetic transport have not been explored.

The goal of these studies is to define the requirement for N-WASP in the biosynthetic traffic of both apical/basolateral proteins and determine if a link exists between PI5K-stimulated apical delivery and N-WASP-mediated actin comets. Here I have examined the effect of inhibition of N-WASP/Arp2/3-mediated actin polymerization on biosynthetic delivery in polarized MDCK cells. To inhibit N-WASP/Arp2/3 function I used a dominant negative

inhibitor of N-WASP, the commercial inhibitor wiskostatin, and an siRNA oligonucleotide directed against N-WASP.

3.2 RESULTS

3.2.1 PI5K Stimulates Actin Comets in MDCK Cells

Because PI5K-stimulated actin comets have been implicated in the transport of raft-associated proteins (158), I asked whether actin comet-mediated propulsion of HA transport carriers could be responsible for the stimulated surface delivery I previously observed. First, I sought to determine the relationship between PI5K and actin in fixed cells. MDCK cells were infected with AV expressing PI5K, then fixed and processed for indirect immunofluorescence 16 h later. Actin filaments were visualized using rhodamine phalloidin and the HA epitope tag on PI5K was detected using a monoclonal mouse antibody. PI5K colocalized extensively with actin filaments in confocal sections of MDCK cells (Figure 3.1A). This is consistent with previous reports that PI5K is found in actin-rich fractions isolated from thrombin-activated platelets (222;223). Next, I used a live cell approach to determine whether PI5K stimulates the formation of actin comets. Actin comets have not previously been reported in MDCK cells. MDCK cells were seeded on glass coverslips, infected with AV encoding PI5K or control AV, and then incubated in the presence of 0.25 ng/ml DOX to suppress PI5K expression. The following day, the DOX was washed out and cells were microinjected with cDNA encoding GFP-actin. Random fields were imaged 5 h later for 4-min intervals using an Olympus IX81 equipped with a 100X Olympus UPlanApo objective. Actin comets were defined as rapidly moving bursts of actin followed by a

fading tail of presumably depolymerizing actin. Comets generated in MDCK cells were distinct but generally smaller than comets described by others using different cell lines, which have been reported to be up to 5 μm in length (158;224;225). Comets were observed in 7.4% of control cells and in 27% of the cells overexpressing PI5K (Table 2.1 and Figure 3.1B).

Additionally, I could increase the frequency of actin comet formation in control cells by addition of the protein kinase C activator PMA, which has been previously demonstrated to stimulate actin comets *in vivo* (Table 2.1) (219). PMA also stimulated the rate of apical delivery of HA to an extent comparable with that observed upon overexpression of PI5K I reported previously (Figure 2.3B). Conversely, addition of 1-butanol, which disrupts phospholipase D-mediated synthesis of the PI5K activator phosphatidic acid (PA), profoundly inhibited the formation of PI5K-stimulated actin comets (Table 2.1) and also blocked delivery of TGN-staged HA to the apical surface (Figure 3.2). 1-Butanol-mediated inhibition of PA synthesis has previously been implicated in the release of secretory vesicles from the TGN of endocrine cells (226). In contrast, *t*-butanol, which does not affect PA synthesis, had no effect on comet formation or HA delivery (Figure 3.2).

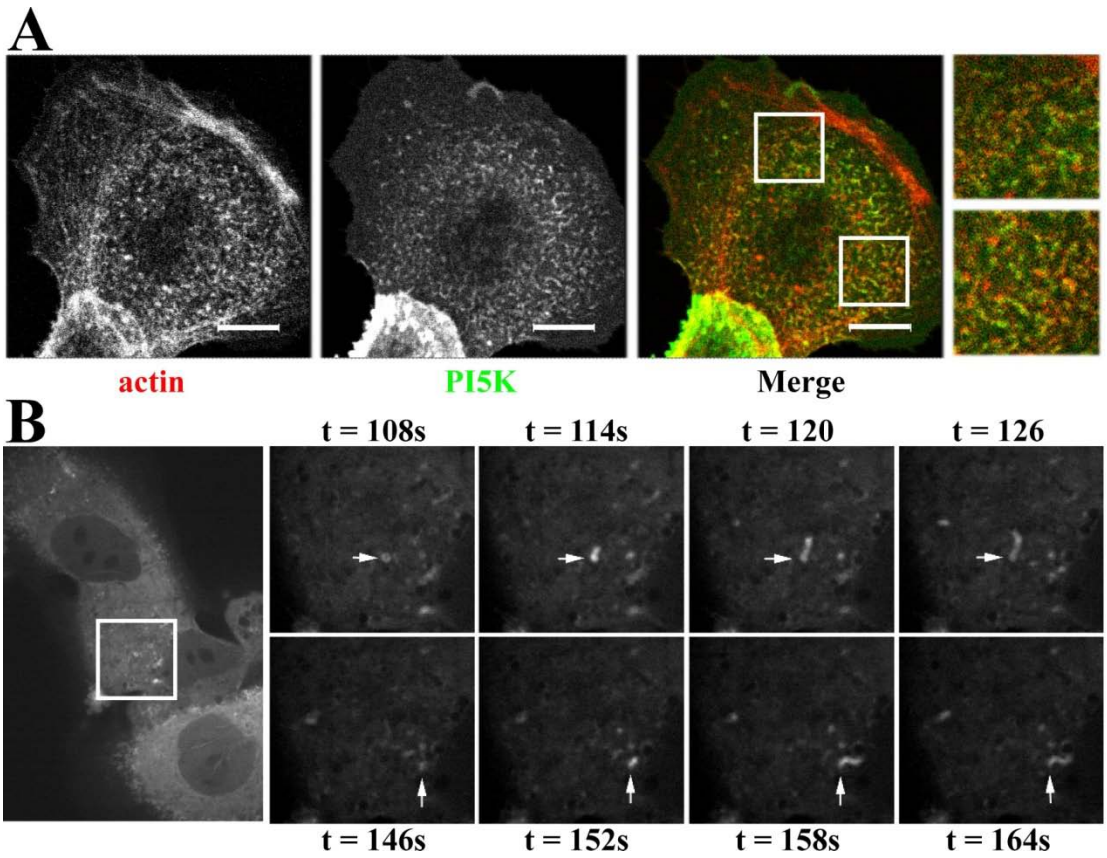

Figure 3.1 PI5K localizes to actin filaments and stimulates actin comet formation in MDCK cells.

A, MDCK cells seeded on coverslips were infected with AV-PI5K and processed for indirect immunofluorescence the following day to detect actin (with rhodamine phalloidin) and the PI5K HA epitope tag (visualized using Alexa 488-conjugated goat anti-mouse secondary antibody). Individual confocal sections and a merged image are shown. The enlarged *insets* highlight areas where colocalization of PI5K with short actin filaments is clearly evident. *Scale bar*, 7.5 µM. *B*, MDCK cells stably expressing GFP-actin were infected with AV-PI5K for 6 h and then imaged every 2 s. Enlarged areas shown are from individual frames from the supplementary movie. Two comets are seen to initiate from the area highlighted by the *square* over the time course; one at 108 s, and the other at 146 s. The starting points for each comet are marked with *white arrowheads* in subsequent frames.

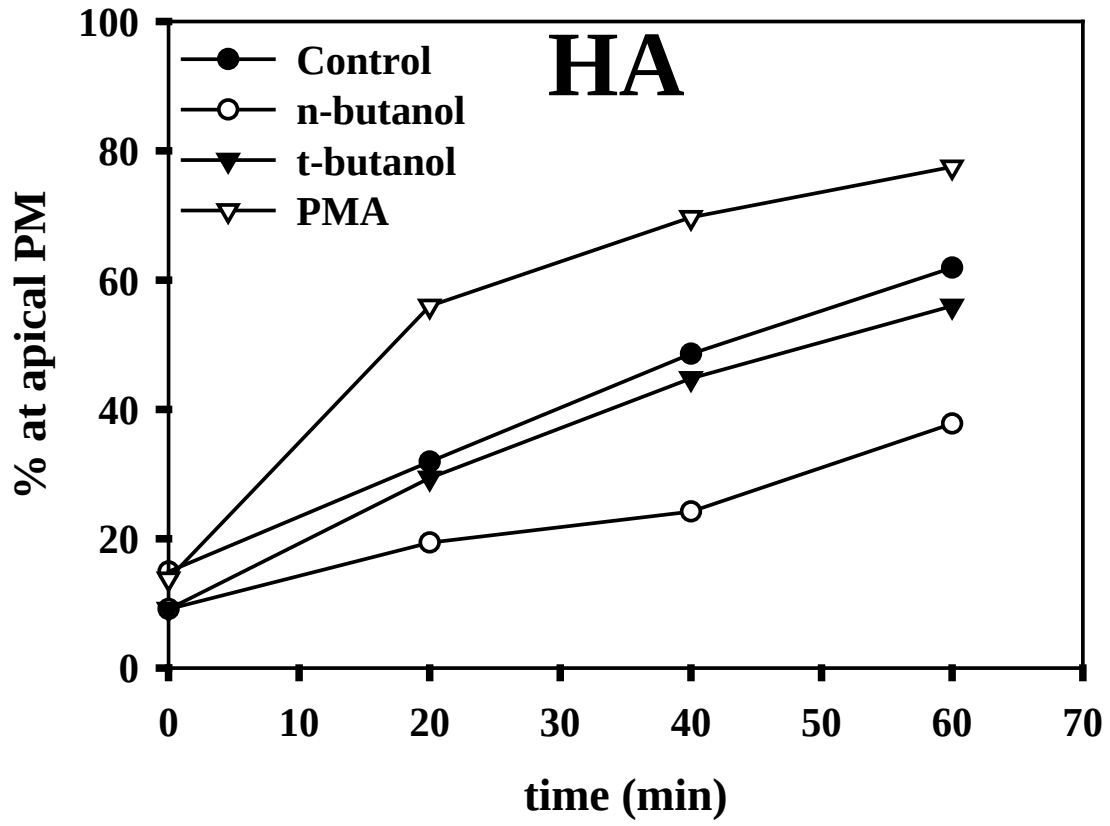

Figure 3.2 PMA and 1-butanol have opposing effects on HA delivery. MDCK cells infected with AV-HA were radiolabeled for 15 min and chased for 2 h at 19°C. PMA (5 µg/ml PMA), 1-butanol (*n*-butanol; 1% v/v), or *t*-butyl alcohol (*t*-butanol; 1% v/v) were added as indicated 10 min prior to the end of the chase period and included upon subsequent incubation at 37 °C for the indicated times. HA delivery to the apical surface was measured by cell surface trypsinization. Similar results were obtained in at least three experiments for each condition.

3.2.2 The Effect of PI5K on HA Delivery is Mediated through Arp2/3

If actin comets are involved in the TGN to apical membrane delivery of HA, then blockade of N-WASP-Arp2/3-mediated actin polymerization would be expected to inhibit HA transport. The WA domain of WASP/WAVE family proteins provides the binding sites for actin monomers and Arp2/3, and when expressed in isolation is a potent inhibitor of N-WASP function (158;161). As a control, I expressed the W domain, which binds to actin monomers but not to Arp2/3 (161).

Infection of MDCK cells with AVs encoding W or WA yielded comparable levels of the expected protein products (W ~16 kDa; WA ~18 kDa Figure 3.3A). As expected, expression of WA abolished PI5K-mediated formation of actin comets, demonstrating effective inhibition of Arp2/3 function (Table 2.1). I next examined the effect of the WA domain and PI5K on the morphology of polarized, filter-grown MDCK cells. Neither the WA domain nor PI5K had any apparent effect on cytoskeletal organization in polarized cells (Figure 3.3B; similar results for W domain, not shown). Moreover, neither tight junction morphology nor the positioning and morphology of the Golgi complex was affected by expression of these constructs (Figure 3.3, C and D), although I did notice in cells expressing very high levels of WA that the Golgi appeared to be somewhat dispersed toward the edges of the cells. As observed previously (Figure 2.1), PI5K was concentrated near the apical membrane, a region that contains the supranuclear Golgi complex and the actin-rich terminal web of these cells (Figure 3.3C). In contrast, WA was diffusely expressed throughout the cytoplasm of polarized MDCK cells (Figure 3.3C).

I next assessed the impact of W or WA domain expression on early transport of HA through the early biosynthetic pathway by monitoring the kinetics of HA acquisition of endo H resistance. Expression of WA or W had no discernable effects on the kinetics of HA traffic through the early Golgi (data not shown). Next, I examined the effects of these domains on HA

delivery from the TGN to the plasma membrane. Expression of WA inhibited kinetics of HA delivery to the apical cell surface by approximately ~50–75% relative to control over a 60-min chase period (Figure 3.4, A and B). Expression of the W domain did not significantly alter the delivery of HA indicating that expression of WA was not generally disrupting actin-driven processes. As with PI5K expression, the effect of WA on HA delivery was on rate rather than sorting, as HA surface polarity measured after long chase times was not compromised (not shown). The stimulatory and inhibitory effects of PI5K and WA on HA delivery kinetics were highly reproducible, and were statistically significant as assessed by Student's *t* test analysis of multiple experiments (Figure 3.4B). The inhibitory effect of the WA domain was specific for lipid raft-enriched apical cargo, as there was no effect of the domain on the apical delivery of p75 (Figure 3.4C). Moreover, expression of WA had no effect on the delivery of the basolateral marker VSV-G (Figure 3.4D).

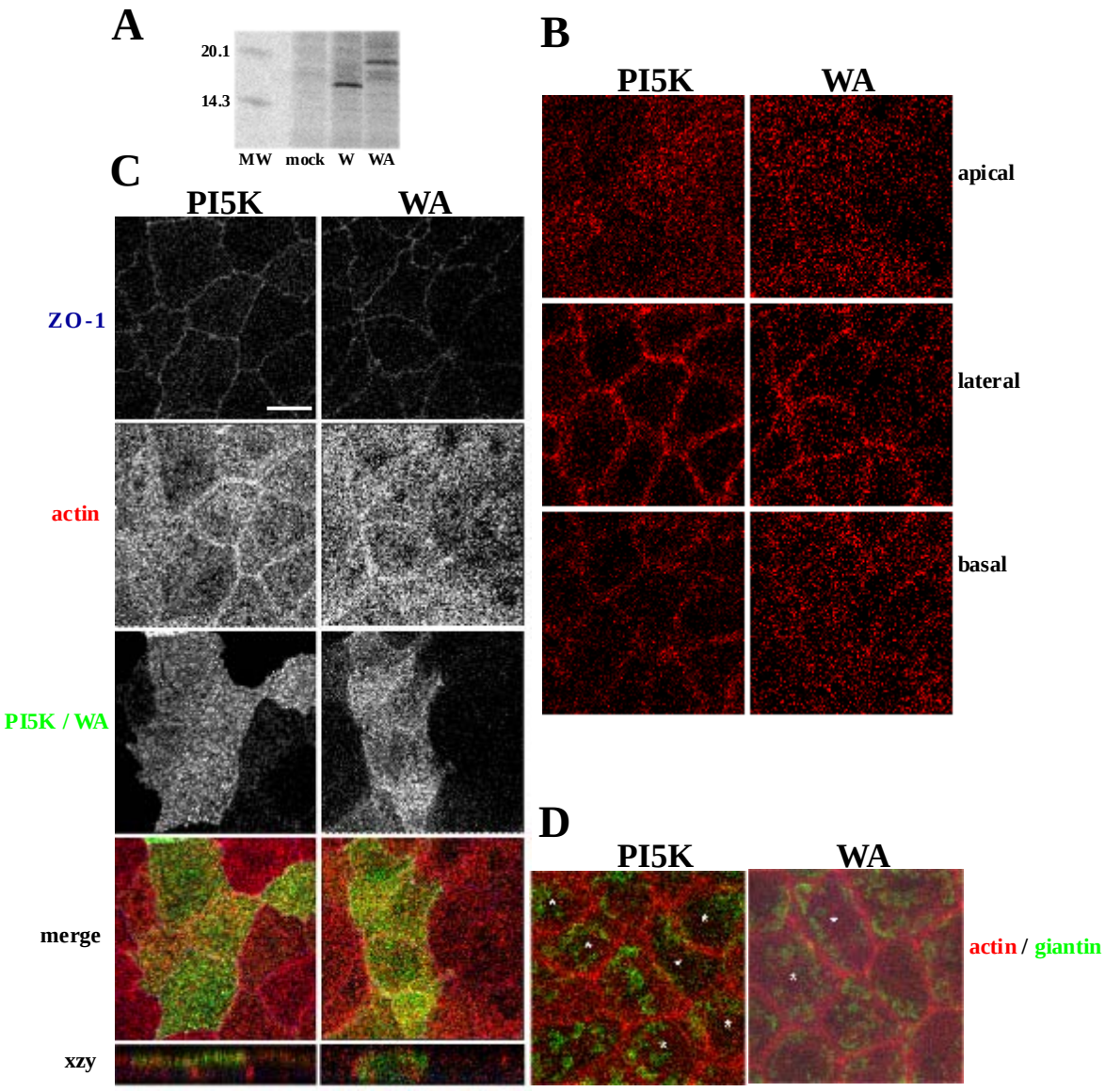

Figure 3.3 Expression of PI5K or the WA domain of Scar1 does not alter Golgi or actin morphology.

A, MDCK cells were mock-infected or infected with AVs encoding the W or WA domain of Scar1, radiolabeled for 1 h, and lysates run on a 15% SDS gel. The positions of molecular weight markers (*MW*) are shown. W and WA migrate at their expected molecular masses (16 and 18 kDa, respectively). *B*, expression of PI5K or WA does not disrupt actin morphology in polarized MDCK cells. Confocal sections from the apical, lateral, and basal portions of rhodamine phalloidin-labeled PI5K- or WA-expressing cells are shown. *C*, expression of PI5K or WA does not alter tight junction morphology of MDCK cells. Filter-grown cells were infected with either PI5K- or WA-expressing AVs. Samples were fixed and processed for indirect immunofluorescence to detect ZO-1, and PI5K or WA. ZO-1 was detected using secondary antibody coupled to Alexa 647 and PI5K or WA was visualized using Alexa 488-conjugated goat anti-mouse secondary antibody. Rhodamine phalloidin was included in the secondary antibody incubations to detect filamentous actin. Samples were imaged by confocal microscopy, and five slices (0.5 μm apart) through the region of the tight junctions were overlaid to make a maximum projection. Individual projections and merged xyz and xzy images are shown. *D*, samples infected as in *B* were stained with rhodamine phalloidin and monoclonal anti-giantin antibody followed by Alexa 488-conjugated secondary antibody. A projection of five sections taken through the Golgi region is shown. AV-infected cells (*asterisks*) were identified by co-labeling to detect PI5K (*left panel*) or WA (*right panel*). *Scale bar* = 7.5 μm for all xyz sections shown.

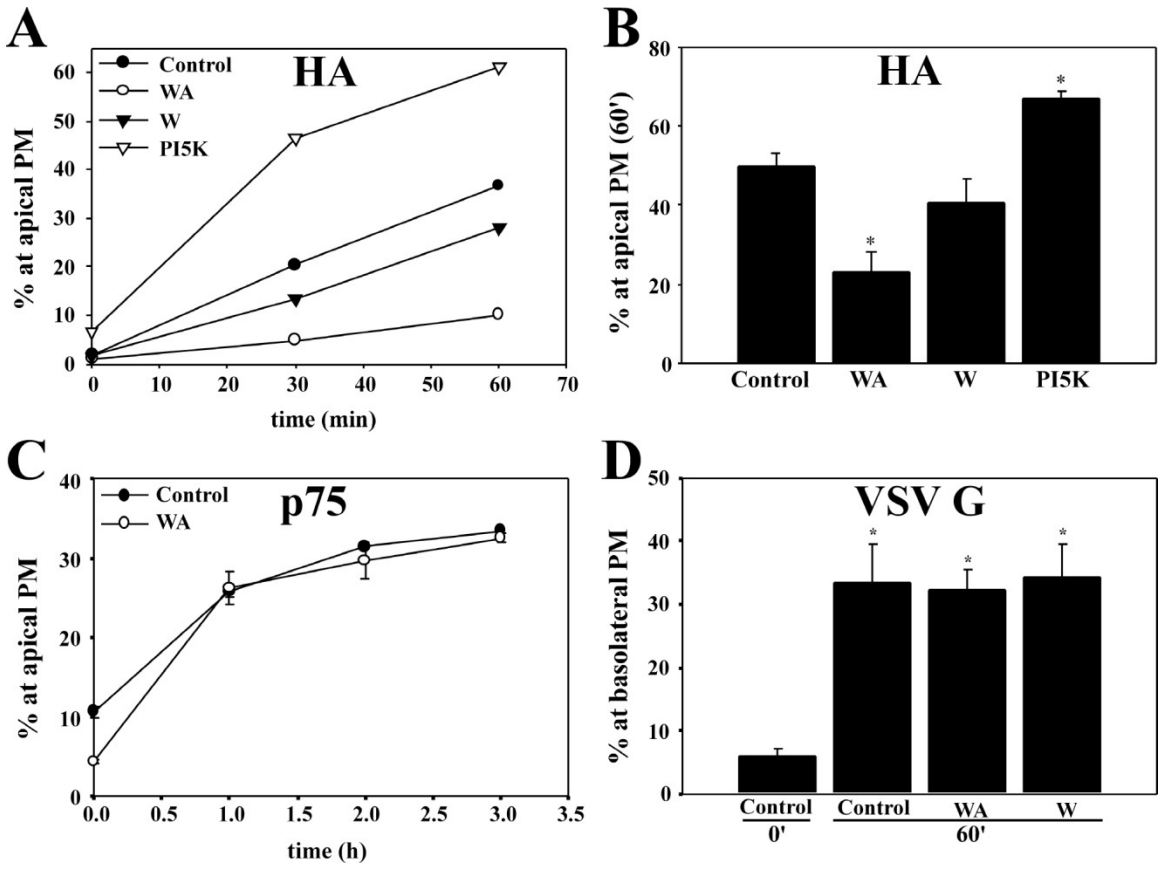

Figure 3.4 Expression of WA selectively inhibits apical delivery of HA.

A, WA inhibits apical delivery of TGN-staged HA. The kinetics of HA surface delivery were quantitated in MDCK cells co-infected with AV-HA, and either control AV or WA-, W-, or PI5K-expressing AVs as described previously. *B*, quantitation of the effects of WA, W, and PI5K on HA delivery. The *bar graph* shows the mean % of total HA (± S.E.) at the apical surface after a 60-min chase in at least 8 experiments for each condition. * denotes statistical significance from control measured using Student's *t* test (WA, $n = 8$, $p \leq 0.001$; PI5K, $n = 13$, $p = 0.001$). *C*, expression of WA has no effect on p75 delivery to the apical surface. Kinetics of p75 delivery were measured as described in the legend to Figure 2.3. Similar results were obtained in three experiments. *D*, WA does not affect basolateral delivery of TGN-staged VSV-G. MDCK cells were co-infected with VSV-G, and control, WA- or W-expressing AVs. VSV-G delivery to the basolateral cell surface was determined by cell surface biotinylation. Each experiment was performed using triplicate or quadruplicate samples, and mean ± S.E. from the indicated number of experiments is plotted. Data for control at 0 and 60 min are the same as those shown in Figure 2.3D. * denotes significant difference from control at 0 min (control at 0 min, $n = 3$; control at 60 min, $n = 8$, $p = 0.02$; WA, $n = 7$, $p = 0.005$; W, $n = 7$, $p = 0.03$; PI5K, $n = 4$, $p = 0.03$).

3.2.3 The Effect of Wiskostatin on Membrane Traffic *in vivo*

Expression of the WA domain of WAVE1 indicated that N-WASP was involved in biosynthetic traffic by significantly decreasing the rate of delivery of lipid-raft cargo, without changing the delivery rate of other types of apical proteins or a basolateral protein. However, the WA domain could also inhibit WAVE proteins, in addition to N-WASP. A rapidly growing number of publications have reported the use of wiskostatin to assess the role of N-WASP in various cellular processes (227-231). In some cases, the effects of wiskostatin on these pathways were interpreted as evidence for known or novel roles for N-WASP in cellular pathways. For example, addition of 50 µM wiskostatin to intestinal epithelial cells was found to inhibit the formation of nascent adherens junctions (227). A more recent report found that addition of 10 µM wiskostatin to B16-F1 cells rapidly dispersed mTuba-containing punctae and inhibited membrane ruffling (229). Another report used 50 µM wiskostatin to show that N-WASP-mediated vesicle motility is a downstream event in nonclassic apoptosis triggered by the adenoviral protein E4orf4 (230). Finally, Haller et al. (228) used 40 µM wiskostatin to demonstrate that N-WASP activation is important for the maturation of immunologic synapses on T-lymphocyte stimulation. In order to determine the role of N-WASP in polarized biosynthetic traffic, I tested the effect of wiskostatin treatment on the biosynthetic delivery of HA.

3.2.3.1 Wiskostatin Inhibits Arp2/3-dependent Apical Biosynthetic Traffic

I chose to use wiskostatin as a more specific inhibitor of N-WASP in order to confirm my results using the WA domain. On the basis of my data in Chapter 2, I hypothesized that wiskostatin would inhibit HA delivery to a level comparable to that of WA expression. HA-expressing MDCK cells (control or overexpressing PI5K) were radiolabeled for 15 min, incubated at 19ºC to

stage newly synthesized membrane proteins in the TGN, and then warmed to 37ºC, and HA surface delivery was monitored after 1 h with a surface trypsinization assay as described in Henkel et al. 2000 (232) As observed previously, HA delivery was stimulated relative to control in cells overexpressing PI5K and inhibited by expression of WA (Figure 3.5A). Inclusion of 50 µM wiskostatin during the 37ºC chase caused a profound inhibition of HA delivery in both control and PI5K-overexpressing cells. In contrast, the effect of WA domain expression on HA delivery was largely rescued by PI5K coexpression.

Next I examined the dose dependence of wiskostatin's effect on HA delivery. HA-expressing MDCK cells were radiolabeled, HA was staged in the TGN at 19ºC for 2 h, and 10–50 µM wiskostatin or vehicle alone was added to the cells before warming to 37ºC and quantitation of surface delivery kinetics. Additionally, some samples were treated with 50 µM wiskostatin during the 2-h stage and then washed extensively before warming to 37ºC to assess the reversibility of wiskostatin's effect (Figure 3.5B). HA surface delivery was unaffected by acute addition of 10 µM wiskostatin, but treatment with higher concentrations (25 or 50 µM) resulted in a virtual blockade in apical delivery. Moreover, the effect of wiskostatin treatment was irreversible over this period, because washout of the drug before warming failed to restore normal delivery kinetics.

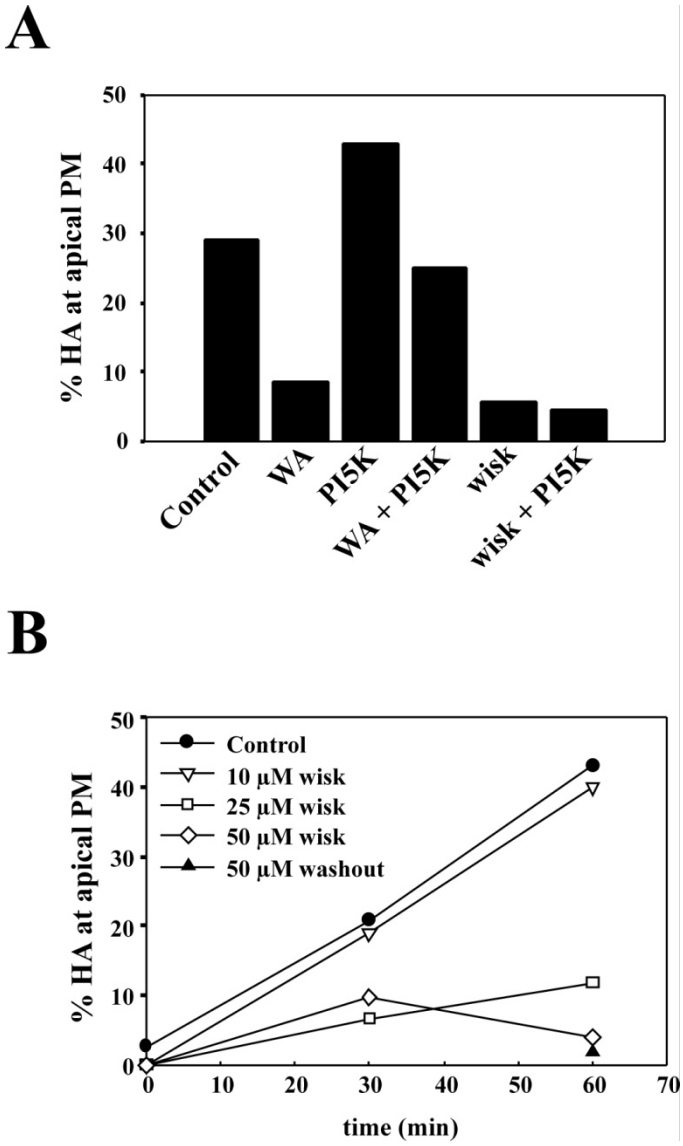

Figure 3.5 Wiskostatin inhibits neuronal Wiskott-Aldrich syndrome protein (N-WASP)-dependent steps in membrane transport.

A: polarized Madin-Darby canine kidney (MDCK) cells were infected with replication-defective recombinant adenoviruses encoding influenza hemagglutinin (HA) and phosphatidylinositol 4-phosphate 5-kinase (PI5K) and/or a construct encoding a dominant-negative inhibitor of N-WASP function (WA) as indicated. The following day, cells were radiolabeled for 15 min and chased for 2 h at 19°C to accumulate newly synthesized proteins in the *trans*-Golgi network. Apical delivery of HA was quantitated after warming to 37°C for 1 h in the presence or absence of 50 µM wiskostatin (wisk). *B*: cells were prepared as in *A* and were treated with wiskostatin at the indicated concentrations or with 50 µM wiskostatin during the 2-h chase followed by washout before warming to 37°C. The results of a single experiment in each case are shown. PM, plasma membrane.

3.2.3.2 Wiskostatin Inhibits N-WASP-independent Steps in Transport

As a control to ensure the selectivity of wiskostatin for N-WASP-dependent cellular processes, I examined the effect of this drug on early steps in biosynthetic transport that are thought to be N-WASP-independent (233;234). MDCK cells expressing HA were starved in methionine-free medium, radiolabeled for 15 min, incubated for 2 h at 19ºC to accumulate mature (sialylated) HA in the TGN, and then either solubilized or warmed to 37°C for 1 h, and surface delivery was assessed (Figure 3.6). Wiskostatin (50, 25, or 10 µM) was added at various stages during this pulse-chase protocol. Addition of wiskostatin for 2 h at 19ºC after the radiolabeling period decreased the accumulation of sialylated HA compared with a mock-treated sample in a dose-dependent manner (Figure 3.6, *lanes C* and *A*, respectively), consistent with inhibition of either intra-Golgi transport or the cellular glycosylation processing machinery. On subsequent warming to 37ºC in the continued presence of wiskostatin, only 1.8% (50 µM), 2.7% (25 µM), or 20% (10 µM) of the total HA reached the cell surface in wiskostatin-treated cells (Figure 3.6, *lane D*). In contrast, 53% of the total HA in mock-treated samples reached the surface during this period, as assessed by the susceptibility of HA to cleavage into HA1 and HA2 fragments on surface trypsinization (Figure 3.6, *lane E*). Moreover, when wiskostatin was added to cells during the 30-min starvation period and in subsequent steps, I observed a loss in the synthesis of radiolabeled HA, particularly at the higher wiskostatin concentrations (Figure 3.6, *lane B*). In cells treated with 50 µM wiskostatin during the starve and pulse, HA recovery was decreased by 92% compared with control, whereas 25 µM and 10 µM wiskostatin decreased recovery by 28% and 7.3%, respectively. Thus wiskostatin appears to inhibit uptake of radioactive methionine and/or disrupt protein synthesis.

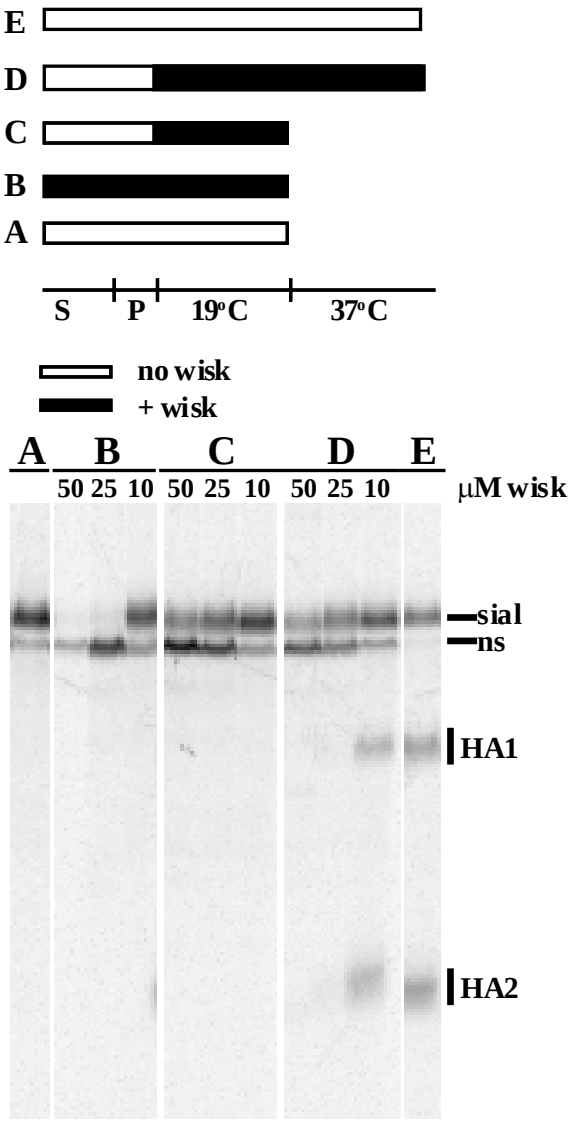

Figure 3.6 Wiskostatin inhibits N-WASP-independent steps in protein processing. HA-expressing MDCK cells were starved (S) for 30 min, radiolabeled (P) for 15 min, incubated for 2 h at 19°C ,and then either solubilized immediately (samples in *lanes A*, *B*, and *C*) or incubated for 1 h at 37°C and trypsinized to quantitate surface delivery of HA before solubilization. HA was visualized after immunoprecipitation and SDS-PAGE. Samples in *lanes A* and *E* were mock-treated, whereas wiskostatin was added to the remaining samples beginning at the starve (*lane B*) or at the start of the 19°C incubation (*lanes C* and *D*). The migration of immature (ns) and sialylated (sial) forms of HA as well as the cleavage products generated on surface trypsinization (HA1 and HA2) are indicated. Surface delivery of HA in the samples in *lanes D* and *E* was 1.8% (50 μM), 2.7% (25 μM), 20% (10 μM), and 53% (control, *lane E*) of the total HA. Similar results were obtained in 2 experiments.

My results described above suggested that wiskostatin inhibits multiple steps along the biosynthetic pathway. To examine its role in postendocytic transport, I measured the effect of wiskostatin on basolateral-to-apical transcytosis of IgA in MDCK cells stably expressing the rabbit pIgR. In this multistep pathway, IgA binds to pIgR at the basolateral cell surface and is transported across the cell, where pIgR is cleaved to release a soluble IgA-pIgR complex into the apical medium. Transcytosis of IgA in these cells has previously been demonstrated to be actin-dependent (235). MDCK cells were incubated for 10 min at 37ºC with basolaterally added ^{125}I-IgA, washed extensively on ice, and then warmed to 37ºC in the presence or absence of the indicated concentrations of wiskostatin. Transcytosis was quantitated as the release of ^{125}I-IgA into the apical medium as described in Henkel et al. 1998 (236). Transcytosis was rapid and efficient, approaching 80% of the internalized ^{125}I-IgA within 1 h of warm-up (Figure 3.7). In contrast, transcytosis was rapidly inhibited in a dose-dependent manner when wiskostatin was added to the cells at the start of the 37°C warm-up period. Inhibition of ^{125}I-IgA transcytosis by wiskostatin could reflect a block in membrane traffic or alternatively, inhibition of the proteolysis step required for the apical release of secretory component. However, when 50 µM wiskostatin was added to cells before the incubation with ^{125}I-IgA, internalization of the radioligand was completely inhibited (data not shown).

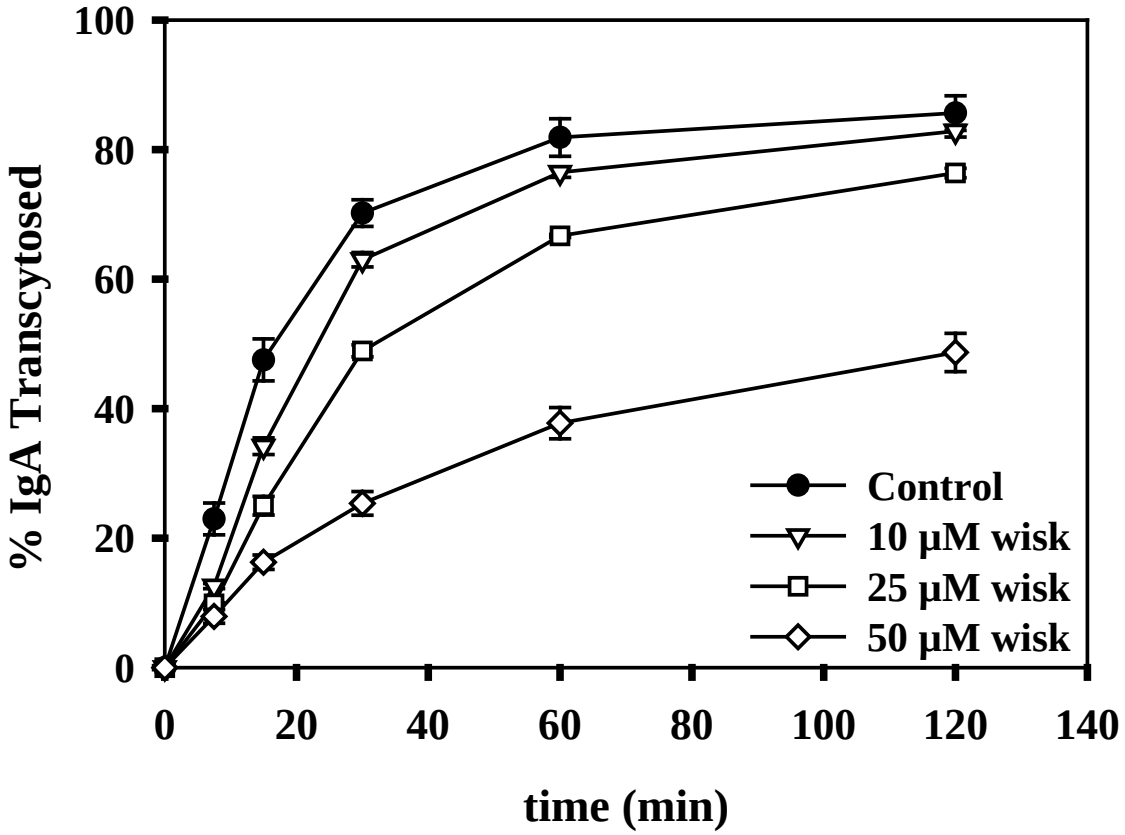

Figure 3.7 Wiskostatin inhibits actin-dependent postendocytic membrane trafficking steps. Polarized MDCK cells were incubated with basolaterally added ^{125}I-labeled IgA for 10 min at 37°C and then washed extensively on ice. Apical release of ^{125}I-IgA was quantitated on warming to 37°C in the presence or absence of the indicated concentrations of wiskostatin added after IgA internalization. Means ± SD of triplicate samples are plotted.

3.2.3.3 Wiskostatin Decreases Cellular ATP Levels

It was shown previously that depletion of cellular ATP by energy poisons such as sodium azide dramatically inhibits protein processing and secretion (237). The rapid and profound effects of wiskostatin on multiple steps in protein synthesis, endocytosis, and membrane traffic suggested that this drug may similarly perturb cellular ATP levels. To examine this possibility, MDCK cells plated in 12-well dishes were treated with wiskostatin at 10, 25, or 50 µM or vehicle for 0–1 h at 37°C. ATP was extracted and quantified with a luminometry-based assay (Figure 3.8). Addition of 25 µM and 50 µM wiskostatin, respectively, resulted in the rapid and nearly complete loss of cellular ATP, decreasing the levels to 57% and 30% of control within 15 min and to 18% and 9.4% of control within 1 h. Treatment with 2% sodium azide resulted in a comparable drop in ATP levels, to 4.6% of control after 1 h of treatment (not shown). Wiskostatin added at a lower concentration (10 µM) had a less dramatic effect on cellular ATP in MDCK cells (84% and 81% of control at 15 min and 1 h, respectively). Washout of the drug for 30 min after a 1 h treatment with any concentration of wiskostatin did not restore normal ATP levels, suggesting that the effects of the drug on cellular energy status are irreversible over this time period.

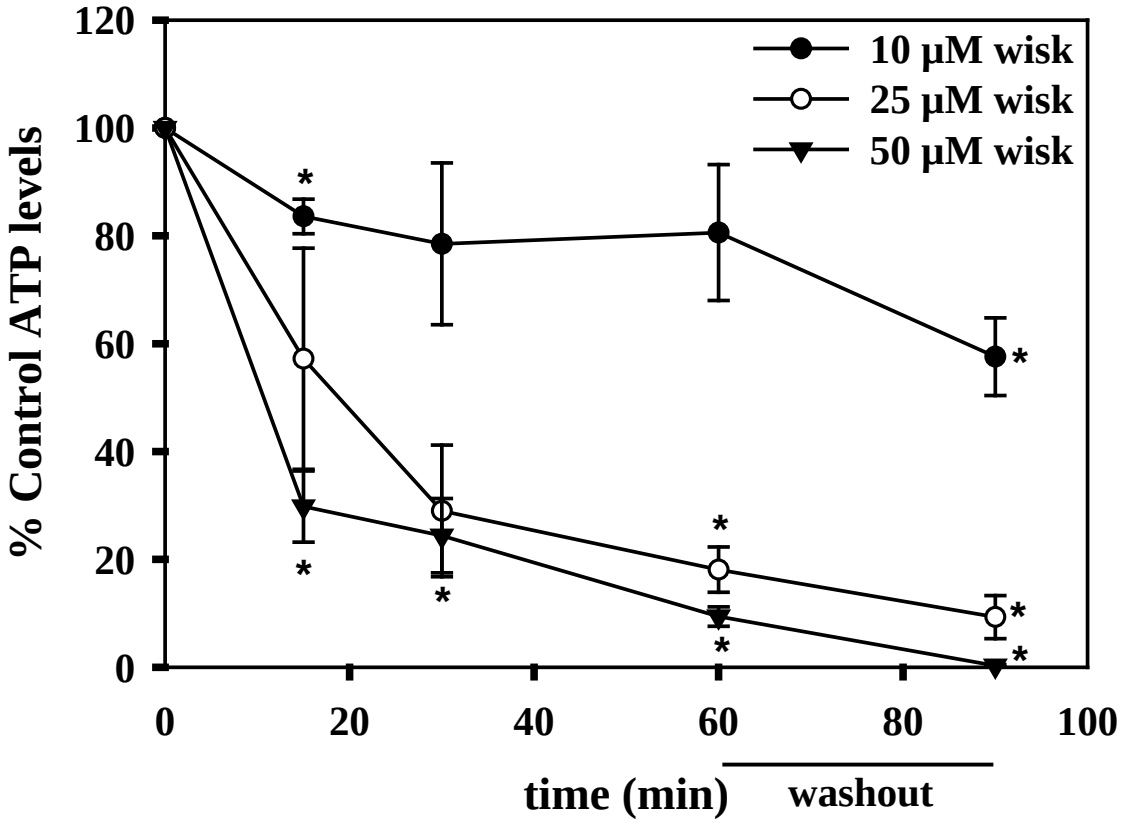

Figure 3.8 Wiskostatin reduces cellular ATP levels.
MDCK cells plated in 12-well dishes were treated with vehicle alone or with wiskostatin at 50, 25, or 10 µM for the indicated time periods. Some drug-treated samples were washed extensively after 1 h of treatment and incubated for an additional 30 min (washout) before assessment of cellular ATP levels as described in materials and methods. The dose- and time-dependent effect of wiskostatin on ATP levels was normalized to control cells and plotted (means ± SE of 3 independent experiments). *$p < 0.05$ compared with control based on paired *t*-test of log-transformed raw data. Treatment with the known energy poison sodium azide (2%) decreased cellular ATP levels to 4.6% of control after 1 h of treatment (not shown).

3.2.4 N-WASP Knockdown Inhibits HA Delivery

The data generated with wiskostatin did not convincingly support a role for N-WASP in biosynthetic traffic, as wiskostatin had multiple off-target effects *in vivo*. To more specifically probe for N-WASP-dependent effects, I chose to use siRNA. This approach was not chosen initially because knockdown in polarized cells is notoriously difficult, but new approaches including siRNA electroporation became available during the course of my work. I designed an siRNA targeting canine N-WASP based on a previously published siRNA oligo (238). I assessed the extent of knockdown using Western blotting and found only modest knockdown, 15-40% (Figure 3.9). However, when I examined the effect of N-WASP knockdown on polarized biosynthetic traffic I found that despite the modest knockdown, the rate of biosynthetic delivery was inhibited by up to 53% relative to control (Figure 3.10). These data confirm my initial observation and support my conclusion that N-WASP-mediated actin polymerization plays an important role in the rate of biosynthetic delivery of lipid raft-associated proteins.

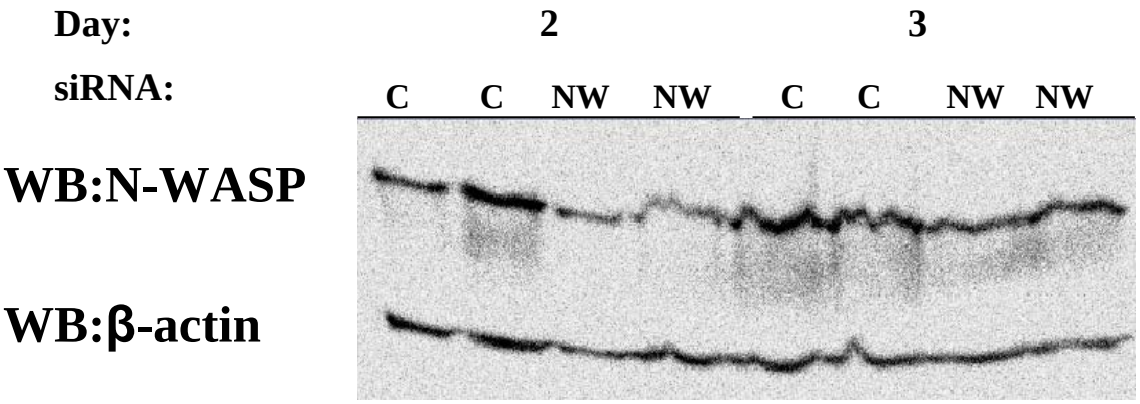

Figure 3.9 Knockdown of N-WASP in polarized MDCK cells.

Low passage MDCK cells grown to 50% confluence were trypsinized and resuspended into Amaxa solution mix at a density of 1 x 10^6 cells/100µl solution. 100 ul of the cells were mixed with 2.5 or 5 ug of control or OCRL siRNA and placed into a cuvette. Samples were nucleofected using program T-020 and were then either put directly onto filters for either two or 3 days. Samples were harvested and analyzed by western blot for N-WASP and β-actin as a loading control. Quantitation of data using a VersaDoc (BioRad) and Quantity One software were performed. The left side of the image is labeled to denote the N-WASP and β-actin bands. Above the image, the days of siRNA treatment is denoted and below individual lanes are labeled C for control siRNA and NW for N-WASP siRNA.

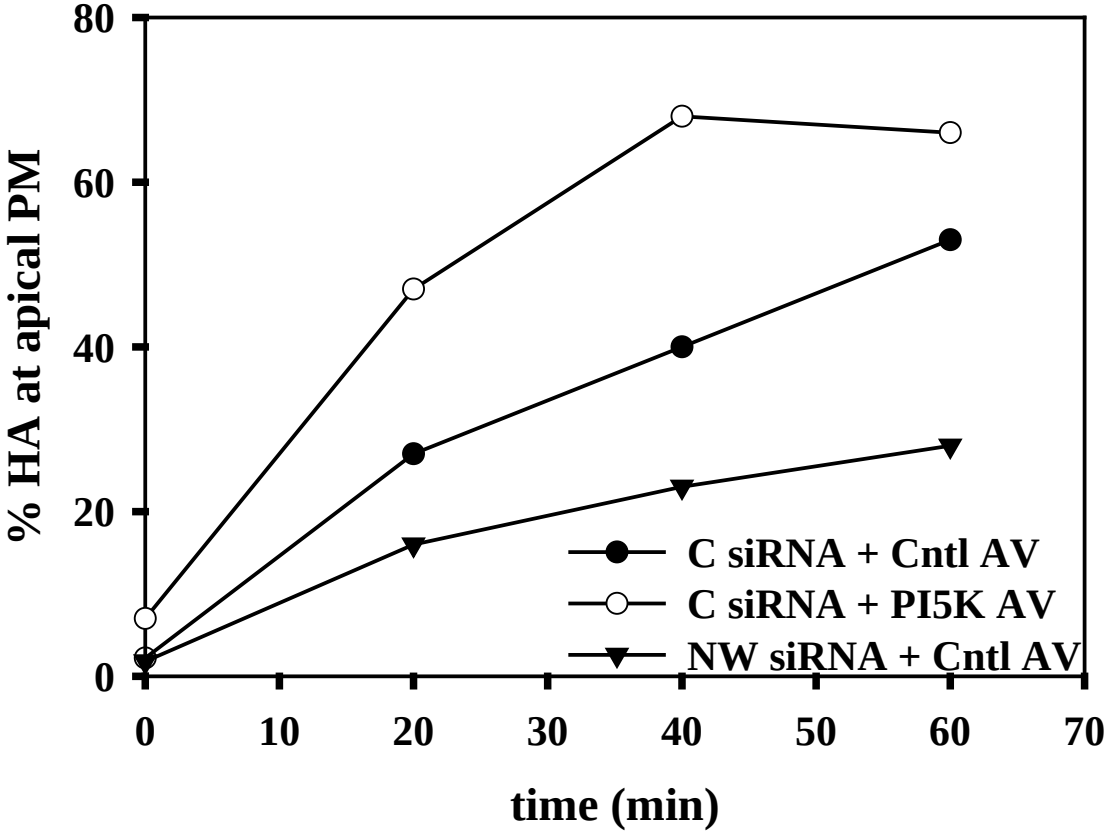

Figure 3.10 N-WASP knockdown inhibits biosynthetic delivery.

MDCK cells were electroporated in buffer containing either control (C) or N-WASP (NW) siRNA oligo. The cells were then seeded onto Transwell filters and infected with control(Cntl)-AV or PI5K-AV before the experiment on day 3. HA infected cells were starved, pulsed with ^{35}S-TransLabel and chased for 2 h. Surface delivery was measured using a cell surface trypsinization assay. The graph represents one experiment from n=3 independent experiments with similar results.

3.2.5 HA is Associated with Actin Comets in MDCK Cells

The data described above suggested the selective involvement of PI5K-stimulated, N-WASP-dependent actin comets in the TGN-to-apical membrane delivery of HA. To test whether newly synthesized HA could be visualized in association with actin comets, MDCK cells seeded on glass coverslips were co-infected with AV-PI5K and AV-HA for 8 h, and then incubated at 19ºC for 2.5 h to accumulate HA in the TGN. Samples were then warmed to 37ºC for 30 min, fixed, and processed for indirect immunofluorescence to visualize actin, HA, and PI5K (Figure 3.11). Numerous actin comets were detected in these cells, many of which stained positively for both PI5K and HA (Figure 3.11, *arrows*). In 25 images I observed 71 comets of which 20 (28%) were positive for both HA and PI5K. By contrast, in 20 images I observed 57 comets of which only 2 (3.5%) were positive for p75 and PI5K.

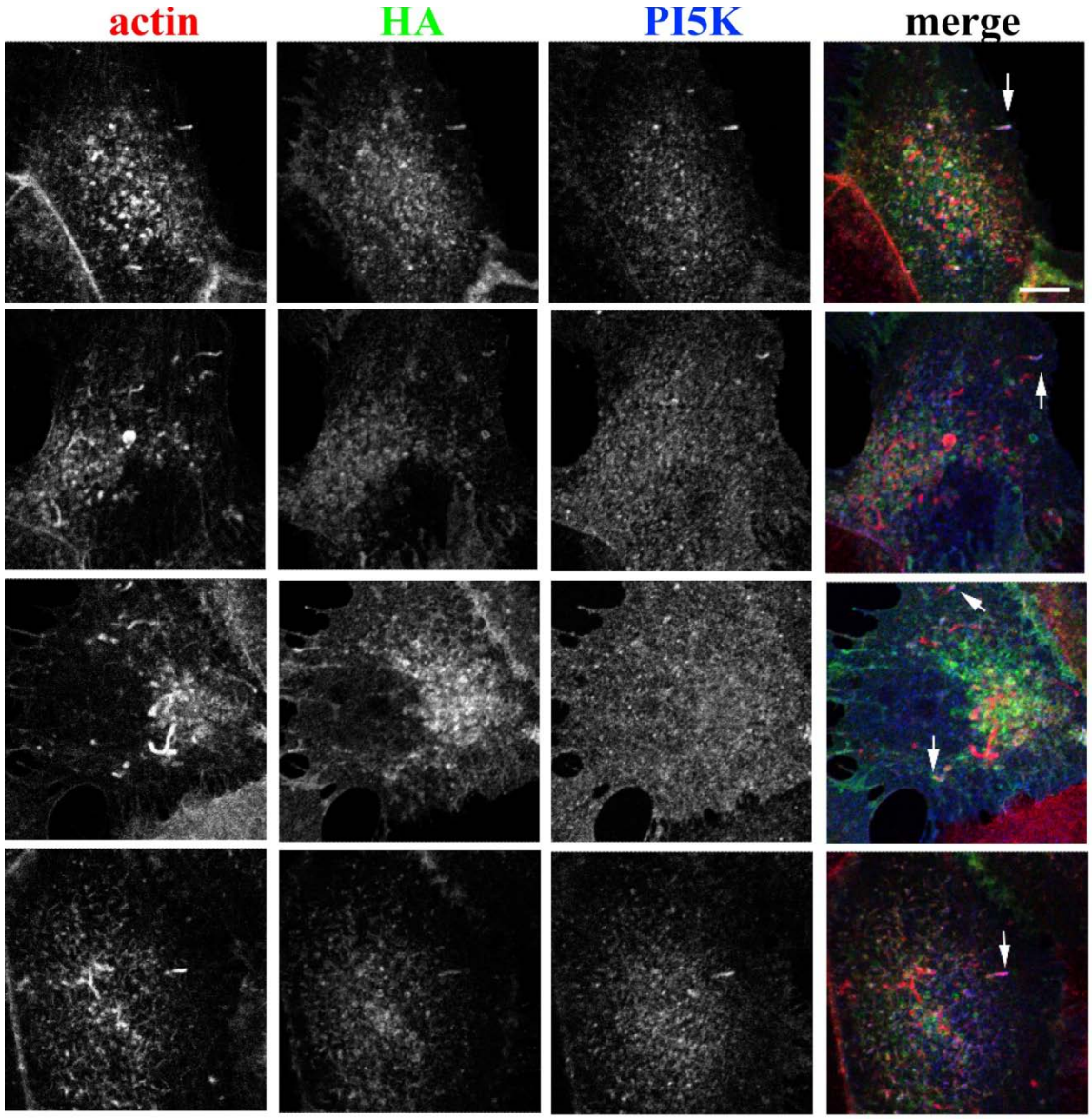

Figure 3.11 HA and PI5K are associated with actin comets in MDCK cells.
MDCK cells grown on coverslips were co-infected with AV-HA and either control or PI5K for 8 h. HA was staged in the TGN for 2.5 h and 19°C, then warmed to 37°C for 30 min prior to fixation and processing for indirect immunofluorescence. Actin was stained using rhodamine phalloidin; HA was visualized using monoclonal antibody Fc125 followed by a Alexa 488-conjugated goat anti-mouse, and the PI5K HA epitope tag was visualized using a polyclonal antibody followed by Alexa 647-conjugated goat anti-rabbit. Individual confocal sections for each channel and a merged image demonstrating several examples of actin comets that co-label with HA and PI5K (marked with *arrows*) are shown. *Scale bar*, 7.5 μm.

3.3 DISCUSSION

I investigated the role of N-WASP in polarized biosynthetic traffic downstream of PI5K activity. I found that MDCK cells are capable of forming actin comets and that expression of AV-PI5K dramatically increases the rate of actin comet formation. Moreover, pharmacological treatments that modify actin comets, such as PMA or 1-butanol have parallel effects on actin comet formation and HA delivery. Inhibition of Arp2/3 via expression of the WAVE1 WA domain significantly inhibited the rate of HA delivery, while having no effect on either another apical marker (p75) or a basolateral maker (VSV-G). Wiskostatin was used to specifically test for N-WASP involvement in comet formation, but was found to have non-specific effects on membrane traffic. Ultimately, knockdown of N-WASP indicated that N-WASP is important in HA delivery, and immunofluorescence microscopy confirmed that both HA and PI5K were found associated with actin comets in fixed cells. Together these biochemical and imaging data provide strong evidence for a novel role for actin comets in polarized biosynthetic delivery of lipid raft-associated proteins.

3.3.1 The Role of Actin in Biosynthetic Traffic

Numerous studies have documented the roles of actin in intra- and post-Golgi transport (239). These have ranged from observations of the presence of actin and actin-associated proteins associated with the Golgi complex (240-242) to more mechanistic insights into the potential roles of actin polymerization in biosynthetic traffic (217). Interestingly, the ADP-ribosylation factor, Arf1 appears to be important for actin assembly on Golgi membranes (241) and this process requires coatomer-bound Cdc42 and activation of the Arp2/3 complex (243;244). Cdc42 may

also regulate recruitment of dynein to coatomer protein complex I vesicles (245). However, the consequences of these signaling cascades on intra-Golgi membrane traffic are not clear. I found no effect of expression of either PI5K or the WA domain of WAVE1 on intra-Golgi transport kinetics, suggesting that PIP_2- and Arp2/3-mediated actin polymerization are not required for the transport or maturation of cargo.

Arf-dependent actin recruitment has also been implicated in post-Golgi transport. Recruitment to Golgi membranes of the actin-binding protein cortactin was shown to be Arf-dependent, and disruption of this complex in BHK cells had profound effects on the surface delivery of VSV-G without affecting intra-Golgi transport (246). However, our laboratory has previously demonstrated that TGN export of HA occurs independently of Arf function (6). Modulation of actin dynamics by the clathrin- and actin-binding protein Hip1R has also been suggested to regulate formation and release of clathrin-coated vesicles from the TGN (247).

3.3.2 The Use of Wiskostatin as a Probe for N-WASP Function

The studies described in this chapter suggest that wiskostatin has global and likely nonspecific effects on membrane traffic and other pathways. Treatment of polarized MDCK cells with this drug inhibited protein synthesis and maturation and disrupted both biosynthetic and postendocytic traffic. The effects of wiskostatin on these transport steps were dose dependent, irreversible, and roughly paralleled in magnitude the effects of the drug on cellular ATP levels. Notably, however, gross cellular morphology and actin structure were not visibly altered after a 1 h incubation with 50 μM wiskostatin, indicating that cell death was not occurring during this period (data not shown).

I can only speculate as to the mechanism by which wiskostatin perturbs cellular ATP levels. Metabolic energy poisons fall into one of four classes, the first two of which are most common: *1*) inhibitors of electron transport, *2*) uncouplers/ionophores, *3*) inhibitors of ATP synthase, and *4*) inhibitors of transport systems (248). Members of the first group include rotenone, cyanide, and sodium azide, which block electron transport by interacting irreversibly or competitively with components of the electron transport chain (249;250). The second group includes 2,4-dinitrophenol (DNP) and carbonyl cyanide *p*-trifluoromethoxyphenylhydrazone (FCCP), which disrupt the proton gradient by acting as proton ionophores (251;252). The aromatic structure of wiskostatin suggests the possibility that, like DNP, it may also disrupt membrane integrity; however, elucidating the mechanism by which this drug interferes with cellular ATP homeostasis requires further study.

The effect of wiskostatin on most cellular transport steps and on ATP levels demonstrated a steep dose-dependent response at concentrations between 10 and 25 µM. Treatment with 10 µM wiskostatin decreased ATP levels by only ~20% after a 1-h treatment and had comparable effects on protein synthesis and maturation when added acutely to cells (Figure 3.6, *lanes B* and *C*). In contrast, treatment with 25 µM wiskostatin decreased ATP levels by 80% over this time period. Interestingly, 10 µM wiskostatin did not affect the efficiency of surface delivery when added acutely after cargo had been prestaged in the TGN (Figure 3.5); however, surface delivery (but not HA maturation) was severely compromised (by 80%) when the drug was added at the start of the 2-h TGN staging period at 19ºC (Figure 3.6, *lane D*). A possible explanation is that post-Golgi transport may be insensitive to acute ATP depletion compared with other steps; however, longer incubations with this concentration of wiskostatin might sufficiently affect ATP levels to inhibit this step or otherwise disrupt other cellular functions required for efficient

membrane traffic. Ironically, it is this very step in membrane transport, namely TGN-to-apical surface delivery of HA, that I found to be N-WASP-dependent based on my studies using the WA domain (234). Previously published studies have utilized variable concentrations of wiskostatin, ranging from 10 to 50 μM (227-231). In all of these reports, rapid and profound effects on the particular cellular function being studied were noted and ascribed to selective inhibition of an N-WASP-dependent pathway. Given the global effects of wiskostatin on cellular transport processes and ATP levels, however, it is clear that this drug is inappropriate for *in vivo* studies aimed at selectively perturbing N-WASP function, or for potential therapeutic use as previously suggested (221). Moreover, novel roles ascribed to N-WASP in cellular pathways based solely on *in vivo* effects observed with wiskostatin merit careful reexamination.

3.3.3 The Role of Actin in Polarized Biosynthetic Traffic

Specific roles for actin polymerization in the transport of apical proteins, and lipid raft-associated cargo in particular, have previously been suggested. Rozelle et al. (158) observed that newly synthesized HA was preferentially localized to the tips of short polymers of actin reminiscent of N-WASP-dependent comets in PI5K-overexpressing cells. In support of this, PIP_2 has been suggested to be enriched in lipid rafts (253-255) although this conclusion has recently been challenged (31;256). Moreover, my observation that expression of either PI5K or WA had no effect on apical delivery of a non-raft-associated protein adds support to the idea that transport of raft-associated and raft-independent proteins is differentially regulated. Jacob *et al.* (9;199) have previously suggested that biosynthetic transport carriers containing the lipid raft-associated hydrolase sucrase isomaltase traffic via actin cables to the cell surface, whereas carriers enriched in the non-raft apical protein lactase-phlorizin hydrolase traffic in separate carriers in an actin-

independent manner. Recently, the same group identified α-kinase 1, which phosphorylates the motor protein myosin I, as a component of sucrase isomaltase but not lactase-phlorizin hydrolase-containing vesicles and demonstrated a role for this motor in apical delivery of sucrase isomaltase (257). Whether α-kinase 1 activity is important for the PI5K-mediated stimulation of HA delivery I observed is not known; however, in a parallel scenario, both myosin motors and N-WASP-Arp2/3-mediated actin polymerization have been suggested as mechanisms that propel internalized endocytic vesicles through the actin-rich cortical cytoskeleton (154;219;258-260).

3.3.4 Concerted Cytoskeletal Function in Polarized Membrane Traffic

Regardless of the role (s) for actin polymerization in apical membrane traffic, it is likely that the long-range directionality of biosynthetic membrane traffic is provided ultimately by the microtubule network. Previous biochemical studies have demonstrated a role for microtubules in polarized membrane transport in MDCK cells (261-264). In addition, live cell imaging has clearly shown that VSV-G-containing transport carriers move to the plasma membrane on microtubule tracks (265;266). I found that disruption of actin with cytochalasin D or by expression of WA in concert with nocodazole treatment virtually abolished delivery of HA to the apical membrane, and ultimately disrupted the polarity of delivery (not shown). In contrast, expression of WA alone had no effect on HA polarity. My data are reminiscent of studies by Maples *et al.* who demonstrated a concerted role for actin and microtubules in basolateral to apical transcytosis of the polymeric immunoglobulin receptor (235). My results do not necessarily suggest that actin comets are obligatory for apical delivery, but rather that they may facilitate apical transport of HA under some conditions. I hypothesize that actin-based movement of HA-containing transport carriers facilitates their access to microtubule tracks that provide the

directionality for efficient transport to the apical membrane, and/or ferries transport carriers across the actin-rich terminal web to their site of fusion.

*Some text in this chapter and Figures 3.1, 3.2, 3.3, 3.4, and 3.11 are published in Guerriero et al. *JBC* 2006 and were used with the permission of the Journal of Biological Chemistry.

**Some text in this chapter and Figures 3.5, 3.6, 3.7, and 3.8 are published in Guerriero et al. *Am J Physiol Cell Physiol* 2007 and were used with the permission of the American Journal of Physiology Cell Physiology.

4.0 CONCLUSION

Protein sorting along the biosynthetic pathway is a multi-step process that requires the coordinated action of both proteins and lipids. In recent years there has been an increasing appreciation of the role of lipid metabolism in membrane trafficking pathways. Diseases of phosphatidylinositol metabolism can disrupt physiological processes like renal protein reabsorption, as observed in Lowe Syndrome, which highlights the importance of lipid metabolism for normal membrane traffic in polarized kidney cells.

In this dissertation, I investigated the role of PIP_2 metabolism in biosynthetic traffic of polarized MDCK cells. Previously, apical biosynthetic traffic was shown to be regulated by levels of PI4P in the Golgi (50). Many lines of evidence also point toward a role for PIP_2 metabolism in normal Golgi function. I found that overexpression of the α isoform of PI5K stimulates the rate of biosynthetic traffic of the lipid raft-associated marker HA. Moreover, decreasing cellular PIP_2 (via OCRL overexpression) inhibits the rate of HA delivery, demonstrating a correlation between PIP_2 levels and biosynthetic traffic of HA. While knockdown of OCRL did not affect biosynthetic traffic, a clear role exists for PIP_2 in surface delivery of newly synthesized HA.

Actin participates in and provides the motile force for many membrane trafficking events, including endocytosis and pathogen motility. An upstream controller of actin-based motility is PIP_2, which can recruit nucleation promoting factors (NPFs) to the surface of the motile

structure. One such NPF, N-WASP is responsible for branched actin filament formation via the Arp2/3 complex and is activated by PIP_2. Using multiple approaches, including dominant negative inhibitors and siRNA-mediated knockdown, I demonstrated that N-WASP is required for HA delivery. Moreover, I found that PI5K and HA are associated with actin comets in MDCK cells, linking PI5K-stimulated HA delivery, PIP_2 metabolism, and actin comet formation. Together, my data support the discovery of a novel role for PIP_2 metabolism and N-WASP-mediated actin comets in the efficient polarized biosynthetic traffic of lipid raft-associated proteins. Below I discuss the implications of my findings with respect to our understanding of polarized membrane traffic and the pathogenesis of Lowe syndrome.

4.1 THE FUNCTION OF OCRL IN POLARIZED EPITHELIAL CELLS

I found that overexpression of OCRL inhibits the rate of HA delivery, likely due to a decrease in cellular PIP_2 levels. To examine the consequences of loss of OCRL I used siRNA-mediated knockdown to silence endogenous canine OCRL. OCRL knockdown stimulated the rate of actin comet formation similar to PI5K overexpression. In addition, knockdown slightly increased PIP_2 levels. Therefore, I predicted that knockdown may also stimulate HA delivery as I saw with PI5K overexpression, but this was not observed. There are several possible explanations for why siRNA knockdown of OCRL did not produce to the hypothesized effects on biosynthetic delivery.

One interpretation for the increase in actin comets without a concomitant trafficking phenotype is that actin comets resulting from OCRL knockdown originate from a different compartment than those stimulated by PI5K overexpression. In live cell microscopy studies I

found that actin comets resulting from PI5K seem to originate from a region localized near the TGN (not shown). While I was unable to directly see comets emanating from the TGN, these data do suggest that comets form in close proximity to the Golgi complex. Comets generated by OCRL knockdown may instead form on endosomes or endocytic vesicles. Live cell microscopy could be used to test if comets in OCRL-deficient cells are more frequently associated with endosomes than comets in PI5K-overexpressing cells. The percentage of comets on endocytic structures could be determined by monitoring actin comet formation in cells preloaded with a fluorescently-tagged dextran to mark endocytic compartments. I predict that OCRL comets will more frequently propel structures loaded with dextran than PI5K-stimulated comets. Another approach to test the origin of OCRL-stimulated comets would be to look for association of comets with biosynthetic cargo in fixed cells. I found that TGN-staged HA was enriched on PI5K-induced actin comets when compared to another apical marker p75. Therefore, a similar approach could be used in OCRL KD cells and determine if OCRL comets are associated with HA to a greater or lesser extent than PI5K-stimulated comets. I found that ~30% of PI5K comets associate with HA, and I predict that OCRL-stimulated comets are less likely to be associated with HA.

A second interpretation of my results is that OCRL's regulation of actin comet formation is not linked to the role of PIP_2 in biosynthetic membrane traffic. OCRL interacts with clathrin and AP-2 and has been found associated with CCVs providing evidence that OCRL may be important for endocytic traffic (74). Additionally, OCRL interacts with the Rab5 effector APPL1, which is found on a subset of peripheral early endosomes (76). Total internal reflection fluorescence microscopy studies showed that a small fraction of OCRL is recruited to CCPs and then moves towards APPL1 positive early endosomes after endocytosis. APPL1 has been

described as an adaptor protein for cell surface receptors such as megalin, with which it interacts as a part of a larger protein complex (267). Therefore, the role of OCRL in vesicular traffic may be more like that of synaptojanin which is important for uncoating of endocytic CCVs. If this were true, then it is possible that actin comet formation on vesicles is only a secondary effect due to an accumulation of PIP_2 on endocytic vesicles. To test if the comets seen in Lowe syndrome cells and OCRL KD are important for membrane traffic, trafficking experiments could be performed under conditions that inhibit actin comets. Megalin endocytosis or CI-MPR trafficking could be assayed in knockdown cells with or without the addition of N-WASP siRNA to inhibit comet formation. I predict that N-WASP siRNA will have no effect on OCRL-mediated membrane traffic. However, these experiments may be difficult to interpret as the endocytosis of some surface receptors is N-WASP-dependent (259). If OCRL is necessary for uncoating of a subset of endocytic vesicles then a defect in this process could lead to problems with vesicle endocytosis or recycling similar to what has been shown in neurons of synaptojanin 1-deficinet mice which accumulate CCVs near the synapse (268).

It is also plausible that the loss of OCRL does not influence PIP_2 levels enough to change the rate of biosynthetic delivery. Indeed, increases in PIP_2 upon OCRL knockdown are modest (~130% of control) and not statistically significant, compared to PI5K overexpression (~225% of control). Since OCRL does not localize to the plasma membrane at steady state, it is reasonable to assume that only modest changes in PIP_2 would be observed after knockdown. However, published studies in primary proximal tubule cells from Lowe syndrome patients report a large increase in PIP_2 (~190% of control) (208). Why do I observe only small increases in PIP_2 levels upon OCRL knockdown? One explanation may be that loss of OCRL could be compensated by another enzyme(s). In support of this, OCRL knockout mice have no discernable Lowe

syndrome phenotype, possibly because mice have higher expression of the OCRL-homologue Inpp5b than humans. OCRL/Inpp5b double knockout mice are embryonically lethal, suggesting that while Inpp5b can compensate for loss of OCRL, the loss of both enzymes is debilitating (211). To test the possibility that Inpp5b can compensate for OCRL, siRNA could be used to simultaneously knock down OCRL and Inpp5b in polarized MDCK cells. If Inpp5b is compensating for loss of OCRL, then double knockdown should more potently increase PIP_2 levels than OCRL knockdown alone and effect biosynthetic delivery.

One caveat of my OCRL knockdown studies is the reliance on immortalized cell lines to recapitulate *in vivo* disease phenotypes. Cultured cells are less than ideal, as often these systems behave differently than they would within an organ due to genetic drift (269). Indeed, while HK2 cells are relevant for studies involving OCRL and megalin because of their proximal tubular identity, they do not form a polarized monolayer and also express much less megalin than *in vivo* proximal tubules (Linton Traub, personal communication). Therefore, it may ultimately be necessary to move to an *in vivo* system, such as an animal model to study OCRL. However, as noted above, knockout of OCRL in mice does not result in a disease phenotype (211). Unpublished observations from our collaborator Dr. Robert Nussbaum suggest that this difference between humans and mice stems from alternate splicing of mouse Inpp5b. In mice 50% of the Inpp5b mRNA uses an alternate splice site, thus producing a mixed population of Inpp5b protein. It is hypothesized that the alternatively spliced mouse Inpp5b is more capable than human Inpp5b at compensating for loss of OCRL. To test this hypothesis, OCRL/Inpp5b knockout mice have recently been engineered to express a single copy of human Inpp5b from a bacterial artificial chromosome. The goal of this experiment is to determine if human Inpp5b is less efficient at compensating for OCRL than mouse Inpp5b. To determine the effect of this

treatment, urine was collected from the mice and analyzed for the presence of low molecular weight proteins. Very preliminary results suggest that double knockout mice supplemented with a single copy of human Inpp5b had proteinuria very similar to that found in Lowe syndrome, while mice containing a single copy of mouse Inpp5b had no discernable proteinuria. These data point to a fundamental difference between the expression or function of human and mouse Inpp5b and open the door for future study. Whole animal studies using iodinated megalin ligands could be performed to examine the ability of megalin to internalize ligands in mice lacking OCRL and Inpp5b that are supplemented with a single copy of human Inpp5b. Additionally, the mouse studies further validate the prediction that Inpp5b can compensate for lack of OCRL activity and increases the probability that experiments designed to study the effect of double knockdown in cell lines will yield positive results.

4.2 THE SITE OF PI5K FUNCTION IN BIOSYNTHETIC TRAFFIC

My data demonstrate that biosynthetic delivery of HA is sensitive to both increases and decreases in cellular PIP_2 levels. Furthermore, biosynthetic delivery of HA is also dependent on actin polymerization via the PIP_2 effector, N-WASP. However, the exact site at which PI5K and N-WASP exert their action(s) cannot be elucidated from my studies. While the TGN has long been thought to be the site where proteins accumulate when subjected to a low temperature block, this has not been exhaustively characterized for all classes of proteins. Indeed, I observed that HA may stage at a site other than the Golgi. Briefly, MDCK cells grown on coverslips were infected with AVs encoding HA, VSV-G, or YFP-p75 for a short period before staging at 19ºC for 3 h followed by fixation and processing for immunofluorescence. Co-staining for each cargo

protein and furin (a TGN marker) revealed that both VSV-G and p75 stage in a compartment that is coincident with furin; however, HA does not localize the furin-containing compartment and does not overlap with YFP-p75 (Figure 4.1). Biochemical studies confirmed that HA expressed under similar conditions is largely mature (sialyated) and intracellular. While I was unable to positively identify the HA-containing compartment, my data does raise the possibility that the PI5K and N-WASP effects occur at a post-TGN site.

Recent studies indicate that different classes of apical proteins traverse distinct endocytic compartments on their way to the apical surface (7). Initially Ang et al. showed that VSV G is delivered to the common recycling endosome of polarized epithelial cells before reaching the basolateral surface (5). Cresawn et al. further demonstrated that a lipid raft-independent apical protein transits through the apical recycling endosome, while lipid raft-dependent proteins move through a different compartment accessible to internalized wheat-germ agglutinin (7). These studies lend support to a role for endosomes in biosynthetic traffic and raise the possibility that PI5K-stimulated comets may be forming on endosomes or endosome-derived vesicles and not the TGN. The site at which PI5K and N-WASP function in biosynthetic delivery of HA could be tested by performing live cell microscopy in cells expressing fluorescent cargo, actin, and different endosomal makers. It would be interesting to compare cells expressing HA and VSV-G, as these cargo move through distinct endosomal intermediates. I predict that actin comets would primarily associate with vesicular or endosomal structures containing HA but not VSV-G. These experiments may help to determine if HA associates with actin comets on vesicles or endosomes. While VSV-G has been shown to transit through the common recycling endosome in polarized cells, the identity of the endosomal compartment involved in apical delivery of HA is less clear, and may represent a previously undescribed apical endosome or a subdomain of a described

organelle (7). An alternative method to identify the HA compartment would be to affinity purify HA- or VSV-G-containing compartments after a 19ºC stage and perform mass spectrometry analysis to identify the components. I predict that N-WASP/Arp2/3 would associate primarily with HA-containing carriers/compartments, and that other proteins revealed by the analysis may uncover the identity of the compartment.

What is the role of lipid rafts in apical delivery? Lipid rafts have been proposed to act as a platform for recruitment of proteins and for the propagation signaling cascades (270). My data revealed that raft-dependent (HA) and raft-independent (p75) apical cargo use different mechanisms for apical delivery based on their differential requirement for N-WASP. HA associates with lipid rafts and segregates in a different compartment than p75 upon low temperature staging (Figure 4.1). These data suggest that because of their sorting signals p-75 (O-glycan-containing stalk) and HA (transmembrane domain) may be found in diverse lipid environments. However, the mechanistic details regarding how rafts mediate apical delivery remain elusive. The disputed existence of rafts and discrepancies regarding their size and composition make this question difficult to explore. It is likely that a component or distinct morphological feature of lipid rafts is responsible for apical sorting of these domains. To answer these questions, specialized tools to alter raft composition must be developed so that researchers can discover the relationship between composition and function.

What mechanism do cells use to direct HA-containing cargo carriers to the apical surface? Lipid raft-association is not sufficient for apical sorting as lipid rafts and raft-enriched cargo do appear at the basolateral cell surface (271;272). Moreover, apically sorted mutants of HA exist that are not associated with lipid rafts (20). However, since the sorting information for HA is located within the transmembrane domain interaction with a lipid such as PIP_2 may be

important. In polarized epithelial cells, most of the PIP_2 is found at the apical plasma membrane, so it is possible that PIP_2 synthesis on Golgi localized lipid raft domains could serve as a marker to direct that membrane to the apical surface. Concentrated PIP_2 at this domain could have a twofold effect. The increased negative charge density on the inner leaflet could affect membrane curvature leading to bowing of the membrane toward the cytoplasm promoting vesicle budding. At this point, a number of scenarios are possible to select the vesicle for apical delivery. Recognition of this of this domain by cytosolic factors could be enhanced by the increased local PIP_2 concentration leading to an overall increased avidity for the membrane. Alternatively, a cytosolic protein(s) could recognize both PIP_2 and a cargo motif resulting in stronger binding to the forming carrier.

If PI5K is necessary to generate PIP_2 on a HA-enriched Golgi domain, then what signal recruits the enzyme? It is possible that the abundance of PI5K's substrate PI4P on the Golgi complex could serve to help recruit PI5K. This theory could be tested *in vitro* by incubating purified enzymes with liposomes containing different ratios of lipid species. It is likely that recruitment of cytosolic factors such as PI5K and N-WASP rely on coincidence detection perhaps with cargo to enhance low affinity interactions. This could be tested using post-TGN vesicles immunoisolated from cells either expressing HA or p75. I predict that PI5K and N-WASP may interact more strongly with HA-containing vesicles, since HA is more frequently found on comets. Subsequently, apical delivery of the vesicle probably relies on the concerted actions of both the microtubule and actin cytoskeletons.

How could cells utilize both microtubules and actin direct the polarized delivery of a Golgi-derived HA carrier? In polarized epithelial cells microtubules originate from the juxtanuclear microtubule organizing center so that their fast growing (plus) ends are directed

toward the nucleus and the slow growing (minus) ends are directed toward the apical membrane (273). However, a recent study also demonstrated that a large number of plus end microtubules are oriented toward the apical pole of polarized cells (274). Therefore, both minus end microtubule motors (dyneins or minus end kinesins) or plus end motors (plus end kinesins) could be utilized to provide ultimate directionality to carriers propelled from the Golgi by comets. The involvement of microtubule motors in apical traffic could be tested by expressing dominant-negative forms of various microtubule motor proteins and measuring the rate and polarity of protein delivery. If microtubules are involved in apical delivery, then disrupting a motor may decrease the rate of delivery or aberrant delivery to the basolateral surface. It is possible that actin comets are necessary for budding of a raft-enriched cargo carrier from the TGN or movement away from the Golgi before contacting and moving along a microtubule for final apical delivery. Answering these questions will help us gain a better understanding of the underlying mechanisms of apical sorting and delivery.

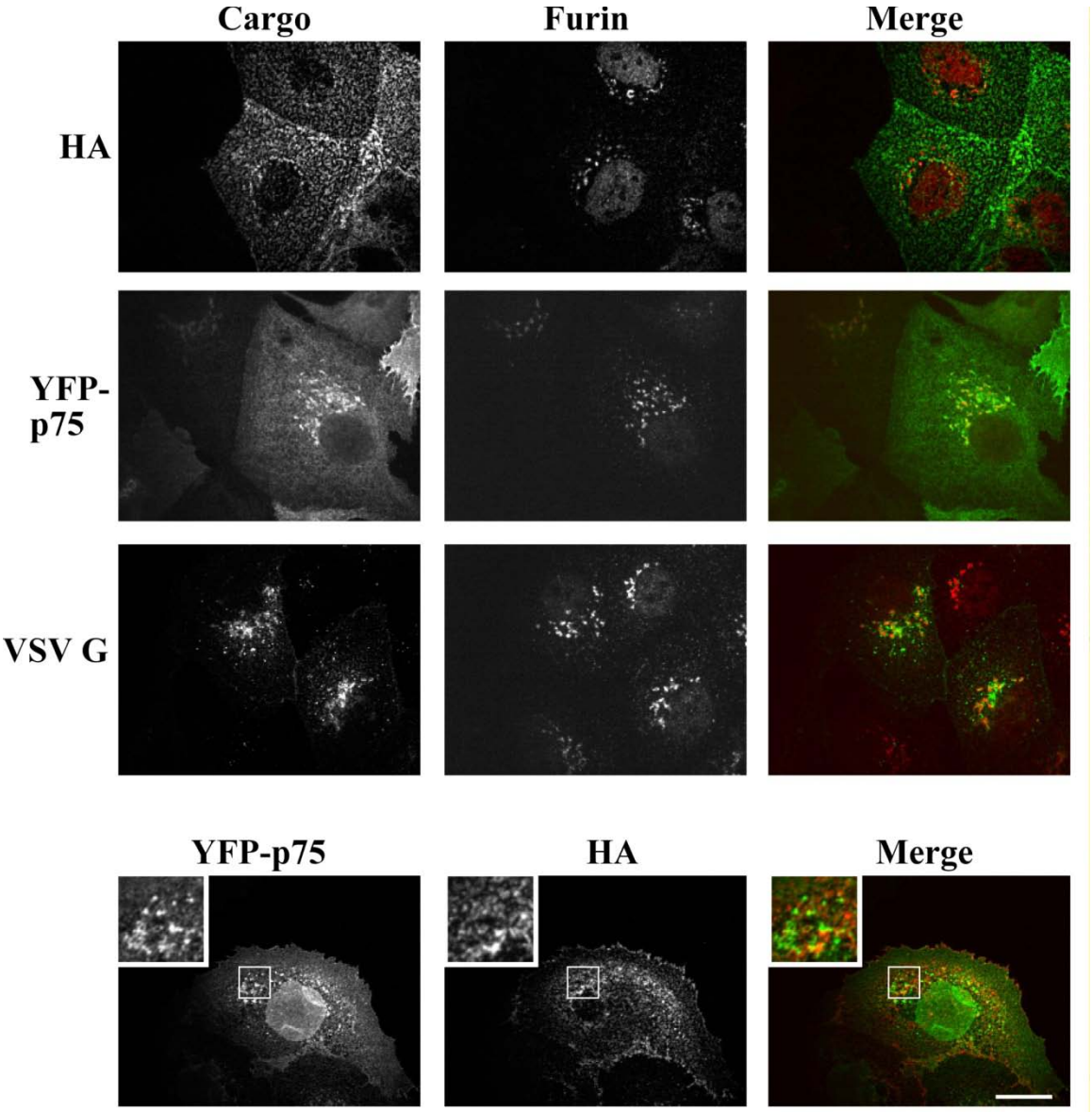

Figure 4.1 YFP-p75 and HA do not co-localize intracellularly after low temperature staging. MDCK cells were infected with adenoviruses encoding YFP-p75, VSV-G, and/or HA for 1 h and then incubated for 5 h at 37 °C and 3 h at 19 °C. Cycloheximide was included during the last hour at 19 °C. The cells were then fixed and processed for immunofluorescence to detect each marker and furin (*rows a–c*) or to visualize co-expressed HA and YFP-p75 (*row d*). The *insets* in *row d* show enlarged versions of the *boxed regions*. Individual confocal sections and a merged image are shown for each condition. *Scale bar*, 30 μM. The nuclear fluorescence in the YFP-p75 panel in *row d* represents background from the polyclonal anti-GFP used in this sample. In contrast, cells in *row b* were labeled using a monoclonal anti-GFP antibody; in both cases, this protocol was used to amplify the fluorescent signal for p75 over that provided by the YFP moiety (see "Materials and Methods").

4.3 DISTINCT FUNCTIONS OF PI5K ISOFORMS IN POLARIZED EPITHELIAL CELLS

As detailed earlier, there are three isoforms of PI5Ks in mammalian cells. What is the purpose of three different enzymes with overlapping substrate specificity? In polarized mouse cortical collecting duct (mCCD) cells, PI5KIα is localized exclusively to the apical pole of the cells, PI5KIβ is present in both the cytoplasm and at membranes, and PI5KIγ localizes primarily to the basolateral surface (Figure 4.2). This raises the possibility that the different isoforms regulate functionally-distinct pools of PIP_2 in polarized cells. I hypothesize that a given isoform will regulate endocytic events at the surface where it localizes. Evidence for this comes from published studies by Padron et al., demonstrating that in nonpolarized cells overexpression of PI5KIα and PI5KIβ, but not PI5KIγ stimulate transferrin (Tfn) endocytosis (204). In contrast, Bairstow et al. showed that in polarized cells, expression of PI5KIγ stimulates Tfn endocytosis (275). One interpretation of these contrasting observations is that in nonpolarized cells, the Tfn receptor is localized throughout the plasma membrane and PI5KIγ may have minimal influence due to the presence of the other two kinase isoforms. However, in polarized cells the Tfn receptor is mainly localized to the basolateral membrane where PI5KIγ is found making PI5KIγ the preferential kinase to influence Tfn endocytosis.

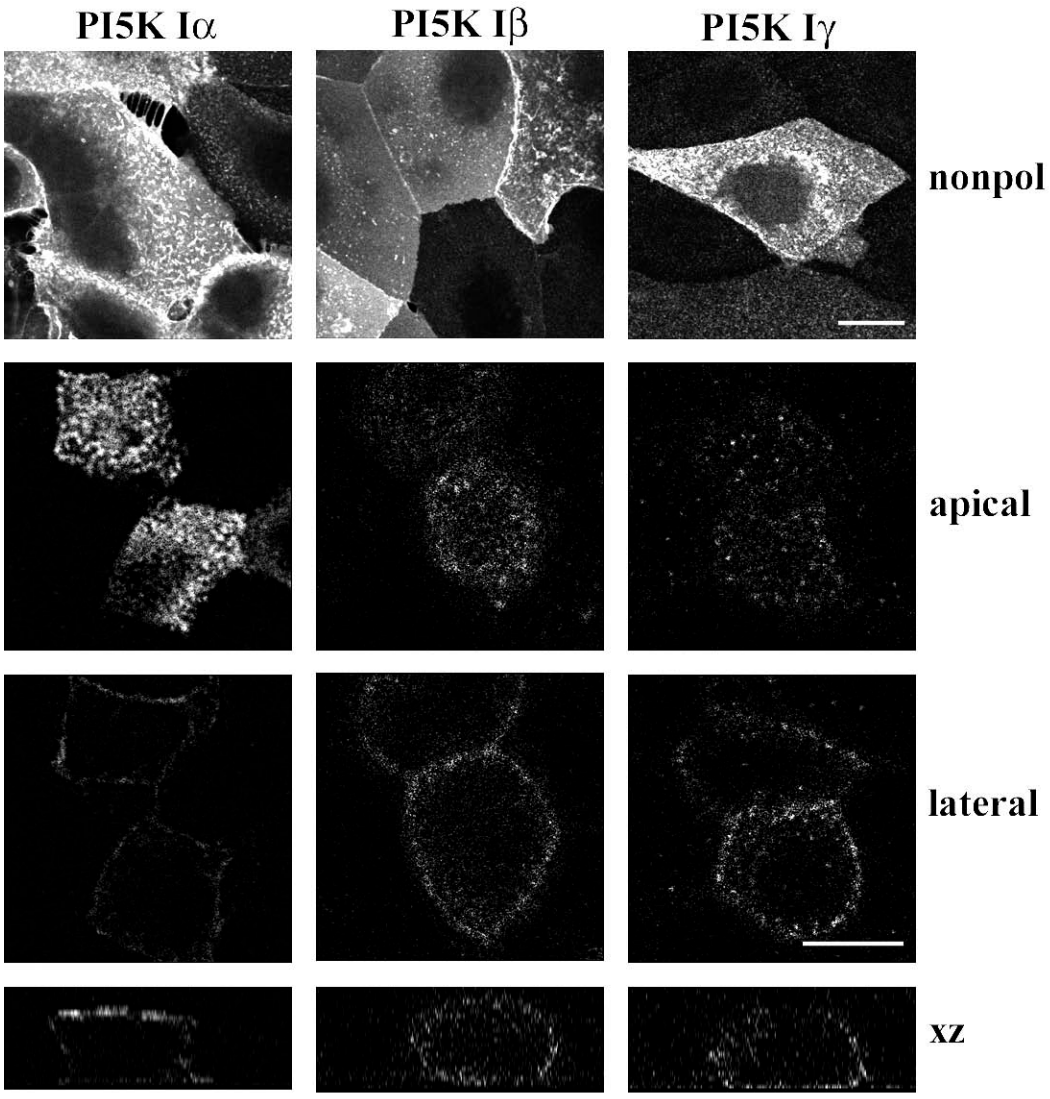

Figure 4.2 Localization of PI5K isoforms in nonpolarized and polarized mCCD cells.
mCCD cells were infected with AVs encoding PI5KIα, PI5KIβ or PI5KIγ and plated sparsely on coverslips (top row) or plated onto Transwell filters for 3 days prior to fixation and processing for immunofluorescence. Confocal sections show representative kinase staining from the apical pole and lateral regions of the cell. The bottom row shows deconvolved xz sections from the filter-grown cells. Scale bars represent ~10μm.

Whether PI5K isoforms differentially regulate endocytic events at polarized membrane domains could be tested by measuring internalization rates of proteins that are endocytosed from both the apical and basolateral surfaces. These studies could be performed using mCCD cells, as there are reagents available for both detection of endogenous PI5Ks and siRNA knockdown. I predict that overexpression of mPI5KIα will increase the endocytosis of proteins from the apical surface, whereas basolateral endocytosis will remain unaffected. In preliminary studies, I examined the rate of endocytosis of the polymeric immunoglobulin receptor (pIgR), using ^{125}I-labeled polymeric IgA that has been pre-bound to the cell surface. Consistent with my hypothesis, overexpression of mPI5KIα stimulated apical endocytosis of pIgR in mCCD cells, but had no effect on basolateral endocytosis of pIgR (Figure 4.3). These studies could be furthered by using siRNA to knock down each isoform. I predict that knockdown will have a negative effect on endocytosis at either the apical or basolateral surface according to kinase localization. The idea that PI5Ks control different endocytic events is appealing and might explain the need for multiple isoforms. PI5Ks may exert this differential action by physically interacting with or producing distinct pools of PIP_2 enabling the recruitment of endocytic adaptors and/or CLASPs required for the endocytosis of a given receptor. CLASPs are PIP_2-binding clathrin-associated sorting adaptors that increase the range of signals recognized for clathrin-mediated endocytosis of cargo proteins. It is likely that CLASPs utilize coincidence detection in order to interact with a receptor more strongly when the receptor is in a PIP_2-rich environment. This phenomenon may give cells a mechanism to up-regulate the endocytosis of certain classes of receptors in response to cell surface changes in PIP_2 levels without globally affecting all endocytic events (Figure 4.4).

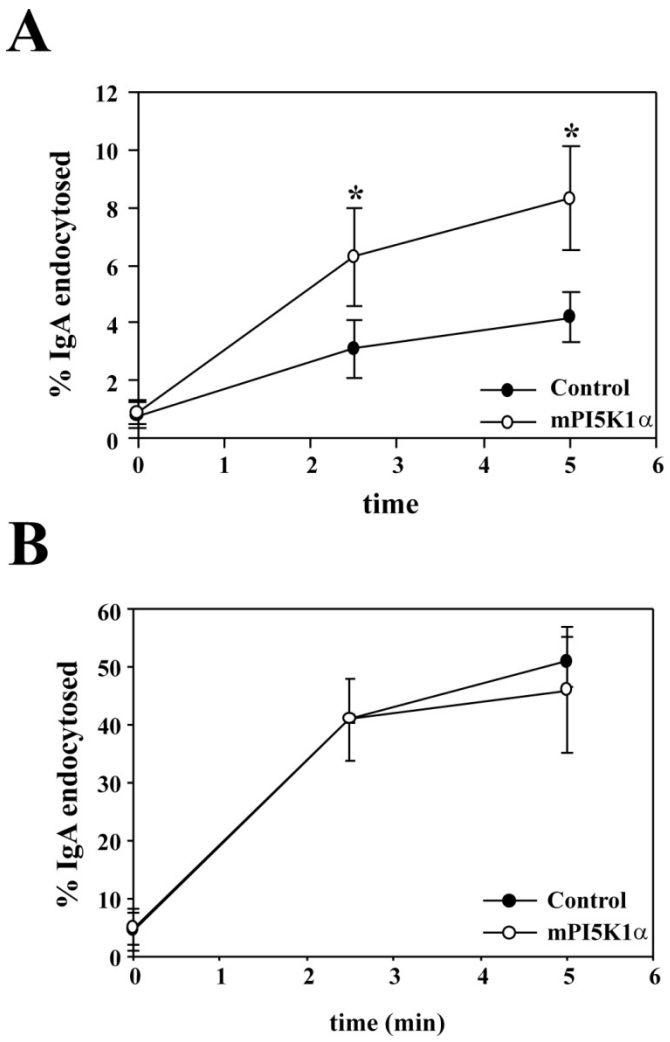

Figure 4.3 mPI5KIα selectively stimulates apical endocytosis of pIgR. mCCD cells were plated onto Transwell filters for 3 days prior to infection with AV-Control or PI5KIα and AV-pIgR. The cells were allowed to recover for 1 night in 1 ng/ml doxycycline (dox). The day after dox washout, I-125 IgA was bound to either the apical surface (A) or the basolateral surface (B) for 1 hr on ice and after extensive washing IgA was internalized for 0, 2.5, or 5 min. The remaining surface counts were stripped using 150mM glycine pH 2.3 and internalized counts were determined using a γ-counter. Error bars represent mean +/- std error from n=4 for apical or mean +/- range for one representative basolateral experiment.

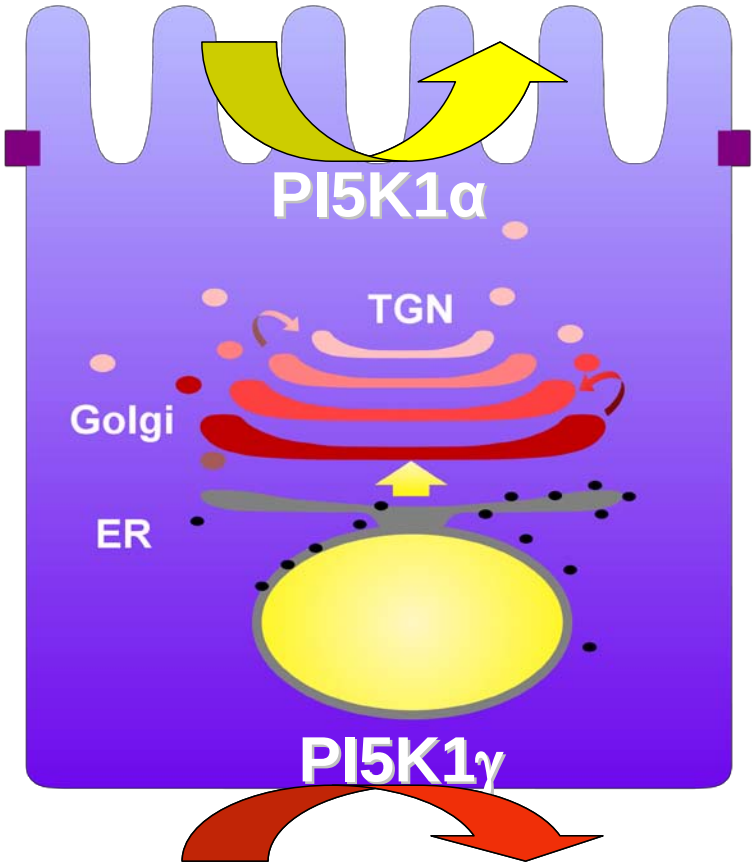

Figure 4.4 Model for differential regulation of endocytosis by PI5K informs. Polarized epithelial cells segregate the different PI5K isoforms to different surface domains. Because PI5KIα is localized exclusively to the apical surface, it will likely be important for apical endocytic events. Conversely, the basolateral localization of PI5KIγ ideally places it to influence basolateral endocytic events. PI5KIβ is found at both surfaces as well as on internal structures and may be involved in endocytosis/recycling or biosynthetic trafficking. This spatial regulation of PIP_2 production could be important for helping cells specifically upregulate the endocytosis of certain ligands, from either surface.

4.4 CONCLUDING COMMENTS

In this dissertation I presented data that help to expand our current knowledge about the contribution of PIP_2 metabolism and actin polymerization in polarized biosynthetic traffic. The discovery that biosynthetic delivery of lipid raft-associated proteins is preferentially sensitive to PIP_2 solidifies the emerging concept that distinct classes of apical proteins use different mechanisms to mediate their apical sorting and trafficking. Furthermore, the identification that N-WASP is important not only for HA delivery under PI5K-stimulated conditions, but under basal conditions as well firmly places N-WASP as a modulator of biosynthetic pathways. Insight gained by these studies regarding regulation of biosynthetic transport is critical to furthering our understanding of basic cell physiology and may one day open the door to therapeutic treatments for diseases such as Lowe syndrome.

* Figure 4.1 from this chapter is published in Guerriero et al. *JBC* 2008 and was used with the permission of the Journal of Biological Chemistry.

5.0 MATERIALS AND METHODS

5.1 DNA, REPLICATION-DEFECTIVE RECOMBINANT ADENOVIRUSES, AND SIRNA OLIGOS

The α isoform of murine phosphatidylinositol 4-phosphate 5-kinase (PI5K) cloned into the pAdtet vector was provided by Dr. Andreas Jeromin (Baylor University). The β isoform of PI5K was the kind gift of Dr. Philip Stahl (Washington University). The γ isoform of PI5K was provided Dr. Richard Anderson via Dr. Linton Traub (University of Pittsburgh). Constructs encoding *myc*-tagged W and WA domains of WAVE1 were generous gifts of Dr. Dorothy Schafer and Dr. James Casanova (University of Virginia). Fluorescent protein-tagged actin constructs were provided by Dr. Ronald Montelaro (University of Pittsburgh). The generation and purification of replication-defective recombinant adenoviruses (AVs) encoding tetracycline-repressible influenza HA (Japan serotype), VSV-G, and a control virus (encoding the influenza Rostock M2 coding sequence in the reverse orientation) has been previously described (50;236). AVs encoding PI5K α, β,γ and human OCRL (both wild type and the phosphatase-deficient mutant R483G; constructs provided by Robert Nussbaum, MD University of California, San Franscisco) were generated using similar methods. AV encoding $p75^{NTR}$ was provided by Dr. Enrique Rodriguez-Boulan (Weill Medical College) with permission from Dr. Moses Chao, and AV-W and WA were kind gifts of Dr. James Casanova (University of Virginia).

Firefly luciferase siRNA was used as a control for siRNA experiments; 5′-GAATATTGTTGCACGATTT-3′. The sequence for the OCRL siRNA was obtained from Dr. Philip Majerus' lab (Dr. Alex Ungewickell) and matches human, mouse, and canine OCRL; 5′-GGTTCCCTGCCATTTTTCA-3′. An siRNA targeting canine N-WASP was based on a published siRNA targeting rat N-WASP; 5′-GGCGAGACCCCCCAAATGC-3′ (238). The OCRL and N-WASP siRNAs have an intentional mismatch at the 3' end of the sense strand which creates a bias for the antisense strand entering the RNA-induced silencing complex (RISC) and increases the rate of target mRNA degradation (205-207). All siRNAs were purchased from Dharmacon and were reconstituted in Dharmacon's 1X siRNA buffer at a concentration of 1 µg/µl (Thermo Scientific, Lafayette, CO).

5.2 ANTIBODIES, REAGENTS AND IMMUNOBLOTTING

Immunoprecipitation (IP) or immunofluorescence (IF) of HA, VSV-G, or p75 was performed using supernatants from cultured hybridomas (Fc125 from Dr. Thomas Braciale, University of Virginia; 8G5 from Dr. Douglas Lyles, Wake Forest University (276); and MA 20.1 from Dr. Enrique Rodriguez-Boulan, Weill Medical College, respectively). Mouse anti-OCRL ascities for western blotting and IF were obtained from Dr. Sharon Suchy and Dr. Robert Nussbaum. Mouse anti-giantin was a gift from Dr. Adam Lindstet (Carnegie Mellon University). Rabbit anti-furin was purchased from Affinity BioReagents (Golden, CO). Mouse anti-HA-tag was obtained from Covance (Berkley, CA) and rat anti-HA-tag was obtained from Roche (Indianapolis, IN). Rabbit monoclonal anti-N-WASP was obtained from Cell Signalling Technology (Danvers, MA). Rabbit anti-GFP was obtained from Invitrogen (Molecular Probes, Carlsbad, CA). Mouse anti-β-

actin, cytochalasin D, nocodazole, n-butanol, t-butanol, and phorbol myristate acetate (PMA) were obtained from Sigma (St. Louis, MO). Wiskostatin was obtained from Calbiochem (San Diego, CA).

Blotting samples were resolved on BioRad 4-15% Criterion precast gels and transferred to nitrocellulose (GE Healthcare, Piscataway, NJ) using the Criterion transfer apparatus (BioRad, Hercules, CA). Nonspecific background was reduced by incubating blots for 1 h in PBS containing 5% non-fat dry milk. Blots were then incubated with 1º antibody for 1-2 h in PBS containing 1% milk, washed with PBS, incubated with a 2º anti-HRP antibody for 1 hr, washed, and incubated with Pierce SuperSignal (Thermo Scientific, Rockford, IL). Exposures were taken using a BioRad VersaDoc and quantitated using Quantity One software (BioRad).

5.3 CELL LINES

Madin-Darby canine kidney (MDCK) type II cells stably expressing the tetracycline transactivator (TA) and the rabbit pIgR were cultured in modified Eagle's medium (Sigma) supplemented with 10% fetal bovine serum (FBS) (Atlanta Biologicals). Mouse cortical collecting duct (mCCD) cells were cultured in 1:1 low glucose Dulbecco's Modified Eagles's Medium (DMEM) (Sigma) and Ham's F12 (Gibco) supplemented with 60 nM sodium selenate, 5 µg/ml transferrin, 2 mM glutamine, 50 nM dexamethasone, 1 nM triiodothyronine, 10 ng/ml epidermal growth factor, 5 µg/ml insulin, 20 mM D-glucose, 20 mM HEPES and 2% heat-inactivated FBS (277). For measurements of intra-Golgi transport, kinetics of surface delivery, surface polarity, transcytosis, and endocytosis; cells were seeded at superconfluence in 12-mm Transwells (0.4-µm pore; Costar, Cambridge, MA) for 2–4 days prior to infection with

recombinant AVs. For IgA transcytosis and endocytosis experiments, pIgR expression was enhanced by incubation with 2 mM sodium butyrate for ≥16 h. Experiments were performed the following day.

HK2 cells were obtained from ATCC and maintained in DMEM:F12 (Sigma) supplemented with 5 µg/ml insulin and 50 nM dexamethasone. Cells were grown in 10 cm culture dishes (Falcon) and plated onto 12-well dishes (Corning) for experimentation.

5.4 ADENOVIRAL INFECTION

On the day prior to the experiment cells were washed two times with PBS supplemented with 1mM $MgCl_2$ (PBS-Mg^{2+}). Cells were then incubated with the intended adenovirus (AV) at the following multiplicity of infection (m.o.i.) (control AV, AV-PI5K, AV-W, AV-WA, AV-OCRL, and AV-OCRL mutant, m.o.i. 100–250; AV-TA, AV-pIgR, AV-HA, AV-p75, AV-YFP-p75, and AV-VSV-G, m.o.i. 25–50) as described in Henkel et al. 1998 (236). Following the infection cells were rinsed with PBS-Mg^{2+} before being returned to culture in normal growth medium. Experiments were performed the following day. CCD cells were allowed to recover for 1 night following infection and virus expression was repressing by including 1 ng/ml DOX in their medium.

5.5 INDIRECT IMMUNOFLUORESCENCE

MDCK cells grown on Transwell filters or coverslips were infected with AVs at the indicated m.o.i. The following day, cells were rinsed with PBS, fixed in 3.7% formaldehyde, rinsed with PBS containing 10 mM glycine (PBS-G), and then permeabilized with 0.5% Triton X-100 in PBS-G for 3 min at room temperature. After washing, nonspecific binding sites were blocked by incubation for 5 min in PBS-G containing 0.25% (w/v) ovalbumin. Coverslips were incubated for 30 min with monoclonal anti-HA tag antibody (1:500 dilution; Covance) followed by washing in blocking buffer. Cells were then incubated for 30 min with secondary antibodies Alexa Fluor goat anti-mouse 488 (1:500; Invitrogen, Carlsbad, CA). Rhodamine phalloidin (1:80; Invitrogen, Molecular Probes) was included in this step where indicated. After extensive washing, coverslips or filters were mounted onto glass slides.

Filter-grown MDCK or mCCD cells were fixed with formaldehyde using a pH-shift protocol with paraformaldyhyde in a cacodylate buffer. For the pH-shift protocol, samples were treated as described in Apodaca et al. 1994 (278). Alternatively, cells were washed by dipping into warm PBS, and samples were fixed for 15 min in 4% paraformaldehyde diluted into 100 mM sodium cacodylate at 37ºC. The fixation was quenched using 20 mM glycine and 75 mM NH_4Cl in PBS, followed by 10 min in 0.1% TX-100, and then blocking in PBS with 1% BSA/0.1% saponin. Images were captured using a Leica TCS-SL confocal microscope equipped with argon and green and red helium neon lasers (Leica, Dearfield, IL). Images were taken with a 100X (1.4 numerical aperture (NA)) plan apochromat oil objective. TIFF images were processed using Adobe Photoshop (Adobe, San Jose, CA). Some fixed samples and all live samples were imaged using an Olympus IX-81 inverted microscope equipped with a Perkin Elmer spinning disc confocal. Images were taken with either an Olympus 60X PlanApo (NA 1.40) or a 100X

UPlanApo (NA 1.35) oil immersion objective. Live images were captured and analyzed using Metamorph imaging software (Molecular Devices, Downington, PA).

5.6 INTRACELLULAR TRANSPORT AND CELL SURFACE DELIVERY ASSAYS

AV-infected filter-grown MDCK cells were starved for 30 min and radiolabeled for 5–10 min (for endoglycosidase H (endo H) kinetics) or 15–20 min (for TGN to surface delivery) on drops containing 1 mCi/ml Tran-^{35}S-label® (MP Biomedicals, Irvine, CA). To measure endo H kinetics, cells were chased in bicarbonate-free modified Eagle's medium for the indicated periods, solubilized, and HA was IPed as previously described in Henkel et al. 1998 (236). After collection of antibody-antigen complexes, samples were eluted, divided in half, and mock-treated or treated overnight with endo H prior to electrophoresis on 10% SDS-PAGE gels. To measure TGN-to- cell surface delivery, radiolabeled cells were chased at 19ºC for 2 h unless otherwise indicated to stage newly synthesized membrane proteins in the TGN. The cells were then rapidly warmed to 32°C or 37°C as indicated. Apical delivery of HA was measured by trypsinization as described in Henkel et al. 2000 (232). Briefly, after each time point samples were rapidly cooled to 4°C, by a wash with cold media. Samples were then incubated in cold media supplemented with TPCK-treated trypsin for 30 min followed by two 10 min washes in media supplemented with soy bean trypsin inhibitor. Basolateral delivery of VSV-G was quantitated using domain selective biotinylation as described in Ref. (279). Briefly, after each time point cells were washed thoroughly with cold PBS containing 1mM $MgCl_2$ and 1mM $CaCl_2$. The apical or basolateral surface was biotinylated twice for 10 min each with sulfo-NHS-SS-biotin (0.5 mg/ml;Cat # 21331, Thermo-Fisher, Pierce) in TEA-buffered saline, pH 7.6. The biotinylation

reaction was quenched by incubation in media containing 10% FBS. To quantitate surface delivery of $p75^{NTR}$ or HA delivery in OCRL-expressing samples, cells were radiolabeled on 25-µl drops of sulfate-free medium containing 100 µCi of [^{35}S]sulfate at 18°C and the rate of surface delivery was assessed using domain selective biotinylation upon subsequent warm-up to 37°C (280).

5.7 VISUALIZATION AND QUANTITATION OF ACTIN COMETS

MDCK cells (2 x 10^5) were seeded on Bioptech 0.17-mm ΔT dishes (Bioptech Inc., Butler, PA). The following day cells were infected with AVs (m.o.i. 100–250) encoding the indicated proteins, and incubated overnight with 0.25 ng/ml doxycycline (DOX) to partially suppress protein expression. The following morning DOX was removed by thorough washing. Cells were then pressure-injected with cDNA encoding GFP- or YFP-actin and were returned to culture for 5 h. Following that time the cells were imaged on an Olympus IX81 microscope using a 100 X Olympus UPlanApo objective (numerical aperture 1.35). Random fields containing cells expressing fluorescent actin were imaged every 2 s for 3-4 min. Data were analyzed using acquisition software (Slidebook or Metamorph) to determine the percentage of cells with comets. Stable cells lines expressing fluorescent protein-tagged actin were generated using Lipofectamine 2000 and mixed populations were isolated by selection in G418. These cells were infected with AV-PI5K where indicated and used for the quantification of actin comets in cells treated with PMA PMA (5 µg/ml), cytochalasin D (25 µg/ml), n-butanol (1% v/v), *t*-butanol (1% v/v), or OCRL siRNA.

5.8 IGA TRANSCYTOSIS

Filter-grown MDCK cells stably expressing pIgR were treated with wiskostatin at the indicated time and concentration. Samples were washed thoroughly with cold MEM + 0.6% BSA and then placed on drops of MEM containing 5 µl dimeric ^{125}I-IgA (~ 0.8-1.5 x 10^6 counts/µl) at 37ºC for 10 min. Next, the cells were washed for 5 min to remove nonspecifically bound ^{125}I-IgA. Apical medium was collected over a 120' time course and the secreted and cell-associated counts per minute were determined and used to calculate the percent IgA transcytosed over time.

5.9 IGA ENDOCYTOSIS

Filter-grown mCCD cells were infected with AV-pIgR and AV-transactivator and either a control AV or AV-mPI5KIα. Cells were kept in 1 ng/ml DOX overnight to allow the cells to recover prior to protein expression. The next day the cells were washed 4 times with media to remove the DOX and were fed with media containing 2% sodium butyrate to induce expression of pIgR. The following day, samples were washed thoroughly with cold MEM containing 0.6% BSA to block nonspecific binding sites. Samples were then placed on drops of MEM containing 5 µl dimeric IgA (for basolateral endocytosis) or incubated with iodinated IgA apically (for apical endocytosis) for 1 h at 4ºC. Samples were washed extensively to remove nonspecific IgA and then warmed for 0, 2.5 or 5 min. At each time point the samples were rapidly cooled and placed into media containing 10 µg/ml TPCK-treated trypsin to remove remaining surface IgA. The samples were then placed in cold PBS containing 150 mM glycine pH 2.3 to further strip IgA from the cell surface. The apical or basolateral media, the trypsin wash, the glycine wash,

and the cells were collected and counted in a γ-counter to determine the relative percentage cell-associated IgA over the time course.

5.10 SIRNA TREATEMENT OF MDCK AND HK2 CELLS

MDCK or HK 2 cells were grown to 50% confluence prior to trypisnization to prepare for electroporation. Cells were counted and reuspended at a density of 1 x 10^6 cells/100 µl Amaxa solution mix (see below). Cells were mixed with 5 µg siRNA/1 x 10^6 cells and electroporated using Amaxa program T-020 in a single cuvette. Cells were immediately plated onto Transwell filters at a density of 0.5 x 10^6 cells/filter and the media was changed the following morning to remove cell debris. Knockdown was assayed using western blot 3 days after electroporation. The recipe for the Amaxa solutions was obtained from Dr. Alex Ungewickell. For Amaxa solution I, a solution of 36 µM ATP and 59 µM $MgCl_2$ were mixed with 10 ml dH_2O, filter sterilized, and stored at -80ºC in 20 µl aliquots. Amaxa solution II contains 440 µM KH_2PO_4, 70 µM $NaHCO_3$, and 11 µM D-Glucose which was dissolved in 500 ml dH_2O, adjusted to pH 7.4 with NaOH, filter sterilized, and stored in 1 ml aliquots. Immediately before cell resuspension, aliquots of each solution were mixed together and kept on ice.

5.11 DETERMINATION OF CELLULAR ATP LEVELS

MDCK cells were plated at 50,000 cells/well in 12-well dishes (Costar). The following day the cells were treated for 0–1 h with vehicle, wiskostatin, or 2% sodium azide (as a positive control)

and then solubilized by the method described in Yang et al. (281). Briefly, cells were washed twice with PBS followed by the addition of 1 ml of boiling distilled H_2O to each well, the cells were removed by pipetting, and the samples were centrifuged at 4ºC for 5 min at 13,000 rpm to pellet debris. To assess the reversibility of drug treatment, cells were rinsed three times and incubated in fresh drug-free medium for 30 min before harvesting. To determine cellular ATP levels after treatment, 20 µl of each lysate was mixed with 100 µl of rLuciferase/Luciferin (Promega) and relative luminescence units were measured with a luminometer (Turner Designs TD-20.20). The ATP concentration in each sample was calculated by comparing the experimental values to a standard curve constructed with known concentrations of ATP and plotted as the percentage of control values obtained for mock-treated samples. Raw data were log transformed and analyzed by paired *t*-test. A *P* value of <0.05 was considered statistically different.

5.12 VISUALIZATION OF CARGO ASSOCIATED WITH ACTIN COMETS

MDCK cells (3×10^5) were seeded onto coverslips in 12-well dishes. The following day the cells were co-infected with AVs encoding HA and either PI5K or control AV. After 8 h at 37ºC, the cells were incubated at 19ºC for 2.5 h to stage HA in the TGN. Dishes were then warmed to 37ºC for 0 or 30 min before fixation and processing for indirect immunofluorescence to detect HA, PI5K, and actin.

BIBLIOGRAPHY

1. Nakatsukasa, K. and Brodsky, J. L. *The recognition and retrotranslocation of misfolded proteins from the endoplasmic reticulum* 2008. Traffic. **9,** 861-870

2. Barlowe, C., Orci, L., Yeung, T., Hosobuchi, M., Hamamoto, S., Salama, N., Rexach, M. F., Ravazzola, M., Amherdt, M., and Schekman, R. *COPII: a membrane coat formed by Sec proteins that drive vesicle budding from the endoplasmic reticulum* 1994 . Cell **77,** 895-907

3. Aridor, M. and Traub, L. M. *Cargo selection in vesicular transport: the making and breaking of a coat* 2002. Traffic. **3,** 537-546

4. Appenzeller-Herzog, C. and Hauri, H. P. *The ER-Golgi intermediate compartment (ERGIC): in search of its identity and function* 2006 . J Cell Sci **119,** 2173-2183

5. Ang, A. L., Taguchi, T., Francis, S., Fölsch, H., Murrells, L. J., Pypaert, M., Warren, G., and Mellman, I. *Recycling endosomes can serve as intermediates during transport from the Golgi to the plasma membrane of MDCK cells.* 2004. J.Cell Biol. **167,** 531-543

6. Ellis, M. A., Potter, B. A., Cresawn, K. O., and Weisz, O. A. *Polarized biosynthetic traffic in renal epithelial cells: sorting, sorting, everywhere* 2006. Am.J Physiol Renal Physiol **291,** p:F707-F713

7. Cresawn, K. O., Potter, B. A., Oztan, A., Guerriero, C. J., Ihrke, G., Goldenring, J. R., Apodaca, G., and Weisz, O. A. *Differential involvement of endocytic compartments in the biosynthetic traffic of apical proteins* 2007. EMBO J **26,** 3737-3748

8. Guerriero, C. J., Lai, Y., and Weisz, O. A. *Differential sorting and golgi export requirements for raft-associated and raft-independent apical proteins along the biosynthetic pathway* 2008. J Biol Chem.

9. Jacob, R. and Naim, H. Y. *Apical membrane proteins are transported in distinct vesicular carriers.* 2001. Curr.Biol **11,** 1444-1450

10. Ellis, M. A., Potter, B. A., Cresawn, K. O., and Weisz, O. A. *Polarized biosynthetic traffic in renal epithelial cells: sorting, sorting, everywhere* 2006. Am.J.Physiol Renal Physiol **291,** p:F707-F713

11. Nakatsu, F. and Ohno, H. *Adaptor protein complexes as the key regulators of protein sorting in the post-Golgi network* 2003. Cell Struct.Funct. **28,** 419-429

12. Ohno, H., Tomemori, T., Nakatsu, F., Okazaki, Y., Aguilar, R. C., Foelsch, H., Mellman, I., Saito, T., Shirasawa, T., and Bonifacino, J. S. *[mu]1B, a novel adaptor medium chain expressed in polarized epithelial cells* 1999. FEBS Letters **449,** 215-220

13. Fölsch, H., Ohno, H., Bonifacino, J. S., and Mellman, I. *A Novel Clathrin Adaptor Complex Mediates Basolateral Targeting in Polarized Epithelial Cells* 1999. Cell **99,** 189-198

14. Deborde, S., Perret, E., Gravotta, D., Deora, A., Salvarezza, S., Schreiner, R., and Rodriguez-Boulan, E. *Clathrin is a key regulator of basolateral polarity* 2008. Nature **452,** 719-723

15. Chuang, J. Z. and Sung, C. H. *The Cytoplasmic Tail of Rhodopsin Acts as a Novel Apical Sorting Signal in Polarized MDCK Cells* 1998. J.Cell Biol. **142,** 1245-1256

16. Takeda, T., Yamazaki, H., and Farquhar, M. G. *Identification of an apical sorting determinant in the cytoplasmic tail of megalin* 2003. Am J Physiol Cell Physiol **284,** p:C1105-C1113

17. Yeaman, C., Gall, A. H., Baldwin, A. N., Monlauzeur, L., Bivic, A. L., and Rodriguez-Boulan, E. *The O-glycosylated Stalk Domain Is Required for Apical Sorting of Neurotrophin Receptors in Polarized MDCK Cells* 1997. J.Cell Biol. **139,** 929-940

18. Potter, B. A., Ihrke, G., Bruns, J. R., Weixel, K. M., and Weisz, O. A. *Specific N-glycans direct apical delivery of transmembrane, but not soluble or glycosylphosphatidylinositol-anchored forms of endolyn in Madin-Darby canine kidney cells.* 2004. Mol.Biol Cell **15,** 1407-1416

19. Paladino, S., Sarnataro, D., and Zurzolo, C. *Detergent-resistant membrane microdomains and apical sorting of GPI-anchored proteins in polarized epithelial cells* 2002. Int.J Med.Microbiol. **291,** 439-445

20. Lin, S., Naim, H. Y., Chapin Rodriguez, A., and Roth, M. G. *Mutations in the Middle of the Transmembrane Domain Reverse the Polarity of Transport of the Influenza Virus Hemagglutinin in MDCK Epithelial Cells* 1998. J.Cell Biol. **142,** 51-57

21. van Meer, G. and Simons, K. *Lipid polarity and sorting in epithelial cells* 1988. J Cell Biochem. **36,** 51-58

22. Brown, D. A. and Rose, J. K. *Sorting of GPI-anchored proteins to glycolipid-enriched membrane subdomains during transport to the apical cell surface* 1992. Cell **68,** 533-544

23. Hanzal-Bayer, M. F. and Hancock, J. F. *Lipid rafts and membrane traffic* 2007. FEBS Lett. **581,** 2098-2104

24. Munro, S. *Lipid rafts: elusive or illusive?* 2003. Cell **115,** 377-388

25. Helms, J. B. and Zurzolo, C. *Lipids as targeting signals: lipid rafts and intracellular trafficking* 2004. Traffic. **5,** 247-254

26. Brown, A. G., Fyffe, R. E., Rose, P. K., and Snow, P. J. *Spinal cord collaterals from axons of type II slowly adapting units in the cat* 1981. J Physiol **316,** 469-480

27. Scheiffele, P., Roth, M. G., and Simons, K. *Interaction of influenza virus haemagglutinin with sphingolipid-cholesterol membrane domains via its transmembrane domain* 1997. EMBO J **16,** 5501-5508

28. Rajendran, L. and Simons, K. *Lipid rafts and membrane dynamics* 2005. J Cell Sci **118,** 1099-1102

29. Schuck, S. and Simons, K. *Polarized sorting in epithelial cells: raft clustering and the biogenesis of the apical membrane* 2004. J Cell Sci **117,** 5955-5964

30. Simons, K. and Toomre, D. *Lipid rafts and signal transduction* 2000. Nat Rev Mol Cell Biol **1,** 31-39

31. van Rheenen, J., Achame, E. M., Janssen, H., Calafat, J., and Jalink, K. *PIP2 signaling in lipid domains: a critical re-evaluation* 2005. EMBO J **24,** 1664-1673

32. Pike, L. J. and Miller, J. M. *Cholesterol Depletion Delocalizes Phosphatidylinositol Bisphosphate and Inhibits Hormone-stimulated Phosphatidylinositol Turnover* 1998. J.Biol.Chem. **273,** 22298-22304

33. Golub, T. and Caroni, P. *PI(4,5)P2-dependent microdomain assemblies capture microtubules to promote and control leading edge motility* 2005. J Cell Biol **169,** 151-165

34. Morris, J. B., Huynh, H., Vasilevski, O., and Woodcock, E. A. *Alpha1-adrenergic receptor signaling is localized to caveolae in neonatal rat cardiomyocytes* 2006. J Mol Cell Cardiol. **41,** 17-25

35. Irvine, R. F. *Nuclear lipid signaling* 2002. Sci STKE. **2002,** p:RE13

36. Di Paolo, G. and De Camilli, P. *Phosphoinositides in cell regulation and membrane dynamics* 2006. Nature **443,** 651-657

37. Downes, C. P., Gray, A., and Lucocq, J. M. *Probing phosphoinositide functions in signaling and membrane trafficking* 2005. Trends in Cell Biology **15,** 259-268

38. Milne, S. B., Ivanova, P. T., DeCamp, D., Hsueh, R. C., and Brown, H. A. *A targeted mass spectrometric analysis of phosphatidylinositol phosphate species* 2005. J.Lipid Res. **46,** 1796-1802

39. De Matteis, M. A. and Godi, A. *PI-loting membrane traffic* 2004. Nat Cell Biol **6,** 487-492

40. D'Angelo, G., Vicinanza, M., Di Campli, A., and De Matteis, M. A. *The multiple roles of PtdIns(4)P - not just the precursor of PtdIns(4,5)P2* 2008. J Cell Sci **121,** 1955-1963

41. Simonsen, A., Wurmser, A. E., Emr, S. D., and Stenmark, H. *The role of phosphoinositides in membrane transport* 2001. Current Opinion in Cell Biology **13,** 485-492

42. Jones, D. H., Morris, J. B., Morgan, C. P., Kondo, H., Irvine, R. F., and Cockcroft, S. *Type I Phosphatidylinositol 4-Phosphate 5-Kinase Directly Interacts with ADP-ribosylation Factor 1 and Is Responsible for Phosphatidylinositol 4,5-Bisphosphate Synthesis in the Golgi Compartment* 2000. J.Biol.Chem. **275,** 13962-13966

43. Watt, S. A., Kilar, G., Fleming I.N., Downes, C. P., and Lucocq, J. M. *Subcellular localization of phosphatidylinositol 4,5-bisphosphate using the pleckstrin homology domain of phospholipase C delta 1.* 2002. Biochemical Journal **363,** 657-666

44. Lowe, M. *Structure and function of the Lowe syndrome protein OCRL1.* 2005. Traffic **6,** 711-719

45. Fruman, D. A., Meyers, R. E., and Cantley, L. C. *Phosphoinositide kinases* 1998. Annu.Rev Biochem. **67,** 481-507

46. Ward, S., Sotsios, Y., Dowden, J., Bruce, I., and Finan, P. *Therapeutic potential of phosphoinositide 3-kinase inhibitors* 2003. Chem.Biol **10,** 207-213

47. Yano, H., Nakanishi, S., Kimura, K., Hanai, N., Saitoh, Y., Fukui, Y., Nonomura, Y., and Matsuda, Y. *Inhibition of histamine secretion by wortmannin through the blockade of phosphatidylinositol 3-kinase in RBL-2H3 cells* 1993. J.Biol.Chem. **268,** 25846-25856

48. Wu, B., Kitagawa, K., Zhang, N. Y., Liu, B., and Inagaki, C. *Pathophysiological concentrations of amyloid beta proteins directly inhibit rat brain and recombinant human type II phosphatidylinositol 4-kinase activity* 2004. J Neurochem. **91,** 1164-1170

49. Weixel, K. M., Blumental-Perry, A., Watkins, S. C., Aridor, M., and Weisz, O. A. *Distinct Golgi populations of phosphatidylinositol 4-phosphate regulated by phosphatidylinositol 4-kinases.* 2005. J Biol Chem. **280,** 10501-10508

50. Bruns, J. R., Ellis, M. A., Jeromin, A., and Weisz, O. A. *Multiple roles for phosphatidylinositol 4-kinase in biosynthetic transport in polarized Madin-Darby canine kidney cells* 2002. J Biol Chem. **277,** 2012-2018

51. Ishihara, H., Shibasaki, Y., Kizuki, N., Katagiri, H., Yazaki, Y., Asano, T., and Oka, Y. *Cloning of cDNAs encoding two isoforms of 68-kDa type I phosphatidylinositol-4-phosphate 5-kinase* 1996. J Biol Chem. **271,** 23611-23614

52. Loijens, J. C. and Anderson, R. A. *Type I phosphatidylinositol-4-phosphate 5-kinases are distinct members of this novel lipid kinase family* 1996. J Biol Chem. **271,** 32937-32943

53. Giudici, M. L., Emson, P. C., and Irvine, R. F. *A novel neuronal-specific splice variant of Type I phosphatidylinositol 4-phosphate 5-kinase isoform gamma* 2004. Biochem.J **379,** 489-496

54. Ishihara, H., Shibasaki, Y., Kizuki, N., Wada, T., Yazaki, Y., Asano, T., and Oka, Y. *Type I phosphatidylinositol-4-phosphate 5-kinases. Cloning of the third isoform and deletion/substitution analysis of members of this novel lipid kinase family* 1998. J Biol Chem. **273,** 8741-8748

55. Mao, Y. S. and Yin, H. L. *Regulation of the actin cytoskeleton by phosphatidylinositol 4-phosphate 5 kinases* 2007. Pflugers Arch. **455,** 5-18

56. Kisseleva, M., Feng, Y., Ward, M., Song, C., Anderson, R. A., and Longmore, G. D. *The LIM protein Ajuba regulates phosphatidylinositol 4,5-bisphosphate levels in migrating cells through an interaction with and activation of PIPKI alpha* 2005. Mol Cell Biol **25,** 3956-3966

57. Saito, K., Tolias, K. F., Saci, A., Koon, H. B., Humphries, L. A., Scharenberg, A., Rawlings, D. J., Kinet, J. P., and Carpenter, C. L. *BTK regulates PtdIns-4,5-P2 synthesis: importance for calcium signaling and PI3K activity* 2003. Immunity. **19,** 669-678

58. Santarius, M., Lee, C. H., and Anderson, R. A. *Supervised membrane swimming: small G-protein lifeguards regulate PIPK signalling and monitor intracellular PtdIns(4,5)P2 pools* 2006. Biochem.J **398,** 1-13

59. Roth, M. G. *Phosphoinositides in constitutive membrane traffic.* 2004. Physiol Rev. **84,** 699-730

60. Takenawa, T. and Itoh, T. *Phosphoinositides, key molecules for regulation of actin cytoskeletal organization and membrane traffic from the plasma membrane* 2001. Biochimica et Biophysica Acta (BBA) - Molecular and Cell Biology of Lipids **1533,** 190-206

61. Norris, F. A., Atkins, R. C., and Majerus, P. W. *The cDNA Cloning and Characterization of Inositol Polyphosphate 4-Phosphatase Type II. Evidence for conserved alternative splicing in the 4-phosphatase family.* 1997. J.Biol.Chem. **272,** 23859-23864

62. Ivetac, I., Munday, A. D., Kisseleva, M. V., Zhang, X. M., Luff, S., Tiganis, T., Whisstock, J. C., Rowe, T., Majerus, P. W., and Mitchell, C. A. *The Type I{alpha} Inositol Polyphosphate 4-Phosphatase Generates and Terminates Phosphoinositide 3-*

Kinase Signals on Endosomes and the Plasma Membrane 2005. Mol.Biol.Cell **16,** 2218-2233

63. Ungewickell, A., Hugge, C., Kisseleva, M., Chang, S. C., Zou, J., Feng, Y., Galyov, E. E., Wilson, M., and Majerus, P. W. *The identification and characterization of two phosphatidylinositol-4,5-bisphosphate 4-phosphatases* 2005. Proc.Natl.Acad.Sci U.S.A **102,** 18854-18859

64. Zou, J., Marjanovic, J., Kisseleva, M. V., Wilson, M., and Majerus, P. W. *Type I phosphatidylinositol-4,5-bisphosphate 4-phosphatase regulates stress-induced apoptosis* 2007. Proc.Natl.Acad.Sci U.S.A **104,** 16834-16839

65. Astle, M. V., Horan, K. A., Ooms, L. M., and Mitchell, C. A. *The inositol polyphosphate 5-phosphatases: traffic controllers, waistline watchers and tumour suppressors?* 2007. Biochem.Soc.Symp. 161-181

66. Astle, M. V., Seaton, G., Davies, E. M., Fedele, C. G., Rahman, P., Arsala, L., and Mitchell, C. A. *Regulation of phosphoinositide signaling by the inositol polyphosphate 5-phosphatases* 2006. IUBMB.Life **58,** 451-456

67. Wenk, M. R. and De Camilli, P. *Inaugural Article: Protein-lipid interactions and phosphoinositide metabolism in membrane traffic: Insights from vesicle recycling in nerve terminals* 2004. PNAS **101,** 8262-8269

68. Peck, J., Douglas, G., Wu, C. H., and Burbelo, P. D. *Human RhoGAP domain-containing proteins: structure, function and evolutionary relationships* 2002. FEBS Lett. **528,** 27-34

69. Williams, C., Choudhury, R., McKenzie, E., and Lowe, M. *Targeting of the type II inositol polyphosphate 5-phosphatase INPP5B to the early secretory pathway* 2007. J Cell Sci **120,** 3941-3951

70. Hellsten, E., Evans, J. P., Bernard, D. J., Janne, P. A., and Nussbaum, R. L. *Disrupted sperm function and fertilin beta processing in mice deficient in the inositol polyphosphate 5-phosphatase Inpp5b* 2001. Dev.Biol **240,** 641-653

71. Johnson, J. M., Castle, J., Garrett-Engele, P., Kan, Z., Loerch, P. M., Armour, C. D., Santos, R., Schadt, E. E., Stoughton, R., and Shoemaker, D. D. *Genome-wide survey of human alternative pre-mRNA splicing with exon junction microarrays* 2003. Science **302,** 2141-2144

72. Olivos-Glander, I. M., Janne, P. A., and Nussbaum, R. L. *The oculocerebrorenal syndrome gene product is a 105-kD protein localized to the Golgi complex* 1995. Am.J Hum.Genet. **57,** 817-823

73. Dressman, M. A., Olivos-Glander, I. M., Nussbaum, R. L., and Suchy, S. F. *Ocrl1, a PtdIns(4,5)P(2) 5-phosphatase, is localized to the trans-Golgi network of fibroblasts and epithelial cells* 2000. J Histochem.Cytochem. **48,** 179-190

74. Ungewickell, A., Ward, M. E., Ungewickell, E., and Majerus, P. W. *The inositol polyphosphate 5-phosphatase Ocrl associates with endosomes that are partially coated with clathrin.* 2004. Proc.Natl.Acad.Sci.U.S.A **101,** 13501-13506

75. Choudhury, R., Diao, A., Zhang, F., Eisenberg, E., Saint-Pol, A., Williams, C., Konstantakopoulos, A., Lucocq, J., Johannes, L., Rabouille, C., Greene, L. E., and Lowe, M. *Lowe Syndrome Protein OCRL1 Interacts with Clathrin and Regulates Protein Trafficking between Endosomes and the Trans-Golgi Network* 2005. Mol.Biol.Cell **16,** 3467-3479

76. Erdmann, K. S., Mao, Y., McCrea, H. J., Zoncu, R., Lee, S., Paradise, S., Modregger, J., Biemesderfer, D., Toomre, D., and De Camilli, P. *A role of the Lowe syndrome protein OCRL in early steps of the endocytic pathway* 2007. Dev.Cell **13,** 377-390

77. Hyvola, N., Diao, A., McKenzie, E., Skippen, A., Cockcroft, S., and Lowe, M. *Membrane targeting and activation of the Lowe syndrome protein OCRL1 by rab GTPases.* 2006. EMBO J **25,** 3750-3761

78. Faucherre, A., Desbois, P., Nagano, F., Satre, V., Lunardi, J., Gacon, G., and Dorseuil, O. *Lowe syndrome protein Ocrl1 is translocated to membrane ruffles upon Rac GTPase activation: a new perspective on Lowe syndrome pathophysiology* 2005. Hum.Mol Genet. **14,** 1441-1448

79. Faucherre, A., Desbois, P., Satre, V., Lunardi, J., Dorseuil, O., and Gacon, G. *Lowe syndrome protein OCRL1 interacts with Rac GTPase in the trans-Golgi network* 2003. Hum.Mol Genet. **12,** 2449-2456

80. Cresawn, K. O., Potter, B. A., Oztan, A., Guerriero, C. J., Ihrke, G., Goldenring, J. R., Apodaca, G., and Weisz, O. A. *Differential involvement of endocytic compartments in the biosynthetic traffic of apical proteins* 2007. EMBO J. **26,** 3737-3748

81. Rhee, S. G. *Regulation of phosphoinositide-specific phospholipase C* 2001. Annu.Rev Biochem. **70,** 281-312

82. Patterson, R. L., Boehning, D., and Snyder, S. H. *Inositol 1,4,5-trisphosphate receptors as signal integrators* 2004. Annu.Rev Biochem. **73,** 437-465

83. Taylor, C. W. *Controlling Calcium Entry* 2002. Cell **111,** 767-769

84. Yang, C. and Kazanietz, M. G. *Divergence and complexities in DAG signaling: looking beyond PKC* 2003. Trends in Pharmacological Sciences **24,** 602-608

85. Jiang, B. H. and Liu, L. Z. *PI3K/PTEN signaling in tumorigenesis and angiogenesis* 2008. Biochim.Biophys.Acta **1784,** 150-158

86. Lemmon, M. A. *Membrane recognition by phospholipid-binding domains* 2008. Nat Rev Mol Cell Biol **9,** 99-111

87. Holz, R. W., Hlubek, M. D., Sorensen, S. D., Fisher, S. K., Balla, T., Ozaki, S., Prestwich, G. D., Stuenkel, E. L., and Bittner, M. A. *A pleckstrin homology domain specific for phosphatidylinositol 4, 5-bisphosphate (PtdIns-4,5-P2) and fused to green fluorescent protein identifies plasma membrane PtdIns-4,5-P2 as being important in exocytosis* 2000. J Biol Chem. **275,** 17878-17885

88. Vérnai, P. and Balla, T. *Live cell imaging of phosphoinositide dynamics with fluorescent protein domains* 2006. Biochimica et Biophysica Acta (BBA) - Molecular and Cell Biology of Lipids **1761,** 957-967

89. Kutateladze, T. G. *Phosphatidylinositol 3-phosphate recognition and membrane docking by the FYVE domain* 2006. Biochim.Biophys.Acta **1761,** 868-877

90. Misra, S. and Hurley, J. H. *Crystal structure of a phosphatidylinositol 3-phosphate-specific membrane-targeting motif, the FYVE domain of Vps27p* 1999. Cell **97,** 657-666

91. Dumas, J. J., Merithew, E., Sudharshan, E., Rajamani, D., Hayes, S., Lawe, D., Corvera, S., and Lambright, D. G. *Multivalent endosome targeting by homodimeric EEA1* 2001. Mol Cell **8,** 947-958

92. Gillooly, D. J., Morrow, I. C., Lindsay, M., Gould, R., Bryant, N. J., Gaullier, J. M., Parton, R. G., and Stenmark, H. *Localization of phosphatidylinositol 3-phosphate in yeast and mammalian cells* 2000. EMBO J **19,** 4577-4588

93. Hayakawa, A., Hayes, S. J., Lawe, D. C., Sudharshan, E., Tuft, R., Fogarty, K., Lambright, D., and Corvera, S. *Structural basis for endosomal targeting by FYVE domains* 2004. J Biol Chem. **279,** 5958-5966

94. Ponting, C. P. *Novel domains in NADPH oxidase subunits, sorting nexins, and PtdIns 3-kinases: binding partners of SH3 domains?* 1996. Protein Sci **5,** 2353-2357

95. Ellson, C. D., Andrews, S., Stephens, L. R., and Hawkins, P. T. *The PX domain: a new phosphoinositide-binding module* 2002. J Cell Sci **115,** 1099-1105

96. Kanai, F., Liu, H., Field, S. J., Akbary, H., Matsuo, T., Brown, G. E., Cantley, L. C., and Yaffe, M. B. *The PX domains of p47phox and p40phox bind to lipid products of PI(3)K* 2001. Nat Cell Biol **3,** 675-678

97. Song, X., Xu, W., Zhang, A., Huang, G., Liang, X., Virbasius, J. V., Czech, M. P., and Zhou, G. W. *Phox homology domains specifically bind phosphatidylinositol phosphates* 2001. Biochemistry **40,** 8940-8944

98. Worby, C. A. and Dixon, J. E. *Sorting out the cellular functions of sorting nexins* 2002. Nat Rev Mol Cell Biol **3,** 919-931

99. Zhong, Q., Watson, M. J., Lazar, C. S., Hounslow, A. M., Waltho, J. P., and Gill, G. N. *Determinants of the endosomal localization of sorting nexin 1* 2005. Mol Biol Cell **16,** 2049-2057

100. Seaman, M. N., McCaffery, J. M., and Emr, S. D. *A membrane coat complex essential for endosome-to-Golgi retrograde transport in yeast* 1998. J Cell Biol **142,** 665-681

101. Harlan, J. E., Hajduk, P. J., Yoon, H. S., and Fesik, S. W. *Pleckstrin homology domains bind to phosphatidylinositol-4,5-bisphosphate* 1994. Nature **371,** 168-170

102. Garcia, P., Gupta, R., Shah, S., Morris, A. J., Rudge, S. A., Scarlata, S., Petrova, V., McLaughlin, S., and Rebecchi, M. J. *The pleckstrin homology domain of phospholipase C-delta 1 binds with high affinity to phosphatidylinositol 4,5-bisphosphate in bilayer membranes* 1995. Biochemistry **34,** 16228-16234

103. Lemmon, M. A., Ferguson, K. M., O'Brien, R., Sigler, P. B., and Schlessinger, J. *Specific and high-affinity binding of inositol phosphates to an isolated pleckstrin homology domain* 1995. Proc.Natl.Acad.Sci U.S.A **92,** 10472-10476

104. Ferguson, K. M., Lemmon, M. A., Schlessinger, J., and Sigler, P. B. *Structure of the high affinity complex of inositol trisphosphate with a phospholipase C pleckstrin homology domain* 1995. Cell **83,** 1037-1046

105. Carlton, J. G. and Cullen, P. J. *Coincidence detection in phosphoinositide signaling* 2005. Trends Cell Biol **15,** 540-547

106. Godi, A., Di Campli, A., Konstantakopoulos, A., Di Tullio, G., Alessi, D. R., Kular, G. S., Daniele, T., Marra, P., Lucocq, J. M., and De Matteis, M. A. *FAPPs control Golgi-to-cell-surface membrane traffic by binding to ARF and PtdIns(4)P* 2004. Nat Cell Biol **6,** 393-404

107. Carlton, J., Bujny, M., Peter, B. J., Oorschot, V. M., Rutherford, A., Mellor, H., Klumperman, J., McMahon, H. T., and Cullen, P. J. *Sorting nexin-1 mediates tubular endosome-to-TGN transport through coincidence sensing of high- curvature membranes and 3-phosphoinositides* 2004. Curr.Biol **14,** 1791-1800

108. Verhage, M. and Toonen, R. F. *Regulated exocytosis: merging ideas on fusing membranes* 2007. Current Opinion in Cell Biology **19,** 402-408

109. Rothman J.E.. *The protein machinery of vesicle budding and fusion* 1996. Protein Science **5,** 185-194

110. Stojilkovic, S. S. *Ca2+-regulated exocytosis and SNARE function* 2005. Trends in Endocrinology and Metabolism **16,** 81-83

111. Martin, T. F. *Phosphoinositide lipids as signaling molecules: common themes for signal transduction, cytoskeletal regulation, and membrane trafficking* 1998. Annu.Rev Cell Dev.Biol **14,** 231-264

112. Bai, J., Tucker, W. C., and Chapman, E. R. *PIP2 increases the speed of response of synaptotagmin and steers its membrane-penetration activity toward the plasma membrane* 2004. Nat Struct.Mol Biol **11,** 36-44

113. Aoyagi, K., Sugaya, T., Umeda, M., Yamamoto, S., Terakawa, S., and Takahashi, M. *The Activation of Exocytotic Sites by the Formation of Phosphatidylinositol 4,5-Bisphosphate Microdomains at Syntaxin Clusters* 2005. J.Biol.Chem. **280,** 17346-17352

114. Milosevic, I., Sorensen, J. B., Lang, T., Krauss, M., Nagy, G., Haucke, V., Jahn, R., and Neher, E. *Plasmalemmal phosphatidylinositol-4,5-bisphosphate level regulates the releasable vesicle pool size in chromaffin cells* 2005. J Neurosci. **25,** 2557-2565

115. Gong, L. W., Di Paolo, G., Diaz, E., Cestra, G., Diaz, M. E., Lindau, M., De Camilli, P., and Toomre, D. *Phosphatidylinositol phosphate kinase type I gamma regulates dynamics of large dense-core vesicle fusion* 2005. Proc.Natl.Acad.Sci U.S.A **102,** 5204-5209

116. Di Paolo, G., Moskowitz, H. S., Gipson, K., Wenk, M. R., Voronov, S., Obayashi, M., Flavell, R., Fitzsimonds, R. M., Ryan, T. A., and De Camilli, P. *Impaired PtdIns(4,5)P2 synthesis in nerve terminals produces defects in synaptic vesicle trafficking* 2004. Nature **431,** 415-422

117. Liu, J., Zuo, X., Yue, P., and Guo, W. *Phosphatidylinositol 4,5-bisphosphate mediates the targeting of the exocyst to the plasma membrane for exocytosis in mammalian cells* 2007. Mol Biol Cell **18,** 4483-4492

118. Gaidarov, I. and Keen, J. H. *Phosphoinositide-AP-2 interactions required for targeting to plasma membrane clathrin-coated pits* 1999. J Cell Biol **146,** 755-764

119. Owen, D. J., Collins, B. M., and Evans, P. R. *Adaptors for clathrin coats: structure and function* 2004. Annu.Rev Cell Dev.Biol **20,** 153-191

120. Brodsky, F. M., Hill, B. L., Acton, S. L., Nathke, I., Wong, D. H., Ponnambalam, S., and Parham, P. *Clathrin light chains: arrays of protein motifs that regulate coated-vesicle dynamics* 1991. Trends Biochem.Sci **16,** 208-213

121. Zheng, J., Cahill, S. M., Lemmon, M. A., Fushman, D., Schlessinger, J., and Cowburn, D. *Identification of the binding site for acidic phospholipids on the pH domain of dynamin: implications for stimulation of GTPase activity* 1996. J Mol Biol **255,** 14-21

122. Conner, S. D. and Schmid, S. L. *Regulated portals of entry into the cell* 2003. Nature **422,** 37-44

123. Traub, L. M. *Sorting it out: AP-2 and alternate clathrin adaptors in endocytic cargo selection* 2003. J Cell Biol **163,** 203-208

124. Smythe, E. and Ayscough, K. R. *Actin regulation in endocytosis* 2006. J Cell Sci **119,** 4589-4598

125. Schafer, D. A. *Coupling actin dynamics and membrane dynamics during endocytosis* 2002. Curr.Opin.Cell Biol **14,** 76-81

126. McPherson, P. S., Garcia, E. P., Slepnev, V. I., David, C., Zhang, X., Grabs, D., Sossin, W. S., Bauerfeind, R., Nemoto, Y., and De Camilli, P. *A presynaptic inositol-5-phosphatase* 1996. Nature **379,** 353-357

127. Weixel, K. M., Edinger, R. S., Kester, L., Guerriero, C. J., Wang, H., Fang, L., Kleyman, T. R., Welling, P. A., Weisz, O. A., and Johnson, J. P. *Phosphatidylinositol 4-Phosphate 5-Kinase Reduces Cell Surface Expression of the Epithelial Sodium Channel (ENaC) in Cultured Collecting Duct Cells.* 2007. J Biol Chem. **282,** 36534-36542

128. Buck, T. M., Wright, C. M., and Brodsky, J. L. *The activities and function of molecular chaperones in the endoplasmic reticulum* 2007. Semin.Cell Dev.Biol **18,** 751-761

129. Ellgaard, L. and Helenius, A. *ER quality control: towards an understanding at the molecular level* 2001. Curr.Opin.Cell Biol **13,** 431-437

130. Pathre, P., Shome, K., Blumental-Perry, A., Bielli, A., Haney, C. J., Alber, S., Watkins, S. C., Romero, G., and Aridor, M. *Activation of phospholipase D by the small GTPase Sar1p is required to support COPII assembly and ER export* 2003. EMBO J **22,** 4059-4069

131. Moritz, A., De Graan, P. N., Gispen, W. H., and Wirtz, K. W. *Phosphatidic acid is a specific activator of phosphatidylinositol-4-phosphate kinase* 1992. J Biol Chem. **267,** 7207-7210

132. Blumental-Perry, A., Haney, C. J., Weixel, K., Watkins, S. C., Weisz, O. A., and Aridor, M. *Phosphatidylinositol 4-Phosphate Formation at ER Exit Sites Regulates ER Export* 2006. Developmental Cell **11,** 671-682

133. Mills, I. G., Praefcke, G. J. K., Vallis, Y., Peter, B. J., Olesen, L. E., Gallop, J. L., Butler, P. J., Evans, P. R., and McMahon, H. T. *EpsinR: an AP1/clathrin interacting protein involved in vesicle trafficking* 2003. J.Cell Biol. **160,** 213-222

134. Godi, A., Pertile, P., Meyers, R., Marra, P., Di Tullio, G., Iurisci, C., Luini, A., Corda, D., and De Matteis, M. A. *ARF mediates recruitment of PtdIns-4-OH kinase-beta and stimulates synthesis of PtdIns(4,5)P2 on the Golgi complex* 1999. Nat Cell Biol **1,** 280-287

135. Hirst, J., Motley, A., Harasaki, K., Peak Chew, S. Y., and Robinson, M. S. *EpsinR: an ENTH domain-containing protein that interacts with AP-1* 2003. Mol Biol Cell **14,** 625-641

136. Levine, T. P. and Munro, S. *Targeting of Golgi-specific pleckstrin homology domains involves both PtdIns 4-kinase-dependent and -independent components* 2002. Curr.Biol **12,** 695-704

137. Kahn, R. A., Yucel, J. K., and Malhotra, V. *ARF signaling: a potential role for phospholipase D in membrane traffic* 1993. Cell **75,** 1045-1048

138. Haynes, L. P., Thomas, G. M., and Burgoyne, R. D. *Interaction of neuronal calcium sensor-1 and ADP-ribosylation factor 1 allows bidirectional control of phosphatidylinositol 4-kinase beta and trans-Golgi network-plasma membrane traffic* 2005. J Biol Chem. **280,** 6047-6054

139. Donaldson, J. G., Honda, A., and Weigert, R. *Multiple activities for Arf1 at the Golgi complex* 2005. Biochimica et Biophysica Acta (BBA) - Molecular Cell Research **1744,** 364-373

140. Hall, A. *Rho GTPases and the Actin Cytoskeleton* 1998. Science **279,** 509-514

141. Takenawa, T. and Miki, H. *WASP and WAVE family proteins: key molecules for rapid rearrangement of cortical actin filaments and cell movement* 2001. J Cell Sci **114,** 1801-1809

142. Sechi, A. S. and Wehland, J. *The actin cytoskeleton and plasma membrane connection: PtdIns(4,5)P(2) influences cytoskeletal protein activity at the plasma membrane* 2000. J Cell Sci **113,** 3685-3695

143. Wiskott A *Familiarer, angeborener morbus Werlhofii.* 1936. Monatschrift Kinderheil **68,** p:212

144. Aldrich, R. A., Steinberg, A. G., and Campbell, D. C. *Pedigree demonstrating a sex-linked recessive condition characterized by draining ears, eczematoid dermatitis and bloody diarrhea.* 1954. Pediatrics **13,** 133-139

145. Remold-O'Donnell, E., Rosen, F. S., and Kenney, D. M. *Defects in Wiskott-Aldrich syndrome blood cells* 1996. Blood **87,** 2621-2631

146. Snapper, S. B., Takeshima, F., Anton, I., Liu, C. H., Thomas, S. M., Nguyen, D., Dudley, D., Fraser, H., Purich, D., Lopez-Ilasaca, M., Klein, C., Davidson, L., Bronson, R., Mulligan, R. C., Southwick, F., Geha, R., Goldberg, M. B., Rosen, F. S., Hartwig, J. H., and Alt, F. W. *N-WASP deficiency reveals distinct pathways for cell surface projections and microbial actin-based motility* 2001. Nat Cell Biol **3,** 897-904

147. Gouin, E., Gantelet, H., Egile, C., Lasa, I., Ohayon, H., Villiers, V., Gounon, P., Sansonetti, P. J., and Cossart, P. *A comparative study of the actin-based motilities of the pathogenic bacteria Listeria monocytogenes, Shigella flexneri and Rickettsia conorii* 1999. J Cell Sci **112 (Pt 11),** 1697-1708

148. Frischknecht, F., Moreau, V., Rottger, S., Gonfloni, S., Reckmann, I., Superti-Furga, G., and Way, M. *Actin-based motility of vaccinia virus mimics receptor tyrosine kinase signalling* 1999. Nature **401,** 926-929

149. Suzuki, T., Miki, H., Takenawa, T., and Sasakawa, C. *Neural Wiskott-Aldrich syndrome protein is implicated in the actin-based motility of Shigella flexneri* 1998. EMBO J **17,** 2767-2776

150. Boujemaa-Paterski, R., Gouin, E., Hansen, G., Samarin, S., Le Clainche, C., Didry, D., Dehoux, P., Cossart, P., Kocks, C., Carlier, M. F., and Pantaloni, D. *Listeria protein ActA mimics WASp family proteins: it activates filament barbed end branching by Arp2/3 complex* 2001. Biochemistry **40,** 11390-11404

151. Miki H, M. K. T. T. *N-WASP, a novel actin-depolymerizing protein, regulates the cortical cytoskeletal rearrangement in a PIP2-dependent manner downstream of tyrosine kinases.* 1996. EMBO J. **15,** 5326-5335

152. Qualmann, B., Roos, J., DiGregorio, P. J., and Kelly, R. B. *Syndapin I, a synaptic dynamin-binding protein that associates with the neural Wiskott-Aldrich syndrome protein* 1999. Mol Biol Cell **10,** 501-513

153. Kessels, M. M. and Qualmann, B. *Syndapins integrate N-WASP in receptor-mediated endocytosis.* 2002. EMBO J **21,** 6083-6094

154. Merrifield, C. J., Qualmann, B., Kessels, M. M., and Almers, W. *Neural Wiskott Aldrich Syndrome Protein (N-WASP) and the Arp2/3 complex are recruited to sites of clathrin-mediated endocytosis in cultured fibroblasts* 2004. Eur.J Cell Biol **83,** 13-18

155. Da Costa, S. R., Sou, E., Xie, J., Yarber, F. A., Okamoto, C. T., Pidgeon, M., Kessels, M. M., Mircheff, A. K., Schechter, J. E., Qualmann, B., and Hamm-Alvarez, S. F. *Impairing actin filament or syndapin functions promotes accumulation of clathrin-coated vesicles at the apical plasma membrane of acinar epithelial cells* 2003. Mol Biol Cell **14,** 4397-4413

156. Frischknecht, F., Cudmore, S., Moreau, V., Reckmann, I., Rottger, S., and Way, M. *Tyrosine phosphorylation is required for actin-based motility of vaccinia but not Listeria or Shigella* 1999. Curr.Biol **9,** 89-92

157. Schmelz, M., Sodeik, B., Ericsson, M., Wolffe, E. J., Shida, H., Hiller, G., and Griffiths, G. *Assembly of vaccinia virus: the second wrapping cisterna is derived from the trans Golgi network* 1994. J Virol. **68,** 130-147

158. Rozelle, A. L., Machesky, L. M., Yamamoto, M., Driessens, M. H. E., Insall, R. H., Roth, M. G., Luby-Phelps, K., Marriott, G., Hall, A., and Yin, H. L. *Phosphatidylinositol 4,5-bisphosphate induces actin-based movement of raft-enriched vesicles through WASP-Arp2/3* 2000. Current Biology **10,** 311-320

159. Rohatgi, R., Ma, L., Miki, H., Lopez, M., Kirchhausen, T., Takenawa, T., and Kirschner, M. W. *The Interaction between N-WASP and the Arp2/3 Complex Links Cdc42-Dependent Signals to Actin Assembly* 1999. Cell **97,** 221-231

160. Miki, H. and Takenawa, T. *Direct binding of the verprolin-homology domain in N-WASP to actin is essential for cytoskeletal reorganization* 1998. Biochem.Biophys.Res.Commun. **243,** 73-78

161. Machesky, L. M. and Insall, R. H. *Scar1 and the related Wiskott-Aldrich syndrome protein, WASP, regulate the actin cytoskeleton through the Arp2/3 complex* 1998. Curr.Biol **8,** 1347-1356

162. Machesky, L. M., Mullins, R. D., Higgs, H. N., Kaiser, D. A., Blanchoin, L., May, R. C., Hall, M. E., and Pollard, T. D. *Scar, a WASp-related protein, activates nucleation of actin filaments by the Arp2/3 complex* 1999. Proc.Natl.Acad.Sci U.S.A **96,** 3739-3744

163. Higgs, H. N. and Pollard, T. D. *Regulation of actin filament network formation through ARP2/3 complex: activation by a diverse array of proteins* 2001. Annu.Rev Biochem. **70,** 649-676

164. Pollard, T. D. *Regulation of actin filament assembly by Arp2/3 complex and formins* 2007. Annu.Rev Biophys.Biomol.Struct. **36,** 451-477

165. Panchal, S. C., Kaiser, D. A., Torres, E., Pollard, T. D., and Rosen, M. K. *A conserved amphipathic helix in WASP/Scar proteins is essential for activation of Arp2/3 complex* 2003. Nat Struct.Biol **10,** 591-598

166. Marchand, J. B., Kaiser, D. A., Pollard, T. D., and Higgs, H. N. *Interaction of WASP/Scar proteins with actin and vertebrate Arp2/3 complex* 2001. Nat Cell Biol **3,** 76-82

167. Prehoda, K. E., Scott, J. A., Mullins, R. D., and Lim, W. A. *Integration of multiple signals through cooperative regulation of the N-WASP-Arp2/3 complex* 2000. Science **290,** 801-806

168. Miki, H. and Takenawa, T. *Regulation of actin dynamics by WASP family proteins* 2003. J Biochem. **134,** 309-313

169. Bompard, G. and Caron, E. *Regulation of WASP/WAVE proteins: making a long story short* 2004. J Cell Biol **166,** 957-962

170. Papayannopoulos, V., Co, C., Prehoda, K. E., Snapper, S., Taunton, J., and Lim, W. A. *A polybasic motif allows N-WASP to act as a sensor of PIP(2) density* 2005. Mol Cell **17,** 181-191

171. Carlier, M. F., Nioche, P., Broutin-L'Hermite, I., Boujemaa, R., Le Clainche, C., Egile, C., Garbay, C., Ducruix, A., Sansonetti, P., and Pantaloni, D. *GRB2 links signaling to actin assembly by enhancing interaction of neural Wiskott-Aldrich syndrome protein (N-WASp) with actin-related protein (ARP2/3) complex* 2000. J Biol Chem. **275,** 21946-21952

172. Fukuoka, M., Suetsugu, S., Miki, H., Fukami, K., Endo, T., and Takenawa, T. *A novel neural Wiskott-Aldrich syndrome protein (N-WASP) binding protein, WISH, induces Arp2/3 complex activation independent of Cdc42* 2001. J Cell Biol **152,** 471-482

173. Rohatgi, R., Nollau, P., Ho, H. Y., Kirschner, M. W., and Mayer, B. J. *Nck and phosphatidylinositol 4,5-bisphosphate synergistically activate actin polymerization through the N-WASP-Arp2/3 pathway* 2001. J Biol Chem. **276,** 26448-26452

174. Suetsugu, S., Hattori, M., Miki, H., Tezuka, T., Yamamoto, T., Mikoshiba, K., and Takenawa, T. *Sustained activation of N-WASP through phosphorylation is essential for neurite extension* 2002. Dev.Cell **3,** 645-658

175. Cory, G. O., Garg, R., Cramer, R., and Ridley, A. J. *Phosphorylation of tyrosine 291 enhances the ability of WASp to stimulate actin polymerization and filopodium formation. Wiskott-Aldrich Syndrome protein* 2002. J Biol Chem. **277,** 45115-45121

176. Cory, G. O., Cramer, R., Blanchoin, L., and Ridley, A. J. *Phosphorylation of the WASP-VCA domain increases its affinity for the Arp2/3 complex and enhances actin polymerization by WASP* 2003. Mol Cell **11,** 1229-1239

177. Zalevsky, J., Lempert, L., Kranitz, H., and Mullins, R. D. *Different WASP family proteins stimulate different Arp2/3 complex-dependent actin-nucleating activities* 2001. Curr.Biol **11,** 1903-1913

178. Peterson, J. R., Bickford, L. C., Morgan, D., Kim, A. S., Ouerfelli, O., Kirschner, M. W., and Rosen, M. K. *Chemical inhibition of N-WASP by stabilization of a native autoinhibited conformation.* 2004. Nat Struct.Mol.Biol **11,** 747-755

179. Pendaries, C., Tronchere, H., Plantavid, M., and Payrastre, B. *Phosphoinositide signaling disorders in human diseases* 2003. FEBS Lett. **546,** 25-31

180. Carnero, A., Blanco-Aparicio, C., Renner, O., Link, W., and Leal, J. F. *The PTEN/PI3K/AKT signalling pathway in cancer, therapeutic implications* 2008. Curr.Cancer Drug Targets. **8,** 187-198

181. Li, J., Yen, C., Liaw, D., Podsypanina, K., Bose, S., Wang, S. I., Puc, J., Miliaresis, C., Rodgers, L., McCombie, R., Bigner, S. H., Giovanella, B. C., Ittmann, M., Tycko, B., Hibshoosh, H., Wigler, M. H., and Parsons, R. *PTEN, a putative protein tyrosine phosphatase gene mutated in human brain, breast, and prostate cancer* 1997. Science **275,** 1943-1947

182. Steck, P. A., Pershouse, M. A., Jasser, S. A., Yung, W. K., Lin, H., Ligon, A. H., Langford, L. A., Baumgard, M. L., Hattier, T., Davis, T., Frye, C., Hu, R., Swedlund, B., Teng, D. H., and Tavtigian, S. V. *Identification of a candidate tumour suppressor gene, MMAC1, at chromosome 10q23.3 that is mutated in multiple advanced cancers* 1997. Nat Genet. **15,** 356-362

183. Wishart, M. J. and Dixon, J. E. *PTEN and myotubularin phosphatases: from 3-phosphoinositide dephosphorylation to disease* 2002. Trends Cell Biol **12,** 579-585

184. Maehama, T. and Dixon, J. E. *PTEN: a tumour suppressor that functions as a phospholipid phosphatase* 1999. Trends Cell Biol **9,** 125-128

185. Toker, A. *Phosphoinositides and signal transduction* 2002. Cell Mol Life Sci **59,** 761-779

186. Katso, R., Okkenhaug, K., Ahmadi, K., White, S., Timms, J., and Waterfield, M. D. *Cellular function of phosphoinositide 3-kinases: implications for development, homeostasis, and cancer* 2001. Annu.Rev Cell Dev.Biol **17,** 615-675

187. Voronov, S. V., Frere, S. G., Giovedi, S., Pollina, E. A., Borel, C., Zhang, H., Schmidt, C., Akeson, E. C., Wenk, M. R., Cimasoni, L., Arancio, O., Davisson, M. T., Antonarakis, S. E., Gardiner, K., De Camilli, P., and Di Paolo, G. *Synaptojanin 1-linked phosphoinositide dyshomeostasis and cognitive deficits in mouse models of Down's syndrome* 2008. PNAS **105,** 9415-9420

188. Attree, O., Olivos, I. M., Okabe, I., Bailey, L. C., Nelson, D. L., Lewis, R. A., McInnes, R. R., and Nussbaum, R. L. *The Lowe's oculocerebrorenal syndrome gene encodes a protein highly homologous to inositol polyphosphate-5-phosphatase* 1992. Nature **358,** 239-242

189. Hoopes, R. R., Jr., Shrimpton, A. E., Knohl, S. J., Hueber, P., Hoppe, B., Matyus, J., Simckes, A., Tasic, V., Toenshoff, B., Suchy, S. F., Nussbaum, R. L., and Scheinman, S. J. *Dent Disease with mutations in OCRL1*. 2005. Am.J Hum.Genet. **76,** 260-267

190. Wrong, O. M., Norden, A. G., and Feest, T. G. *Dent's disease; a familial proximal renal tubular syndrome with low-molecular-weight proteinuria, hypercalciuria, nephrocalcinosis, metabolic bone disease, progressive renal failure and a marked male predominance.* 1994. QJM. **87,** 473-493

191. Cho, H. Y., Lee, B. H., Choi, H. J., Ha, I. S., Choi, Y., and Cheong, H. I. *Renal manifestations of Dent disease and Lowe syndrome* 2008. Pediatr.Nephrol. **23,** 243-249

192. Bockenhauer, D., Bokenkamp, A., van't Hoff, W., Levtchenko, E., Kist-van Holthe, J. E., Tasic, V., and Ludwig, M. *Renal phenotype in Lowe Syndrome: a selective proximal tubular dysfunction* 2008. Clin.J Am Soc.Nephrol. **3,** 1430-1436

193. Sekine, T., Nozu, K., Iyengar, R., Fu, X. J., Matsuo, M., Tanaka, R., Iijima, K., Matsui, E., Harita, Y., Inatomi, J., and Igarashi, T. *OCRL1 mutations in patients with Dent disease phenotype in Japan* 2007. Pediatr.Nephrol. **22,** 975-980

194. Hryciw, D. H., Ekberg, J., Pollock, C. A., and Poronnik, P. *ClC-5: A chloride channel with multiple roles in renal tubular albumin uptake.* 2005. Int.J Biochem Cell Biol

195. Verroust, P. J. and Christensen, E. I. *Megalin and cubilin--the story of two multipurpose receptors unfolds.* 2002. Nephrol.Dial.Transplant. **17,** 1867-1871

196. Norden, A. G., Lapsley, M., Igarashi, T., Kelleher, C. L., Lee, P. J., Matsuyama, T., Scheinman, S. J., Shiraga, H., Sundin, D. P., Thakker, R. V., Unwin, R. J., Verroust, P., and Moestrup, S. K. *Urinary megalin deficiency implicates abnormal tubular endocytic function in Fanconi syndrome.* 2002. J Am Soc.Nephrol. **13,** 125-133

197. Zou, Z., Chung, B., Nguyen, T., Mentone, S., Thomson, B., and Biemesderfer, D. *Linking Receptor-mediated Endocytosis and Cell Signaling: Evidnece for Regulated Iintramembrane Proteolysis of Megamin in Proximal Tubule* 2004. J.Biol.Chem. **279,** 34302-34310

198. Rodriguez-Boulan, E., Kreitzer, G., and Musch, A. *Organization of vesicular trafficking in epithelia* 2005. Nat Rev Mol Cell Biol **6,** 233-247

199. Jacob, R., Heine, M., Alfalah, M., and Naim, H. Y. *Distinct cytoskeletal tracks direct individual vesicle populations to the apical membrane of epithelial cells.* 2003. Curr.Biol **13,** 607-612

200. Wei, Y. J., Sun, H. Q., Yamamoto, M., Wlodarski, P., Kunii, K., Martinez, M., Barylko, B., Albanesi, J. P., and Yin, H. L. *Type II Phosphatidylinositol 4-Kinase beta Is a Cytosolic and Peripheral Membrane Protein That Is Recruited to the Plasma Membrane and Activated by Rac-GTP* 2002. J.Biol.Chem. **277,** 46586-46593

201. Lorra, C. and Huttner, W. B. *The mesh hypothesis of Golgi dynamics* 1999. Nat Cell Biol **1,** p:E113-E115

202. Huijbregts, R. P., Topalof, L., and Bankaitis, V. A. *Lipid metabolism and regulation of membrane trafficking* 2000. Traffic. **1,** 195-202

203. Zhang, X., Jefferson, A. B., Auethavekiat, V., and Majerus, P. W. *The protein deficient in Lowe syndrome is a phosphatidylinositol-4,5-bisphosphate 5-phosphatase.* 1995. Proc.Natl.Acad.Sci.U.S.A **92,** 4853-4856

204. Padron, D., Wang, Y. J., Yamamoto, M., Yin, H., and Roth, M. G. *Phosphatidylinositol phosphate 5-kinase I{beta} recruits AP-2 to the plasma membrane and regulates rates of constitutive endocytosis* 2003. J.Cell Biol. **162,** 693-701

205. Gong, D. and Ferrell, J. E., Jr. *Picking a winner: new mechanistic insights into the design of effective siRNAs* 2004. Trends Biotechnol. **22,** 451-454

206. Schwarz, D. S., Hutvagner, G., Du, T., Xu, Z., Aronin, N., and Zamore, P. D. *Asymmetry in the assembly of the RNAi enzyme complex* 2003. Cell **115,** 199-208

207. Hohjoh, H. *Enhancement of RNAi activity by improved siRNA duplexes* 2004. FEBS Lett. **557,** 193-198

208. Zhang, X., Hartz, P. A., Philip, E., Racusen, L. C., and Majerus, P. W. *Cell Lines from Kidney Proximal Tubules of a Patient with Lowe Syndrome Lack OCRL Inositol Polyphosphate 5-Phosphatase and Accumulate Phosphatidylinositol 4,5-Bisphosphate* 1998. J.Biol.Chem. **273,** 1574-1582

209. Suchy, S. F. and Nussbaum, R. L. *The deficiency of PIP 5 phosphatase in Lowe Syndrome affects actin polymerization.* 2002. Am.J Hum.Genet. **71,** 1420-1427

210. Allen, P. G. *Actin filament uncapping localizes to ruffling lamellae and rocketing vesicles.* 2003. Nat Cell Biol **5,** 972-979

211. Janne, P. A., Suchy, S. F., Bernard, D., MacDonald, M., Crawley, J., Grinberg, A., Wynshaw-Boris, A., Westphal, H., and Nussbaum, R. L. *Functional overlap between murine Inpp5b and Ocrl1 may explain why deficiency of the murine ortholog for OCRL1 does not cause Lowe syndrome in mice* 1998. J Clin.Invest **101,** 2042-2053

212. Nagai, M., Meerloo, T., Takeda, T., and Farquhar, M. G. *The adaptor protein ARH escorts megalin to and through endosomes* 2003. Mol.Biol Cell **14,** 4984-4996

213. Orzech, E., Cohen, S., Weiss, A., and Aroeti, B. *Interactions between the Exocytic and Endocytic Pathways in Polarized Madin-Darby Canine Kidney Cells* 2000. J.Biol.Chem. **275,** 15207-15219

214. Polishchuk, R., Di Pentima, A., and Lippincott-Schwartz, J. *Delivery of raft-associated, GPI-anchored proteins to the apical surface of polarized MDCK cells by a transcytotic pathway* 2004. Nat Cell Biol **6,** 297-307

215. Khurana, S. *Role of actin cytoskeleton in regulation of ion transport: examples from epithelial cells* 2000. J Membr.Biol **178,** 73-87

216. Pollard, T. D. *Cellular motility powered by actin filament assembly and disassembly* 2002. Harvey Lect. **98,** 1-17

217. Stamnes, M. *Regulating the actin cytoskeleton during vesicular transport* 2002. Curr.Opin.Cell Biol **14,** 428-433

218. Ibarra, N., Pollitt, A., and Insall, R. H. *Regulation of actin assembly by SCAR/WAVE proteins* 2005. Biochem.Soc.Trans. **33,** 1243-1246

219. Taunton, J., Rowning, B. A., Coughlin, M. L., Wu, M., Moon, R. T., Mitchison, T. J., and Larabell, C. A. *Actin-dependent Propulsion of Endosomes and Lysosomes by Recruitment of N-WASP* 2000. J.Cell Biol. **148,** 519-530

220. Miki, H., Miura, K., and Takenawa, T. *N-WASP, a novel actin-depolymerizing protein, regulates the cortical cytoskeletal rearrangement in a PIP2-dependent manner downstream of tyrosine kinases.* 1996. EMBO J. **15,** 5326-5335

221. Peterson, J. R., Lokey, R. S., Mitchison, T. J., and Kirschner, M. W. *A chemical inhibitor of N-WASP reveals a new mechanism for targeting protein interactions* 2001. Proc.Natl.Acad.Sci U.S.A **98,** 10624-10629

222. Hinchliffe, K. A., Irvine, R. F., and Divecha, N. *Aggregation-dependent, integrin-mediated increases in cytoskeletally associated PtdInsP2 (4,5) levels in human platelets are controlled by translocation of PtdIns 4-P 5-kinase C to the cytoskeleton* 1996. EMBO J **15,** 6516-6524

223. Yang, S. A., Carpenter, C. L., and Abrams, C. S. *Rho and Rho-kinase mediate thrombin-induced phosphatidylinositol 4-phosphate 5-kinase trafficking in platelets* 2004. J Biol Chem. **279,** 42331-42336

224. Orth, J. D., Krueger, E. W., Cao, H., and McNiven, M. A. *The large GTPase dynamin regulates actin comet formation and movement in living cells* 2002. Proc.Natl.Acad.Sci U.S.A **99,** 167-172

225. Lee, E. and De Camilli, P. *From the Cover: Dynamin at actin tails* 2002. PNAS **99,** 161-166

226. Chen, Y. G., Siddhanta, A., Austin, C. D., Hammond, S. M., Sung, T. C., Frohman, M. A., Morris, A. J., and Shields, D. *Phospholipase D stimulates release of nascent secretory vesicles from the trans-Golgi network* 1997. J Cell Biol **138,** 495-504

227. Ivanov, A. I., Hunt, D., Utech, M., Nusrat, A., and Parkos, C. A. *Differential roles for actin polymerization and a myosin II motor in assembly of the epithelial apical junctional complex.* 2005. Mol.Biol Cell **16,** 2636-2650

228. Haller, C., Rauch, S., Michel, N., Hannemann, S., Lehmann, M. J., Keppler, O. T., and Fackler, O. T. *The HIV-1 pathogenicity factor Nef interferes with maturation of stimulatory T-lymphocyte contacts by modulation of N-Wasp activity* 2006. J Biol Chem. **281,** 19618-19630

229. Kovacs, E. M., Makar, R. S., and Gertler, F. B. *Tuba stimulates intracellular N-WASP-dependent actin assembly* 2006. J Cell Sci **119,** 2715-2726

230. Robert, A., Smadja-Lamere, N., Landry, M. C., Champagne, C., Petrie, R., Lamarche-Vane, N., Hosoya, H., and Lavoie, J. N. *Adenovirus E4orf4 hijacks rho GTPase-dependent actin dynamics to kill cells: a role for endosome-associated actin assembly* 2006. Mol Biol Cell **17,** 3329-3344

231. ten Klooster, J. P., Evers, E. E., Janssen, L., Machesky, L. M., Michiels, F., Hordijk, P., and Collard, J. G. *Interaction between Tiam1 and the Arp2/3 complex links activation of Rac to actin polymerization* 2006. Biochem.J **397,** 39-45

232. Henkel, J. R., Gibson, G. A., Poland, P. A., Ellis, M. A., Hughey, R. P., and Weisz, O. A. *Influenza M2 proton channel activity selectively inhibits trans-Golgi network release of apical membrane and secreted proteins in polarized Madin-Darby canine kidney cells* 2000. J Cell Biol **148,** 495-504

233. Duran, J. M., Valderrama, F., Castel, S., Magdalena, J., Tomas, M., Hosoya, H., Renau-Piqueras, J., Malhotra, V., and Egea, G. *Myosin motors and not actin comets are mediators of the actin-based Golgi-to-endoplasmic reticulum protein transport* 2003. Mol Biol Cell **14,** 445-459

234. Guerriero, C. J., Weixel, K. M., Bruns, J. R., and Weisz, O. A. *Phosphatidylinositol 5-kinase stimulates apical biosynthetic delivery via an Arp2/3-dependent mechanism* 2006. J Biol Chem.

235. Maples, C. J., Ruiz, W. G., and Apodaca, G. *Both microtubules and actin filaments are required for efficient postendocytotic traffic of the polymeric immunoglobulin receptor in polarized Madin-Darby canine kidney cells* 1997. J Biol Chem. **272,** 6741-6751

236. Henkel, J. R., Apodaca, G., Altschuler, Y., Hardy, S., and Weisz, O. A. *Selective perturbation of apical membrane traffic by expression of influenza M2, an acid-activated ion channel, in polarized madin-darby canine kidney cells.* 1998. Mol.Biol Cell **9,** 2477-2490

237. Persson, R., Ahlstrom, E., and Fries, E. *Differential arrest of secretory protein transport in cultured rat hepatocytes by azide treatment* 1988. J Cell Biol **107,** 2503-2510

238. Kempiak, S. J., Yamaguchi, H., Sarmiento, C., Sidani, M., Ghosh, M., Eddy, R. J., Desmarais, V., Way, M., Condeelis, J., and Segall, J. E. *A neural Wiskott-Aldrich Syndrome protein-mediated pathway for localized activation of actin polymerization that is regulated by cortactin.* 2005. J Biol Chem. **280,** 5836-5842

239. Allan, V. J., Thompson, H. M., and McNiven, M. A. *Motoring around the Golgi* 2002. Nat.Cell Biol. **4,** p:E236-E242

240. Heimann, K., Percival, J. M., Weinberger, R., Gunning, P., and Stow, J. L. *Specific Isoforms of Actin-binding Proteins on Distinct Populations of Golgi-derived Vesicles* 1999. J.Biol.Chem. **274,** 10743-10750

241. Fucini, R. V., Navarrete, A., Vadakkan, C., Lacomis, L., Erdjument-Bromage, H., Tempst, P., and Stamnes, M. *Activated ADP-ribosylation Factor Assembles Distinct Pools of Actin on Golgi Membranes* 2000. J.Biol.Chem. **275,** 18824-18829

242. Matas, O. B., Martinez-Menarguez, J. A., and Egea, G. *Association of Cdc42/N-WASP/Arp2/3 signaling pathway with Golgi membranes* 2004. Traffic. **5,** 838-846

243. Fucini, R. V., Chen, J. L., Sharma, C., Kessels, M. M., and Stamnes, M. *Golgi Vesicle Proteins Are Linked to the Assembly of an Actin Complex Defined by mAbp1* 2002. Mol.Biol.Cell **13,** 621-631

244. Dubois, T., Paleotti, O., Mironov, A. A., Fraisier, V., Stradal, T. E., De Matteis, M. A., Franco, M., and Chavrier, P. *Golgi-localized GAP for Cdc42 functions downstream of ARF1 to control Arp2/3 complex and F-actin dynamics* 2005. Nat.Cell Biol. **7,** 353-364

245. Chen, J. L., Fucini, R. V., Lacomis, L., Erdjument-Bromage, H., Tempst, P., and Stamnes, M. *Coatomer-bound Cdc42 regulates dynein recruitment to COPI vesicles* 2005. J Cell Biol **169,** 383-389

246. Cao, H., Weller, S., Orth, J. D., Chen, J., Huang, B., Chen, J. L., Stamnes, M., and McNiven, M. A. *Actin and Arf1-dependent recruitment of a cortactin-dynamin complex to the Golgi regulates post-Golgi transport* 2005. Nat.Cell Biol. **7,** 483-492

247. Carreno, S., Engqvist-Goldstein, A. E., Zhang, C. X., McDonald, K. L., and Drubin, D. G. *Actin dynamics coupled to clathrin-coated vesicle formation at the trans-Golgi network* 2004. J.Cell Biol. **165,** 781-788

248. Scheffler, I. E. (1999) *Mitochondria*, Wiley-Liss, New York

249. Ball, E. G. and Cooper, O. *The reaction of cytochrome oxidase with cyanide* 1952. J Biol Chem. **198,** 629-638

250. Oberg, K. E. *The site of the action of rotenone in the respiratory chain* 1961. Exp.Cell Res. **24,** 163-164

251. Linnett, P. E. and Beechey, R. B. *Inhibitors of the ATP synthethase system* 1979. Methods Enzymol. **55,** 472-518

252. Stubbs, M. *Inhibitors of the adenine nucleotide translocase* 1979. Pharmacol.Ther. **7,** 329-350

253. Hope, H. R. and Pike, L. J. *Phosphoinositides and phosphoinositide-utilizing enzymes in detergent- insoluble lipid domains* 1996. Mol.Biol.Cell **7,** 843-851

254. Laux, T., Fukami, K., Thelen, M., Golub, T., Frey, D., and Caroni, P. *GAP43, MARCKS, and CAP23 Modulate PI(4,5)P2 at Plasmalemmal Rafts, and Regulate Cell Cortex Actin Dynamics through a Common Mechanism* 2000. J.Cell Biol. **149,** 1455-1472

255. Caroni, P. *New EMBO members' review: actin cytoskeleton regulation through modulation of PI(4,5)P(2) rafts* 2001. EMBO J. **20,** 4332-4336

256. Brough, D., Bhatti, F., and Irvine, R. F. *Mobility of proteins associated with the plasma membrane by interaction with inositol lipids* 2005. J Cell Sci **118,** 3019-3025

257. Heine, M., Cramm-Behrens, C. I., Ansari, A., Chu, H. P., Ryazanov, A. G., Naim, H. Y., and Jacob, R. *{alpha}-Kinase 1, a New Component in Apical Protein Transport* 2005. J.Biol.Chem. **280,** 25637-25643

258. Morris, S. M., Arden, S. D., Roberts, R. C., Kendrick-Jones, J., Cooper, J. A., Luzio, J. P., and Buss, F. *Myosin VI binds to and localises with Dab2, potentially linking receptor-mediated endocytosis and the actin cytoskeleton* 2002. Traffic. **3,** 331-341

259. Benesch, S., Polo, S., Lai, F. P. L., Anderson, K. I., Stradal, T. E. B., Wehland, J., and Rottner, K. *N-WASP deficiency impairs EGF internalization and actin assembly at clathrin-coated pits* 2005. J Cell Sci **118,** 3103-3115

260. Merrifield, C. J. *Seeing is believing: imaging actin dynamics at single sites of endocytosis* 2004. Trends Cell Biol. **14,** 352-358

261. Parczyk, K., Haase, W., and Kondor-Koch, C. *Microtubules are involved in the secretion of proteins at the apical cell surface of the polarized epithelial cell, Madin-Darby canine kidney* 1989. J.Biol.Chem. **264,** 16837-16846

262. Grindstaff, K. K., Yeaman, C., Anandasabapathy, N., Hsu, S. C., Rodriguez-Boulan, E., Scheller, R. H., and Nelson, W. J. *Sec6/8 complex is recruited to cell-cell contacts and specifies transport vesicle delivery to the basal-lateral membrane in epithelial cells* 1998. Cell **93,** 731-740

263. Boll, W., Partin, J. S., Katz, A. I., Caplan, M. J., and Jamieson, J. D. *Distinct pathways for basolateral targeting of membrane and secretory proteins in polarized epithelial cells* 1991. Proceedings of the National Academy of Sciences of the United States of America **88,** 8592-8596

264. Breitfeld, P. P., McKinnon, W. C., and Mostov, K. E. *Effect of nocodazole on vesicular traffic to the apical and basolateral surfaces of polarized MDCK cells* 1990. J.Cell Biol. **111,** 2365-2373

265. Hirschberg, K., Miller, C. M., Ellenberg, J., Presley, J. F., Siggia, E. D., Phair, R. D., and Lippincott-Schwartz, J. *Kinetic Analysis of Secretory Protein Traffic and Characterization of Golgi to Plasma Membrane Transport Intermediates in Living Cells* 1998. J.Cell Biol. **143,** 1485-1503

266. Toomre, D., Keller, P., White, J., Olivo, J. C., and Simons, K. *Dual-color visualization of trans-Golgi network to plasma membrane traffic along microtubules in living cells* 1999. J Cell Sci **112,** 21-33

267. Lou, X., McQuistan, T., Orlando, R. A., and Farquhar, M. G. *GAIP, GIPC and Galphai3 are concentrated in endocytic compartments of proximal tubule cells: putative role in regulating megalin's function* 2002. J Am Soc.Nephrol. **13,** 918-927

268. Cremona, O., Di Paolo, G., Wenk, M. R., Luthi, A., Kim, W. T., Takei, K., Daniell, L., Nemoto, Y., Shears, S. B., Flavell, R. A., McCormick, D. A., and De Camilli, P. *Essential role of phosphoinositide metabolism in synaptic vesicle recycling* 1999. Cell **99,** 179-188

269. Hughes, P., Marshall, D., Reid, Y., Parkes, H., and Gelber, C. *The costs of using unauthenticated, over-passaged cell lines: how much more data do we need?* 2007. Biotechniques **43,** 575, 577-2

270. Simons K, I. E. *Functional rafts in cell membranes.* 1997. Nature **387,** 569-572

271. Purkerson, J. M., Kittelberger, A. M., and Schwartz, G. J. *Basolateral carbonic anhydrase IV in the proximal tubule is a glycosylphosphatidylinositol-anchored protein* 2007. Kidney Int. **71,** 407-416

272. Sarnataro, D., Paladino, S., Campana, V., Grassi, J., Nitsch, L., and Zurzolo, C. *PrPC is sorted to the basolateral membrane of epithelial cells independently of its association with rafts* 2002. Traffic. **3,** 810-821

273. Bacallao, R., Antony, C., Dotti, C., Karsenti, E., Stelzer, E. H., and Simons, K. *The subcellular organization of Madin-Darby canine kidney cells during the formation of a polarized epithelium* 1989. J Cell Biol **109,** 2817-2832

274. Jaulin, F., Xue, X., Rodriguez-Boulan, E., and Kreitzer, G. *Polarization-dependent selective transport to the apical membrane by KIF5B in MDCK cells* 2007. Dev.Cell **13,** 511-522

275. Bairstow, S. F., Ling, K., Su, X., Firestone, A. J., Carbonara, C., and Anderson, R. A. *Type I{gamma}661 Phosphatidylinositol Phosphate Kinase Directly Interacts with AP2 and Regulates Endocytosis* 2006. J.Biol.Chem. **281,** 20632-20642

276. Lefrancois, L. and Lyles, D. S. *The interaction of antibody with the major surface glycoprotein of vesicular stomatitis virus. II. Monoclonal antibodies of nonneutralizing and cross-reactive epitopes of Indiana and New Jersey serotypes* 1982. Virology **121,** 168-174

277. Butterworth, M. B., Edinger, R. S., Johnson, J. P., and Frizzell, R. A. *Acute ENaC Stimulation by cAMP in a Kidney Cell Line is Mediated by Exocytic Insertion from a Recycling Channel Pool* 2004. J.Gen.Physiol. **125,** 81-101

278. Apodaca, G., Katz, L. A., and Mostov, K. E. *Receptor-mediated transcytosis of IgA in MDCK cells is via apical recycling endosomes* 1994. J.Cell Biol. **125,** 67-86

279. Altschuler, Y., Kinlough, C. L., Poland, P. A., Bruns, J. B., Apodaca, G., Weisz, O. A., and Hughey, R. P. *Clathrin-mediated endocytosis of MUC1 is modulated by its glycosylation state* 2000. Mol.Biol.Cell **11,** 819-831

280. Celis, J. E. (1998) *Cell biology a laboratory handbook*, 2nd ed Ed., Academic Press, San Diego

281. Yang, N. C., Ho, W. M., Chen, Y. H., and Hu, M. L. *A convenient one-step extraction of cellular ATP using boiling water for the luciferin-luciferase assay of ATP* 2002. Anal.Biochem. **306,** 323-327